NEURAL RESPONSES DURING TRACE CONDITIONING WITH FACE AND NON-FACE STIMULI RECORDED WITH MAGNETOENCEPHALOGRAPHY

by

Nicholas L. Balderston

A Dissertation Submitted in

Partial Fulfillment of the

Requirements for the Degree of

Doctor of Philosophy

in Psychology

at

The University of Wisconsin-Milwaukee

December 2013

ABSTRACT
NEURAL RESPONSES DURING TRACE CONDITIONING WITH FACE AND NON-FACE STIMULI RECORDED WITH MAGNETOENCEPHALOGRAPHY

by

Nicholas L. Balderston

The University of Wisconsin-Milwaukee, 2013
Under the Supervision of Fred Helmstetter

During fear conditioning a subject is presented with an initially innocuous stimulus like an image (conditioned stimulus; CS) that predicts an aversive outcome like a mild electric shock (unconditioned stimulus; UCS). Subjects rapidly learn that the CS predicts the UCS, and show autonomic fear responses (CRs) during the presentation of the CS. When the CS and the UCS coterminate, as is the case for delay conditioning, individuals can acquire CRs even if they are unable to predict the occurrence of the UCS. However when there is a temporal gap between the CS and the UCS, CR expression is typically dependent upon explicit awareness of the CS-UCS pairing. Research with non-human animals suggests that both the hippocampus and the prefrontal cortex are needed for trace but not delay fear conditioning, and that communication between these areas may help to maintain the CS during the trace interval. We tested this hypothesis by exposing subjects to differential delay and trace fear conditioning while we recorded their brain activity with magnetoencephalography. Faces and houses served as CSs and an aversive electrical stimulation served as the UCS. As predicted, subjects show evidence of conditioning on both implicit and explicit measures. In addition, there is a learning related increase in theta coherence between the left parahippocampal gyrus and several frontal and parietal cortical regions for trace but not delay conditioning. These results suggest that trace

conditioning recruits a network of cortical regions, and that the activity of these regions is coordinated by the medial temporal lobe.

TABLE OF CONTENTS

LIST OF FIGURES

LIST OF TABLES

During Pavlovian fear conditioning, an initially innocuous stimulus (CS) is repeatedly paired with an aversive outcome (UCS) (Kim & Jung, 2006; See Figure 1). After this experience, humans acquire the ability to explicitly state the nature of the cue-outcome contingencies. In addition, they express a conditioned emotional response (CR) when they later encounter the CS (Cheng, Knight, Smith, & Helmstetter, 2006a). During delay fear conditioning these two stimuli overlap in time, (Balderston & Helmstetter, 2010; Knight, Waters, & Bandettini, 2009; Schultz & Helmstetter, 2010a; Weike, Schupp, & Hamm, 2007). During trace conditioning the CS and the UCS are separated by a stimulus free period (Knight, Nguyen, & Bandettini, 2006; Weike et al., 2007). Learning is typically measured using variables that index either changes in physiological arousal (implicit) or declarative knowledge of the experimental contingencies (explicit).

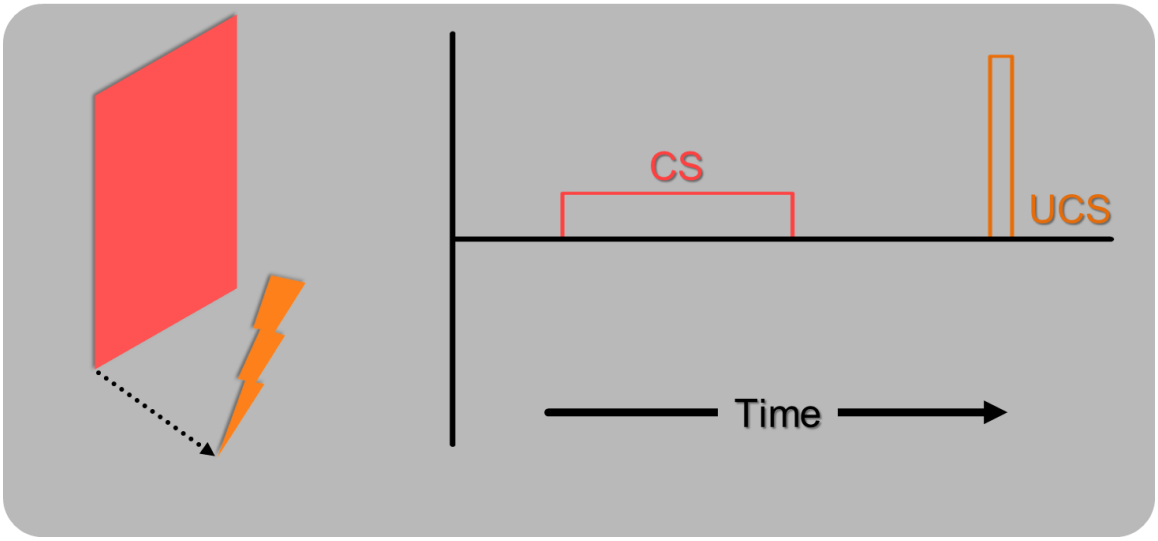

Figure 1. Typical fear conditioning experiment. The square predicts the occurrence of the shock. Notice the gap between the offset of the CS and the onset of the UCS, indicating that this is an example of trace conditioning.

1.1 Implicit measures of fear learning

To show that the conditioning procedure is inducing a state of heightened fear in the subject, most studies of fear conditioning measure changes in autonomic arousal. Skin conductance responses (SCRs) are the most common measure of arousal in trace fear conditioning with humans (Ahs, Frans, Tibblin, Kumlien, & Fredrikson, 2010; Carter, Hofstotter, Tsuchiya, & Koch, 2003; Knight, Cheng, Smith, Stein, & Helmstetter, 2004; Knight et al., 2006; Weike et al., 2007). SCRs are typically bimodal in time, but most current studies focus on the second interval response (SIR), which usually occurs just prior to UCS delivery (Ahs et al., 2010; Büchel, Dolan, Armony, & Friston, 1999; Knight, Cheng, et al., 2004; Knight et al., 2006). However, first interval responses (FIRs) are sometimes used when there are other stimuli like startle probes that may affect expression of the SIR (Weike et al., 2007). SCRs tend to habituate rapidly, and studies that include large numbers of trials tend to show differential SCRs only on early trials (Büchel et al., 1999; Knight, Cheng, et al., 2004). In addition, SCRs are susceptible to interference from attentional processes, so conditional SCR expression may not be apparent when attentionally demanding tasks are introduced (Carter et al., 2003).

Heart rate has also been commonly used as a measure of conditioning in both humans and laboratory animals (Headley & Weinberger, 2011; Hermans, Henckens, Roelofs, & Fernández, 2012; LeDoux, 2000). The most common pattern of heart rate changes in emotional paradigms is to show a decrease in heart rate in response to emotional or conditional stimuli (Headley & Weinberger, 2011; Hermans et al., 2012; Minati et al., 2009). However, others have shown both increases and decreases in heart rate in subjects during conditioning, and that different patterns of heart rate changes are

associated with different patterns of neural activity (Moratti, Keil, & Miller, 2006; Moratti & Keil, 2005).

In addition to SCRs, recent studies have begun to use changes in pupil diameter as a measure of autonomic arousal (Sterpenich et al., 2006). One study found that changes in pupil diameter evoked by emotional images correlated with changes in activity in the locus coeruleus, an area thought to modulate arousal (Sterpenich et al., 2006). Other studies have shown that positively and negatively valenced arousing images evoke increases in pupil diameter, independent of luminosity (Bradley, Miccoli, Escrig, & Lang, 2008; van Steenbergen, Band, & Hommel, 2011). Finally, some studies have shown that differential fear conditioning with simple (Reinhard & Lachnit, 2002) and compound (Reinhard, Lachnit, & König, 2006) visual stimuli evoke increases in pupil diameter. Interestingly, auditory CSs (Kluge et al., 2011) and unseen emotional faces/bodies (Tamietto et al., 2009) also evoke increases in pupil diameter, suggesting that this effect seems to be a general index of arousal, and not dependent upon visual perception. Using changes in pupil diameter is an attractive new method to measure changes in arousal during conditioning for two reasons. First, unlike SCRs, pupil responses are rapid, and conditioned pupil dilation can be seen as early as 2 s after CS onset (Kluge et al., 2011; Reinhard et al., 2006; Reinhard & Lachnit, 2002). Second, unlike fear potentiated startle, additional probes are not needed to assess learning.

1.2 Explicit measures of fear learning

Unlike non-human animals, humans can express conscious awareness of the CS-UCS contingencies during trace fear conditioning. There are two common methods used

to assess awareness in trace fear conditioning, post-experimental questionnaires (PEQs) and online UCS expectancy. Some researchers choose to administer a questionnaire after the experiment (Asli, Kulvedrøsten, Solbakken, Flaten, & Kulvedrosten, 2009; Carter, O'Doherty, Seymour, Koch, & Dolan, 2006; R. E. Clark & Squire, 1998; Weike et al., 2007). PEQs can be used to assess the subject's awareness of the CS-UCS contingencies, as well as the subject's evaluative ratings of the CSs, which can change after conditioning (Asli et al., 2009; Dawson, Rissling, Schell, & Wilcox, 2007; Wamsley & Antrobus, 2009). However, using a PEQ to assess awareness is not ideal because it may not accurately reflect the individuals explicit knowledge of the CS-UCS contingencies during the training (Lovibond & Shanks, 2002). For instance, if there are intervening tasks between the training and the PEQ, the individual may forget details about the CS-UCS relationship or timing (Lovibond & Shanks, 2002). This is especially crucial if the contingencies change during the intervening task like during extinction.

For this reason, online measures of UCS expectancy are often preferred over post-experimental measures. One common way to measure awareness during training is to have the individual continuously rate his or her expectation of receiving the UCS throughout the experiment (Balderston & Helmstetter, 2010; Cheng, Knight, Smith, & Helmstetter, 2006b; Cheng, Knight, Smith, Stein, & Helmstetter, 2003; Cheng, Richards, & Helmstetter, 2007a; Knight, Cheng, et al., 2004; Knight, Smith, Cheng, Stein, & Helmstetter, 2004; Knight, Smith, Stein, & Helmstetter, 1999; Schultz & Helmstetter, 2010a). This is typically done using a continuously updated visual analog scale, which the subject controls with a response device. This method has the added benefit of not only telling the researcher whether the individual expects to receive the stimulation, but also

when the individual expects to receive the stimulation (Balderston & Helmstetter, 2010; Cheng et al., 2006b, 2003, 2007a; Knight, Cheng, et al., 2004; Knight, Smith, et al., 2004; Knight et al., 1999; Schultz & Helmstetter, 2010a). This is especially important for trace conditioning where the subject may learn the timing of the CS and UCS as well as the contingency.

1.3 Brain processes that mediate delay and trace fear conditioning

The primary goal of neuroscientific research into the Pavlovian conditioning process is to understand the neural circuitry mediating the conditional fear response (Kim & Jung, 2006). The amygdala is commonly thought to be the "fear-center" of the brain (Ledoux, 2000; Öhman & Mineka, 2001); however, research with non-human animals shows that fear conditioning is dependent upon distributed plasticity in a wide network of structures (Helmstetter, Parsons, & Gafford, 2008; Parsons, Gafford, & Helmstetter, 2006). These results are largely consistent with functional neuroimaging results (Cheng et al., 2006a; Dunsmoor, Kragel, Martin, & Labar, 2013), suggesting that learning is mediated by changes at the network level, rather than the structure level. Understanding how specific structures contribute to the learning process is a matter of current interest.

1.3.1 Amygdala. Anatomical connectivity of the amygdala suggests that this structure is the primary associative node in the neural network mediating fear learning. The amygdala has reciprocal connections with the thalamus (Ottersen & Ben-Ari, 1979) and sensory cortical regions (Krettek & Price, 1977; Pessoa & Adolphs, 2010). The central nucleus projects to the hypothalamus and brainstem, and activation of the central nucleus leads to changes in hormone levels, increases in autonomic arousal, and species-specific fear behaviors (i.e. freezing; Kim & Jung, 2006).

As indicated by the anatomical connectivity, impaired amygdala functioning is associated with impaired fear learning. For instance lesions of the amygdala in rodents (Koo, Han, & Kim, 2004) and humans (Bechara et al., 1995) blocks fear expression. Blocking activity or plasticity in the amygdala impairs both delay and trace conditioning (Kwapis, Jarome, Schiff, & Helmstetter, 2011). Finally, blocking either protein degradation (Jarome, Werner, Kwapis, & Helmstetter, 2011) or synthesis (Parsons et al., 2006).

In humans, amygdala activity is associated with CR expression. For instance, skin conductance responses (SCRs) are correlated with blood oxygenation-level dependent (BOLD) responses in the amygdala during learning (Cheng et al., 2006a, 2007a; Knight, Nguyen, & Bandettini, 2005). Like delay conditioning, amygdala activity during trace conditioning seems to mediate CR expression. Carter et al. (2006) found that left amygdala activity was correlated with SCR magnitude during both delay and trace conditioning. Preliminary data from the Knight et al. (2004) study suggest that the amygdala is selectively engaged on delay and trace trials where the subject shows a conditional SCR. Similarly, data from the Büchel et al. (1999) study suggest that the amygdala is activated on early trials and deactivated on later trials, which is consistent with the observation that SCRs are expressed early in training and habituate rapidly after repeated presentations of the CS.

1.3.2 Sensory cortices. Fear conditioning in non-human animals induces plasticity in a distributed network of regions including sensory areas of the thalamus (Helmstetter et al., 2008). Functional neuroimaging studies show learning related changes in sensory cortical activity as well. Both Knight et al. (2004) and Büchel et al. (1999)

showed differential activity in modality-specific sensory cortical regions. These results suggest that humans also experience plasticity in regions of sensory cortex specific to the modality of the CS used, and have been seen in other fMRI studies of fear conditioning (Cheng et al., 2003). In a recent study, Dunsmoor et al. (Dunsmoor et al., 2013) exposed subjects to conditioning with

Some models of fear conditioning suggest that through learning the CS comes to activate an internal representation of the UCS (Mackintosh, 1983). Büchel and colleagues (1999) report greater activation of the dorsal ACC and anterior insula for the CS+ compared to the CS-. These findings are consistent with those of several delay fear fMRI studies and suggest that, delay and trace CSs evoke activity in regions of the brain important for the experience of aversive events like the anterior cingulate cortex and the insular cortex (Dunsmoor, Bandettini, & Knight, 2007; Knight et al., 2009; Phelps, Delgado, Nearing, & LeDoux, 2004). Interestingly, in the Knight et al. (2004) study, the dorsal ACC showed the largest BOLD response to the period just prior to the UCS (i.e. the delay CS+ and the trace interval), suggesting that ACC activity during fear conditioning is related to the anticipation of the UCS, not necessarily the CS itself.

Gamma oscillations in sensory regions may also be a marker for active processing of sensory stimuli, while coherent gamma oscillations across regions may represent the binding of sensory information into a single representation (Fell & Axmacher, 2011). For instance, attended stimuli tend to evoke increases in gamma power in sensory cortex, and these gamma oscillations may influence activity in downstream cortical areas (Bauer, Oostenveld, Peeters, & Fries, 2006; Bichot, Rossi, & Desimone, 2005; Fries, Reynolds, Rorie, & Desimone, 2001; Steinmetz, Roy, Fitzgerald, Hsiao, & Johnson, 2000). In recent

EEG study, researchers identified electrodes that responded to face presentations, then they measured gamma power from these electrodes while subjects attended to either faces or houses (Engell & McCarthy, 2010). They found increases in gamma power in these electrodes when subjects attended to faces, compared to when they attended to houses.

There are also several studies that suggest gamma oscillations play a role in long term memory formation. Several studies have shown that increases in gamma power during the encoding stage of declarative memory tasks are predictive of subsequent recall during testing (Gruber, Tsivilis, Montaldi, & Müller, 2004; Osipova et al., 2006; Sederberg et al., 2007; Sederberg, Kahana, Howard, Donner, & Madsen, 2003). In one recent contextual cueing study, subjects showed increases in frontal gamma power during the initial learning, but not during subsequent cueing trials after the learning had taken place (Chaumon, Schwartz, & Tallon-Baudry, 2009). Popescu and colleagues have also shown that gamma power is related to memory during associative tasks as well (Popescu, Popa, & Paré, 2009). They showed that during appetitive conditioning, coherent oscillations between the amygdala and the striatum were correlated with conditioned responding. In addition, others have shown using electroencephalography (EEG) that there are broad increases in gamma phase coherence following fear conditioning (Kaiser, Ripper, Birbaumer, & Lutzenberger, 2003). Finally, in addition to memory formation, gamma oscillations seem to play an important role in fear processing in the amygdala (Sato et al., 2011; Sato, Kochiyama, Uono, & Yoshikawa, 2010).

Taken together, these results suggest that the amygdala is the central associative node in the fear learning network (See Figure 2). Representations of the CS and UCS converge on the amygdala. Through this convergence the CS comes to activate the central

nucleus of the amygdala, which ultimately leads to CR expression. Although this model is sufficient to describe delay conditioning, it is not sufficient to describe trace conditioning. This is because trace conditioning requires the subjects to maintain a representation of the CS during the empty trace interval, meaning that there is no opportunity for CS and UCS representations to directly overlap in the amygdala.

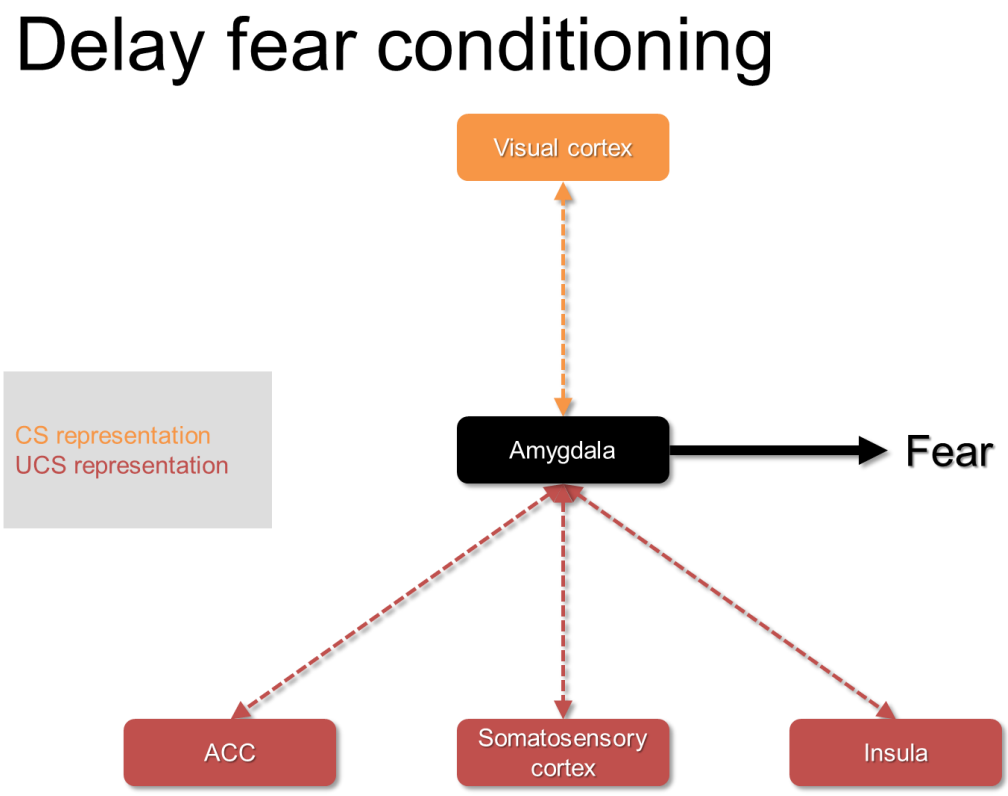

Figure 2. Schematic representation of the neural substrates of delay fear conditioning. CS and UCS representations converge on the amygdala, which initiates the conditioned fear response.

1.4 The role of awareness in CR expression during delay and trace conditioning

In the previous sections I described a number of ways to measure what subjects learn during fear conditioning. These can roughly be divided into two categories, those that reflect the subject's explicit awareness of the CS-UCS contingencies and those that

reflect implicit knowledge of the CS-UCS contingencies, which are outside of the subject's direct conscious control (Lovibond & Shanks, 2002). Because the CS and UCS overlap during delay conditioning, it is possible to dissociate implicit and explicit responding. For instance, I showed that delay conditioning affects performance on a subsequent reacquisition test, even though subjects' ability to explicitly learn the contingencies was blocked with backward masking (Balderston & Helmstetter, 2010).

However during trace conditioning, CR expression seems to be dependent on an individual's ability to explicitly learn the CS-UCS contingencies (Carter et al., 2003; Knight et al., 2006; Weike et al., 2007). In a typical study, Knight and colleagues differentially conditioned subjects to fear tones that were presented slightly above or slightly below the subjects' perception threshold. When the tone co-terminated with the 100 dB white noise UCS, subjects showed differential SCRs on both perceived and unperceived trials; however, when there was a stimulus free period separating the tone and the white noise, subjects only showed differential SCRs on perceived trials.

Taken together, these results suggest that an active representation of the CS must be present during the presentation of the UCS. During delay conditioning, the CS is actively being processed by sensory regions of the brain, some of which operate outside the realm of conscious awareness (Liddell et al., 2005; Morris, DeGelder, Weiskrantz, Dolan, & de Gelder, 2001; Noguchi & Kakigi, 2005; Öhman, Morris, & Dolan, 1999). It is possible that this processing is what is associated with the UCS, even when awareness is blocked. In contrast during trace conditioning, the CS is no longer being actively processed by sensory regions of the brain. Therefore, awareness is needed to bridge the gap between the CS and the UCS, and the active maintenance of the CS at the time of the

UCS is what becomes associated with the UCS. Understanding how the brain contributes to this process may help to explain the role of conscious perception in emotional learning.

1.5 Brain processes that specifically mediate trace fear conditioning

In the basic model of laboratory fear conditioning sensory input corresponding to a CS representation converges on the amygdala with sensory input corresponding to the UCS (Kim & Jung, 2006). However, as with the functional neuroimaging studies, work with laboratory animals suggests that additional brain regions are necessary for trace fear conditioning. For instance, interfering with activity in either the hippocampus (Beylin et al., 2001) or the prefrontal cortex (Gilmartin & Helmstetter, 2010) interferes with trace but not delay conditioning. Thus it is known that these structures are necessary for trace fear conditioning. However, the specific role that each region plays is still unclear.

1.5.1 Prefrontal cortex. One possible explanation is that these structures bridge the gap between the CS and the UCS during trace fear conditioning. If this is the case, then there should be persistent neural activity in these regions during the trace interval. Recording from single units in rats, Gilmartin and McEchron have shown this to be the case for the prefrontal cortex (Gilmartin & McEchron, 2005a), but not the hippocampus (Gilmartin & McEchron, 2005b). Consistent with a bridging role, in a recent paper from our lab Dr. Gilmartin also showed with optogenetics that interfering with prefrontal activity during the trace interval impairs trace fear conditioning (Gilmartin, Miyawaki, Helmstetter, & Diba, 2013).

In functional neuroimaging studies, maintaining the CS during the trace interval seems to engage working memory processes (Baddeley, 1992; Bledowski & Kaiser, 2010; Courtney, Petit, Maisog, Ungerleider, & Haxby, 1998). Knight and colleagues

(2004) observed bilateral activation of the middle frontal gyrus and activation of the right inferior parietal lobule. Büchel and colleagues (1999) observed similar activations in the dorsolateral prefrontal cortex. Carter et al. (2006) found that activity in the middle frontal gyrus was correlated with UCS expectancy on delay and trace trials, and activity in this region also predicted performance on the PEQ. The fact that they observed a correlation between contingency awareness and middle frontal gyrus activity even with delay conditioning is interesting, and may be due to the fact that they used partial reinforcement. Like trace conditioning learning with partial reinforcement is slower (Gottlieb, 2004; Svartdal, 2003), and requires additional cognitive resources.

1.5.2 Hippocampus. Although necessary for trace fear conditioning, the hippocampus does not appear to be playing a bridging role. Another possibility is that the hippocampus may be coordinating activity of other regions during the trace interval (Battaglia, Benchenane, Sirota, Pennartz, & Wiener, 2011). Functional neuroimaging studies tend to find hippocampal activity on early but not later trials (Büchel et al., 1999; Knight, Cheng, et al., 2004), and hippocampal activity is greater in individuals who time the presentation of the UCS (Knight, Cheng, et al., 2004).

The hippocampus is known to have a strong rhythm in the theta frequency band (Buzsáki & Moser, 2013), this theta rhythm has been shown to be important in eyeblink conditioning (Hoffmann & Berry, 2009; Seager, Johnson, Chabot, Asaka, & Berry, 2002), and humans show theta oscillations in the hippocampus during spatial navigation (Kaplan et al., 2012). In addition, at least one study has shown that local field potentials in the hippocampus and prefrontal cortex are coherent in the theta frequency band at decision points in a y-maze task (Benchenane et al., 2010), suggesting that hippocampal theta is

coordinating the activity of the prefrontal cortex during decision making.

1.6 Purpose

Trace conditioning requires the subject to maintain a representation of the CS during the trace interval. In humans this requires conscious awareness of the stimulus contingencies (Knight et al., 2006). Trace conditioning also requires the functioning of the hippocampus and the prefrontal cortex (Bangasser, Waxler, Santollo, & Shors, 2006; Gilmartin et al., 2013). Although recent research suggests that the prefronal cortex may play a bridging role during the trace interval (Gilmartin et al., 2013), the role of the hippocampus in trace conditioning is not entirely clear (Gilmartin & McEchron, 2005b). I hypothesize that the hippocampus coordinates the activity of a distributed network of cortical regions in order to maintain a representation of the CS during the trace interval (See Figure 3).

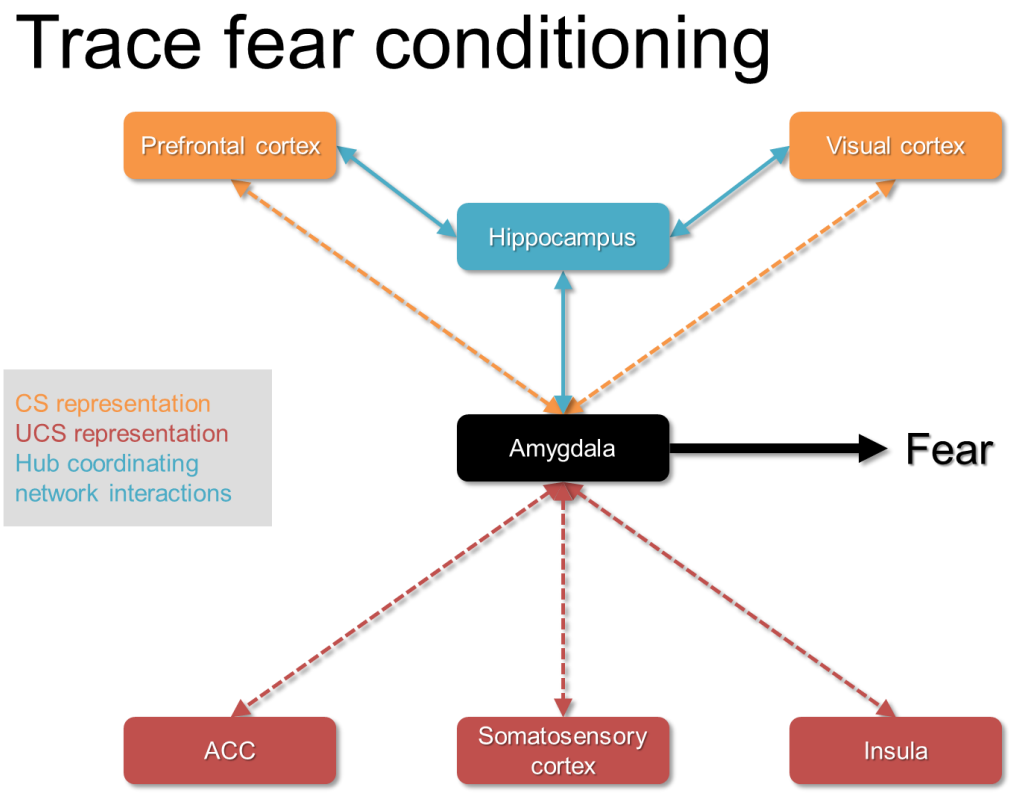

Figure 3. Schematic representation of the neural substrates of trace conditioning. As with delay fear conditioning, information about the CS and UCS must converge on the amygdala. Unlike delay conditioning, additional input from the hippocampus and prefrontal cortex is necessary. I hypothesize that the hippocampus coordinates the activity of the prefrontal and visual cortices to maintain the CS during the trace interval.

The previous fMRI studies have two major drawbacks related to the timecourse of the BOLD response (Carter et al., 2003; Knight et al., 2006; Weike et al., 2007). First, because the BOLD response resolves at such a slow rate (on the order of seconds) it is difficult show timing differences in activated regions using fMRI. Second, because it is only possible to collect a few data points during the trace interval, it is difficult to correlate activity across regions during specific intervals. Given that coherent patterns of activity can indicate communication across regions (Fell & Axmacher, 2011); it is difficult to identify patterns of communication across activated regions using fMRI. One

way to address these drawbacks is to record neural activity during the trace interval using magnetoencephalography (MEG). Because MEG allows the user to directly record brain activity at high temporal resolutions, it is possible to precisely determine the timing of activations. Also, because MEG is collected at high sampling rates (~2 kHz) there are enough data points to identify common patterns of neural activity, indicative of neural communication.

The purpose of this experiment was to use MEG to investigate the neural mechanisms that might maintain a representation of the CS during the trace interval. I trained subjects with both delay and trace conditioning using faces and houses as CSs and an aversive electrical stimulation as the UCS. Because of the precise temporal resolution of MEG, it is possible to asses multiple measures of neural activity during a given window of time. For instance, it is possible to record precisely timed evoked responses, increases in power within specific frequency bands, as well as coherent oscillations within specific frequency bands across neural regions. The goal is to determine whether there are differences between delay and trace conditioning on any of these measures.

1.7 Hypotheses

1.7.1 Implicit measures of learning. In order to demonstrate evidence of learning, I included several physiological measures. During the conditioning trials I recorded heart rate and pupil dilation. Subjects should show significantly larger increases in pupil diameter during the CS+ presentations than during the CS- presentations, indicating a heightened state of arousal (Reinhard et al., 2006; Reinhard & Lachnit, 2002). In addition, subjects should show conditioned bradycardia (Headley & Weinberger, 2011; Hermans et al., 2012). However, because there is no manipulation of

awareness, there should be no differences between delay and trace conditioning on either of these measures.

1.7.2 Explicit measures of learning. In this experiment I recorded UCS expectancy during the conditioning trials, as an indication of the subjects' explicit knowledge of the stimulus contingencies. Because it is quite easy to learn differential conditioning, subjects should rapidly learn the contingencies, and show that they expect the shock more on CS+ trials than on CS- trials for both delay and trace conditioning. In addition to the UCS expectancy measure, I also gave subjects a post experimental questionnaire, where I asked them to rate the pictures on arousal and valence scales. Similar to previous work with evaluative conditioning, subjects should rate the CS+ as more arousing and negative than the CS- for both delay and trace conditioning (Tabbert et al., 2010).

1.7.3 Recordings. Based on the previous work with fMRI, I should expect to see differential evoked responses for both delay and trace conditioning in regions like the amygdala, visual cortex, and insula. I also expect to see differential evoked responses specifically for trace conditioning in the hippocampus and prefrontal cortex. Previous work has suggested that local gamma oscillations may play a role in the maintenance of object representations (Bertrand & Tallon-Baudry, 2000). Given the hypothesis that the CS is maintained by different mechanisms during the trace interval, I should expect to see gamma oscillations in different regions for delay and trace conditioning. For delay conditioning, I expect to see gamma oscillations in visual regions. For trace conditioning, I expect to see gamma oscillations in frontal regions. Finally, previous work suggests that hippocampal theta oscillations might be important for coordinating the activity in task

specific cortical regions. Accordingly, I expect to see coherent oscillations between the hippocampus and prefrontal cortex in the theta frequency band for trace conditioning.

2 Method

2.1 Participants

Fifteen neurologically healthy adults participated in this study. Six were female. Subjects were college-aged (M = 24; SD = 2.3) and recruited from the community. Subjects were paid 80 euros for their participation. All procedures were approved by the official ethical committee of INSERM.

2.2 Procedure

Subjects were brought into the MEG suite, and given a copy of the consent form. After completing the consent form, the subjects were given a hospital gown to change into, and escorted to the prep area, where I began prepping them for the MEG acquisition.

2.2.1 Setup First I attached electrodes to monitor the subject's physiological measures and to administer the stimulation (See Figure 4). Next I setup the head position monitoring system. I attached four head position indicator (HPI) coils to the subject, one above each eye and one behind each ear. Next I identified several fiducial points (nasion, and left and right tragi), as well as the position of the HPI coils. This allowed us to align the subject's head relative to the HPI coils, which were used to track the position of the subject's head in the MEG system. Finally, I identified 50-100 points on the subject's scalp to further refine the alignment between the fiducial points and the HPI coils.

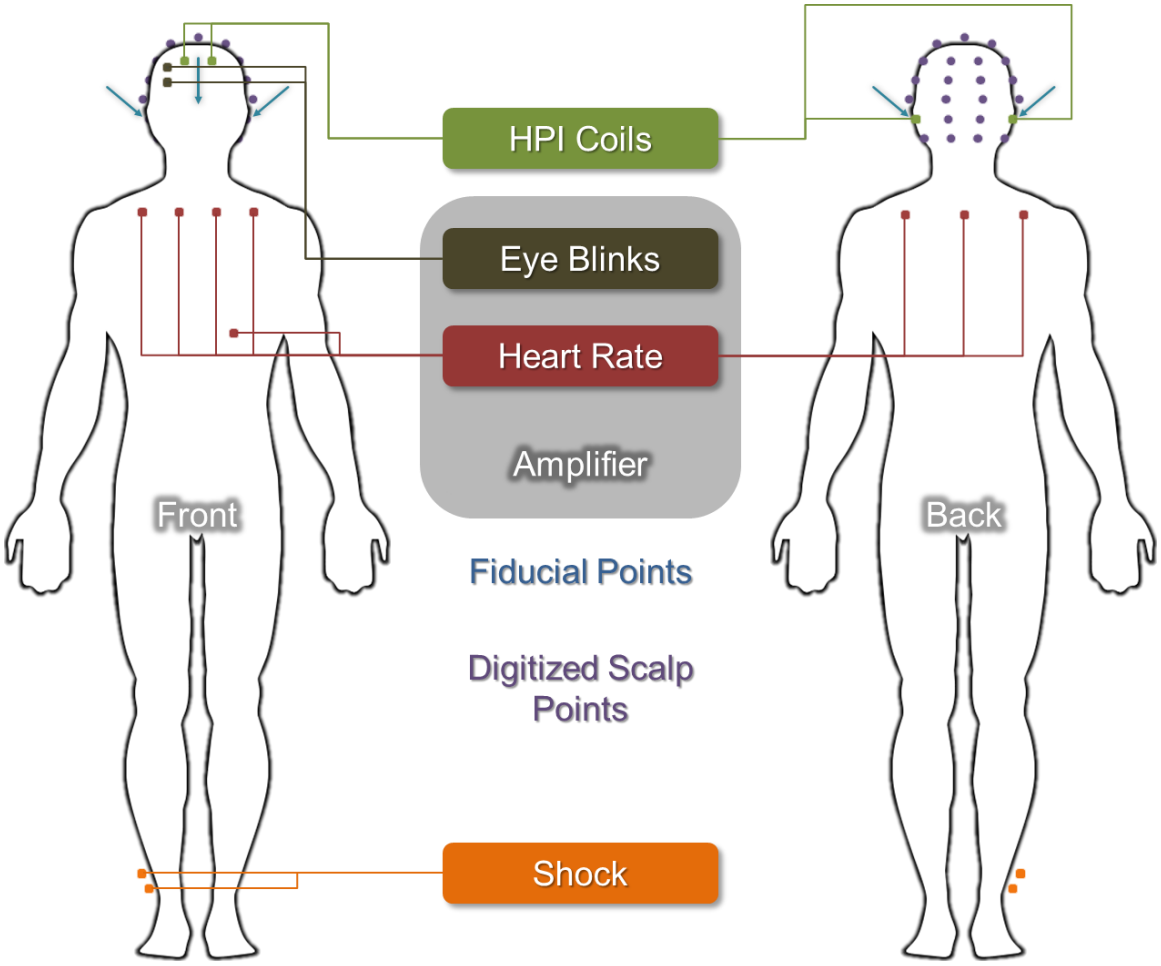

Figure 4. Illustration showing the location of each of the sensors and fiducial points described in the text. Dots with attached lines correspond to the labeled sensors and leads. Blue arrows represent the fiducial points used to register the MEG recordings with the MRI anatomical volume. Purple points represent digitized scalp points used to further refine the MEG-MRI coregistration.

After I attached the necessary electrodes and sensors, I escorted the subject to the MEG system and connected the electrodes and sensors to the appropriate interface. I plugged the disposable electrode leads and HPI coils into the MEG system. Next I raised the chair so that the subject's head is touching the top of the MEG helmet, and positioned the screen so that the projected image was in focus. Once the subject was positioned, I adjusted the camera for the eye tracking unit, and calibrated the eye tracker. Once the setup was completed, I instructed the subject on the proper use of the dial, and set the

level of stimulation that the individual would receive during the experiment.

2.2.2 Conditioning (See Figure 5)**.** During the conditioning session I presented six blocks of differential delay and trace conditioning. During each block, subjects saw four images, two faces and two houses. One face and one scene was paired with a shock, while the other face and house was presented unpaired. On half of the blocks faces served as delay CSs and houses served as trace CSs, while on the other half of the blocks house served as delay CSs and faces served as trace CSs. On delay trials, images were presented for 2.6 seconds, and the shock was presented during the final 100 ms of the delay CS+ (See Figure 6). On trace trials, images were presented for 500 ms and the shock was presented on the trace CS+ trials after a 2 second stimulus free interval. There were a total of 40 training trials, 10 trials of each type (Delay +/-; Trace +/-) within a given training block, and trials were separated by a variable 6 s intertrial interval. In addition, four 10 second probe trials were presented at the end of each training block. Block and trial order was counterbalanced across subjects. Stimuli were chosen randomly for each subject, and novel stimuli were used for each training block.

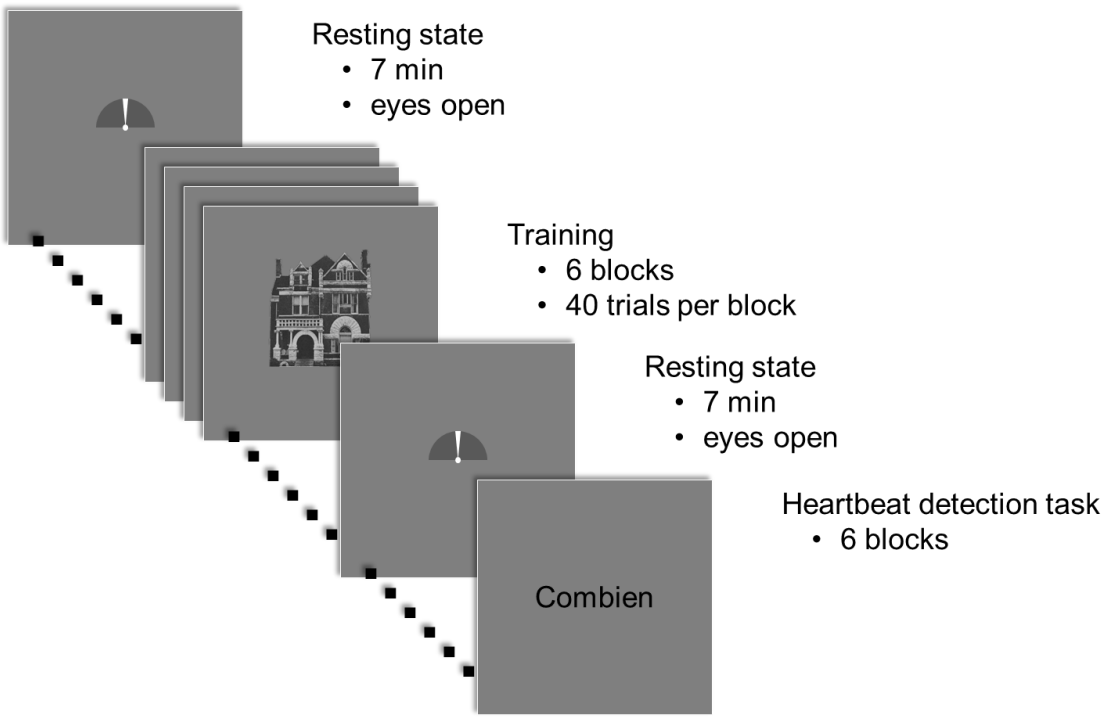

Figure 5. Schematic representing the sequence of scans in the experiment. There were 6 blocks of conditioning. There were resting scans before and after conditioning. The session ended with 6 blocks of a heartbeat detection task.

To minimize habituation to the UCS, the subjects were asked to provide a subjective rating of the UCS at the end of each conditioning block. If this rating was lower than an 8, the shock was recalibrated so that the subject continued to rate it as a 10.

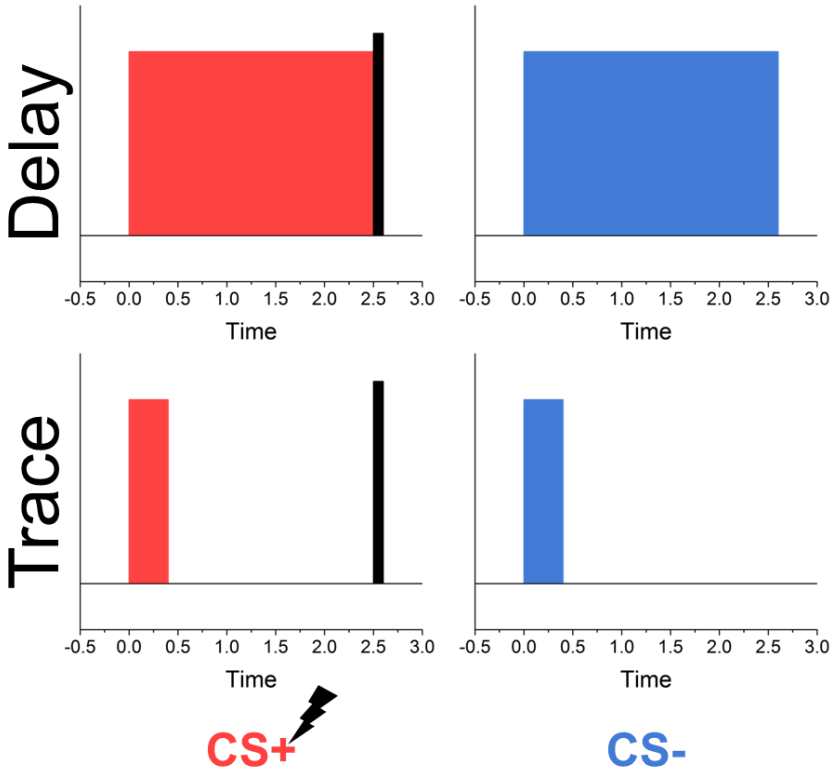

Figure 6. Schematics of the 4 trial types in the experiment. Delay stimuli were presented for 2.6 s. Trace stimuli were presented for 500 ms. The 100 ms shock was presented 2.5 s after the onset of the CS+ on all CS+ trials.

2.2.3 Resting. Resting state recordings were made before and after the conditioning session. Each of these lasted 7 minutes, and participants were instructed to sit comfortably, and focus their eyes on the fixation point at the center of the screen.

2.3 Stimuli

Images of faces and houses were chosen as CSs. For faces, I used images of males and females with neutral expressions, and forward facing gaze (See Figure 7). For houses, I used images of typical houses, centered with a grey background. I collected a bank of both types of images, and resizing them to 250 x 284 px. I then converted them to black and white, and equated them for contrast and luminance using custom matlab

scripts. Next I had an independent group of subjects rate the images for arousal and valence. I then selected the images from the larger bank so that faces and houses would be closely equated for arousal and valence.

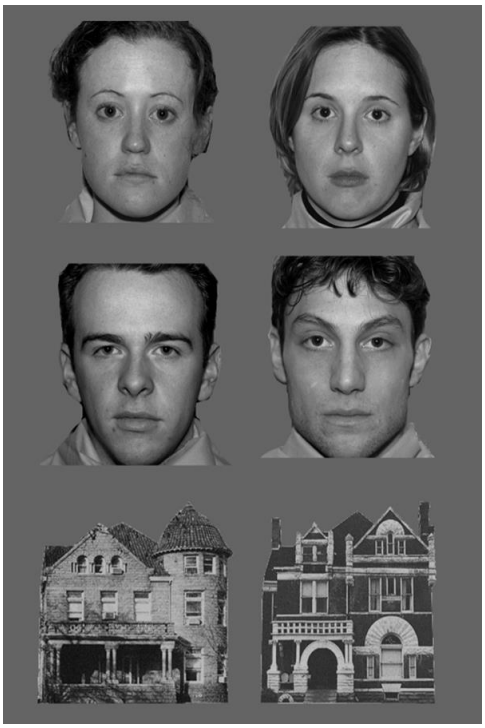

Figure 7. Example stimuli used in the experiment. Both male and female faces were used, and counterbalanced across runs.

2.4 Shock

On each of the CS+ trials, the subjects received a 100 ms presentation of an electrical stimulation, administered to the skin above the right tibial nerve, over the right medial malleolus (Balderston & Helmstetter, 2010). The stimulation was presented as a train of 2ms bursts using an AC source (Digitimer model DS7A). Prior to the experiment I set the level of the stimulation by administering several presentations and having the subject rate the intensity of the presentations on a scale from 0 (not perceived) to 10 (uncomfortable but not painful). I increased the intensity of the stimulation until I reached a level that the subject rated as a level 10. Stimulations during the experiment were

administered at the subject's level 10, and adjusted between runs as needed.

2.5 Shock expectancy

Each trial began with a 2 second presentation of the rating scale/fixation point. This was presented centrally, and remained on the screen until the end of the trial. During each trial, the subjects rated their expectation of receiving the electrical stimulation (Balderston & Helmstetter, 2010). They controlled a cursor, which moved around the fixation point using a button box. The subjects place the cursor all the way to the right if they were absolutely sure that they would receive the stimulation. The subjects placed the cursor all the way to the left if they were absolutely sure that they would not receive the stimulation.

2.6 Heartbeat detection task

After the conditioning session, subjects were given 6 blocks of a heartbeat detection task (Pollatos, Kirsch, & Schandry, 2005). During the task, subjects were asked to count the number of heartbeats they could perceive during a given period of time, ranging between 30 and 120 seconds. Subjects were instructed not to take their own pulse, or position themselves so that they could feel their heartbeats artificially (Pollatos et al., 2005). After the experiment I compared the subjects' estimates to the actual number of heartbeats within each block, and created a perception score according to the following formula. High perception scores indicate higher accuracy.

$$\textit{Perception score} = (\Sigma(1 - (\textit{recorded} - \textit{counted}) / \textit{recorded}) / 6)$$

2.7 Post-experimental questionnaire

Following the experiment, subjects were asked to rate the arousal and valence of the images (Lang, Bradley, & Cuthbert, 2008). Subjects responded to each question using a nine-point likert type scale anchored with appropriate descriptors (arousal: excited-

calm; valence happy-unhappy). Pictures were presented in a random order on a computer in a quiet room near the MRI suite. Subjects were given as much time as needed to complete the questionnaire. In addition, subjects also completed the French version of the state-trait anxiety questionnaire.

2.8 Physiological monitoring

I recorded heart rate, eye blinks, and SCRs throughout the conditioning session via disposable electrodes using the EEG amp built in to the MEG system. As with the MEG recordings, these measures were sampled at 2 kHz.

2.9 Pupil dilation

I recorded eye movements and pupil diameter at 1 kHz using an eye tracking unit (SR Research EyeLink 1000) integrated with the MEG system. The signals from the EyeLink unit were passed through a digital to analog converter, which was connected to the MEG system. These signals were then recorded by the acquisition system along with the neural recordings. I used the built-in eyelink detection software to identify blinks and saccades. These markers were then transferred to the neural recordings using custom software.

2.10 MEG acquisition

I acquired the recordings at 2 KHz using the the Elekta-Neuromag TRIUX MEG, which has 306 sensors at 102 sites in its whole-head sensor array. Sensors at each site are grouped into triplets consisting of 2 orthogonal planar gradiometers and 1 planar magnetometer. Recording took place inside a magnetically-shielded room.

2.11 MEG preprocessing

I used source imaging to analyze the MEG recordings (See Figure 8). Raw data were initially processed using Elekta-Neuromag's MaxField software, which uses signal

source separation to attenuate signals from far-field sources (Taulu & Hari, 2009; Taulu, Kajola, & Simola, 2004). Runs were then aligned using the fiducials identified during setup. Next markers were placed in the recordings to record the timing of the following: stimulus onset, shock onset, button presses, heartbeats, eyeblinks, and saccades. Next, raw recordings were visually inspected for other artifacts, such as muscle movements and sensor steps. I then classified clean trials as those that were free of blinks, muscle movements, sensor steps, and saccades larger than 3 degrees of visual angle. For evoked responses I selected trials that were clean during the following peristimulus time window: -200 – 800 ms (87.6% of total trials). For the coherence analysis, I were specifically interested in trace interval activity, so I increased the time window of interest to: -200 – 2500 ms (70.6% of total trials). Only clean trials were used in the subsequent analyses.

I then imported the clean data into Brainstorm (Tadel, Baillet, Mosher, Pantazis, & Leahy, 2011), and aligned the recordings to the SPGR volume using the fiducial points and head points collected during the set up.

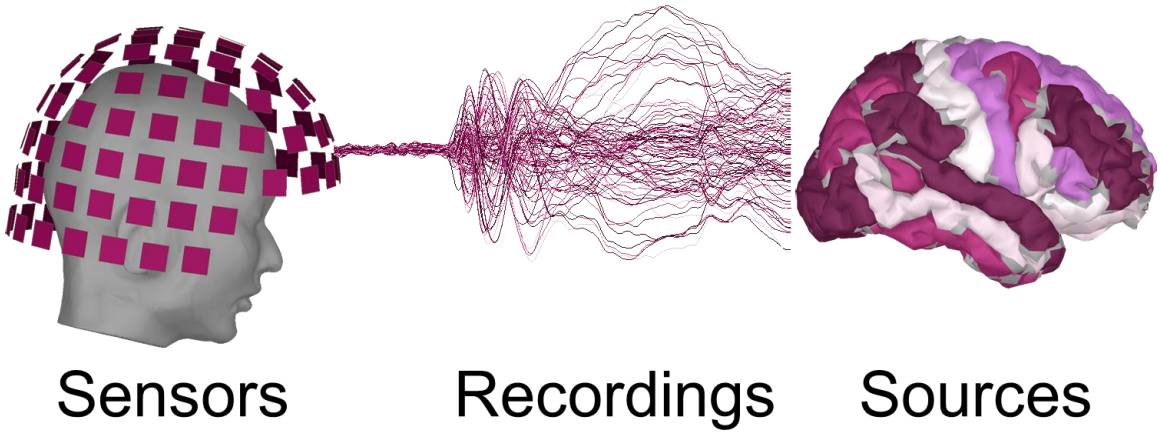

Figure 8. We recorded signals from 306 sensors in a whole-head MEG system. The figure on the left represents an example subject's position in the helmet. The middle figure represents the recordings averaged across all subjects and all trial types. We used source imaging to localize the neural generators of the MEG signal. We distributed current dipoles evenly across the cortex, then downsampled the cortical map to one consisting of 72 regions of interest.

Next I projected the recordings into source space. First I computed the forward model using an overlapping spheres approach, applying an elementary dipole current source normally oriented at each of the vertices of the cortical surface (Huang, Mosher, & Leahy, 1999). Next I estimated the noise covariance statistics, using the baseline period as input (Pascual-Marqui, 2002). Finally I computed the inverse model using the weighted minimum-norm estimate approach (Hämäläinen & Ilmoniemi, 1994), and estimate the amplitude for each of the 18,000 current dipoles distributed across the cortex, amygdala, and hippocampal surfaces.

For the evoked responses I lowpass filtered the source data at 30 Hz, converted these values to z-scores, and averaged the maps across trials. Next I projected the source maps for each subject on to the default anatomy and downsampled these maps to the Desikan-Killiany atlas (See Table 1; Desikan et al., 2006).

For the time-frequency decompositions I downsampled the source maps for each trial to the Desikan-Killiany atlas (Desikan et al., 2006). I then computed the time-frequency decompositions for each atlas region by convolving the signal with a complex morelet wavelet, with a carrier frequency of 1Hz and a time resolution of 3 s (Tallon-Baudry & Bertrand, 1999). I averaged the resulting time frequency maps across trials, and converted the values to Z-scores based on the variability in the baseline period. The resulting normalized time frequency maps were then used for group-level analyses.

For the coherence analysis downsampled the source maps for each trial to the Desikan-Killiany atlas (Desikan et al., 2006), computed the pairwise coherence between each atlas region for each trial at the following frequency bands: delta (2-4 Hz), theta (5-7 Hz), alpha (8-12 Hz), beta (15-29 Hz), low gamma (30-59 Hz), high gamma (60-90 Hz). I then averaged these coherence estimates across trials.

Table 1. Regions of the Desikan-Killiany atlas.

Frontal	Parietal	Temporal	Occipital
caudal anterior cingulate	inferior parietal	amygdala	cuneus
caudal middle frontal	isthmus cingulate	bank sts	fusiform
frontal pole	paracentral	entorhinal	lateral occipital
insula	postcentral	hippocampus	lingual
lateral orbitofrontal	posterior cingulate	inferior temporal	pericalcarine
medial orbitofrontal	precuneus	middle temporal	
parsopercularis	superior parietal	parahippocampal	
parsorbitalis	supramarginal	superior temporal	
parstriangularis		temporal pole	
precentral		transverse temporal	
rostral anterior cingulate			
rostral middle frontal			
superior frontal			

2.12 Permutation tests

To identify effects within the recordings I computed a series of paired sample t-tests, using the trial averages as input. This same basic procedure was used to analyze the evoked responses, the time-frequency decomposition maps, and the coherence maps. To correct for multiple comparisons I conducted a series of permutation tests. For each permutation I randomly shuffled the condition assignments of the individual trial data,

and then averaged across trials according to the new shuffled labels. Next I computed a paired sample t-test based on these trial averages. This procedure will allow us to estimate the true probability of type 1 error, given the actual number of comparisons in each of our data types. I then repeated these permutations several hundred times in order to obtain a distribution of type 1 errors. Once the permutation tests were conducted, I then used them to identify an alpha threshold in the original comparisons. For this I used a different method, appropriate for each of the data types.

2.12.1 Evoked responses. For our evoked responses I conducted a t-test at each time sample. Because evoked responses represent data collected across time, adjacent comparisons are not independent. Therefore I used a temporal clustering algorithm to cluster the data across time. First I apply an alpha threshold of 0.05 to our permutation p-maps. Then I identify temporal clusters within the resulting t-maps and sum the t-values across the temporal cluster. Next I collect the summed t-values and sort them according to size. I then identify the summed t-value at the 95^{th} percentile, and use that as the threshold. Finally, I apply this dual threshold to our original evoked maps. First I threshold with a timepoint alpha of 0.05, then I identify clusters with a summed t-value larger than our threshold. I computed 837 permutations collapsed across the delay and trace conditions. I pooled these permutations and used the resulting summed t-value (89.71) as my threshold.

2.12.2 Time-frequency decompositions. As with the evoked responses I computed t-tests at each sample of the time-frequency maps. Similar to the evoked responses, adjacent time samples in these maps are not independent. However, these maps also have a second, frequency, dimension that contains non-independent samples.

Therefore, when correcting for multiple comparisons with this data type I identified clusters that were contiguous across both the time and frequency dimensions. As before, the first step is to apply an alpha threshold of 0.05 to the permutation p-maps, and identify the clusters of connected samples within the thresholded t-maps. I categorized time-frequency clusters using an approach similar to the AFNI AlphaSim program (Cox, 1996). First I counted the number of samples in each cluster, then I sorted the clusters according to size. Next I identified the cluster size at the 95th percentile, and used that as the threshold. Finally, I applied this dual threshold to our original time-frequency maps. I computed 140 permutation tests with an alpha threshold of 0.05, and I identified a cluster size threshold of 590 connected samples.

2.12.3 Coherence. Like the evoked responses and the time-frequency decompositions, the coherence analysis required computing a large number of t-tests for each comparison. However, because the maps reflect coherence estimates between atlas regions, rather than a continuous set of time or frequency samples, a clustering algorithm is not appropriate. Therefore, I thresholded the coherence maps with an alpha of 0.05 and then sorted the resulting p-values by size and identified the p-value at the 95th percentile. I computed 1000 permutations for both the Delay CS+ > Delay CS- and the Trace CS+ > Trace CS- comparisons. For both delay and trace I identified a p-threshold of 0.025.

2.13 MRI acquisition

For this experiment I selected subjects who had previously participated in an MRI study through the Centre de neuro-imagerie de reserche (CENIR). High resolution spoiled gradient recalled (SPGR) images were collected as part of these previous studies using a 3T (Siemans VERIO 3T Magnetom) MRI scanner. These images were used to

create the surfaces needed to model the neural sources of the MEG signal.

2.14 MRI preprocessing

In order to model the sources of the MEG signal, I created 3d surfaces of each subject's skull, cortex, amygdala, and hippocampus, using their MRI volume. First I processed each subject's MRI volume using freesurfer (Fischl et al., 2002; Fischl, Salat, et al., 2004; Fischl, van der Kouwe, et al., 2004). Using freesurfer I generated 3d surfaces of the subject's cortex and skull, and 3d volumes of each subject's amygdala and hippocampus. The 3d volumes were converted to surfaces, and all surfaces were imported into the brainstorm database. In addition to the surfaces, I also imported the volumetric MRI data into Brainstorm. This was used to align the surfaces to the recordings, based on the fiducial points identified during the set up.

3 Results

3.1 Individual differences

Below is a summary of the results from several behavioral measures hypothesized to affect learning (See Figure 9). Individual differences in these scores will later be used to predict conditional responding.

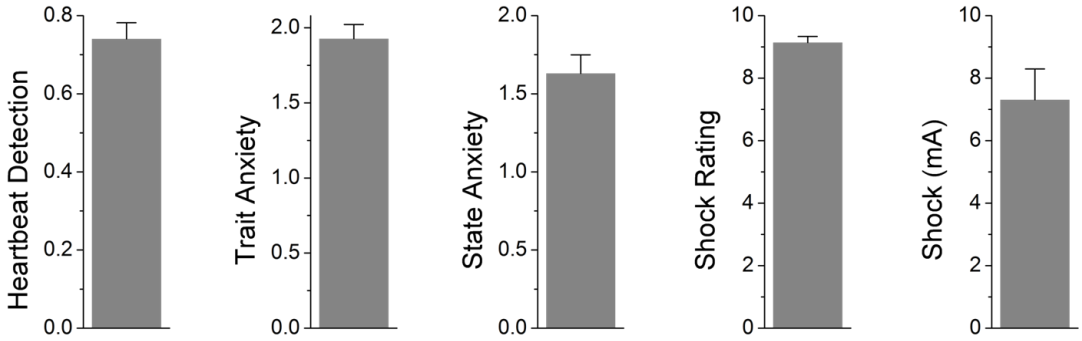

Figure 9. These graphs represent the mean ± SEM on several measures of individual differences.

3.1.1 Shock ratings. At the beginning of the experiment, and prior to each run I asked the subjects to rate the intensity of the UCS on a scale from 0 to 10. The average ratings for UCS intensity can be found in Figure 9. Because the shock intensity is calibrated at the beginning of the experiment to the subject's level 10, these values reflect some degree of habituation ($F(6,84) = 4.58$; $p < 0.001$). Figure 10 shows that the majority of this habituation occurs during the first training block, and is counteracted by the recalibrations done after each run ($t(14) = 2.54$; $p = 0.024$)

3.1.2 Shock intensity. Prior to the experiment I calibrate the shock intensity so that it is at a level that the subjects rate as uncomfortable but not painful, which corresponds to a level 10 on the 0 to 10 scale that I instruct them to use. The average UCS intensity across the entire session can be found in Figure 10. However, as mentioned in the previous section, subjects tend to show habituation to the UCS. Because I recalibrate the shock as needed after each run, there is an overall increase in the intensity of the shock ($F(6,84) = 6.69$; $p < 0.001$), which is largest when going from the first run to the second ($t(14) = 2.86$; $p = 0.012$).

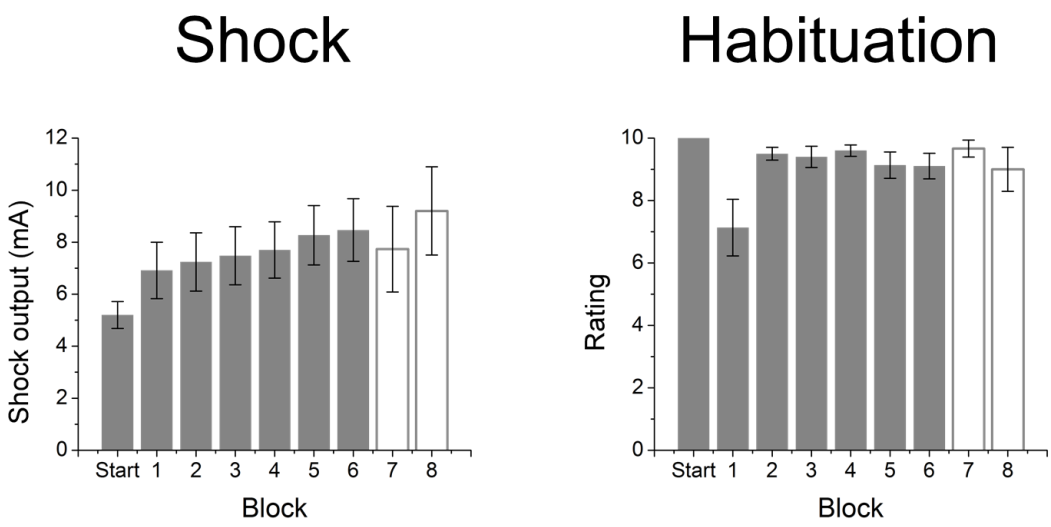

Figure 10. Graphs represent the shock intensity and ratings measured across conditioning blocks. Bars represent mean ± SEM. White bars are optional runs that were only undertaken if there was an issue with one of the training runs.

3.1.3 Heartbeat detection. After the conditioning runs, subjects performed a heartbeat detection task. The average perception score for this task can be found in Figure 9 (Pollatos et al., 2005).

3.1.4 State/trait anxiety. After being removed from the MEG suite, subjects completed a post-experimental questionnaire. The average scores for these scales can be found in Figure 9.

3.2 Behavioral measures of learning

3.2.1 UCS expectancy. As an explicit measure of learning, I asked the subjects to indicate the degree to which they expected the UCS. To determine how our training protocol affected explicit UCS expectancy, I performed a CS x picture content (face vs. house) x training protocol (trace vs. delay) repeated-measures ANOVA, which is summarized in Figure 11. Unsurprisingly, I found that subjects expected the shock more on CS+ trials than on CS- trials ($F(1,14) = 1804.94$; $p < 0.001$). In addition to the main

effect for CS, there was also a CS x picture content interaction ($F(1,14) = 5.67$; $p = 0.032$), which seemed to be driving a main effect for picture content ($F(1,14) = 6.47$; $p = 0.023$).

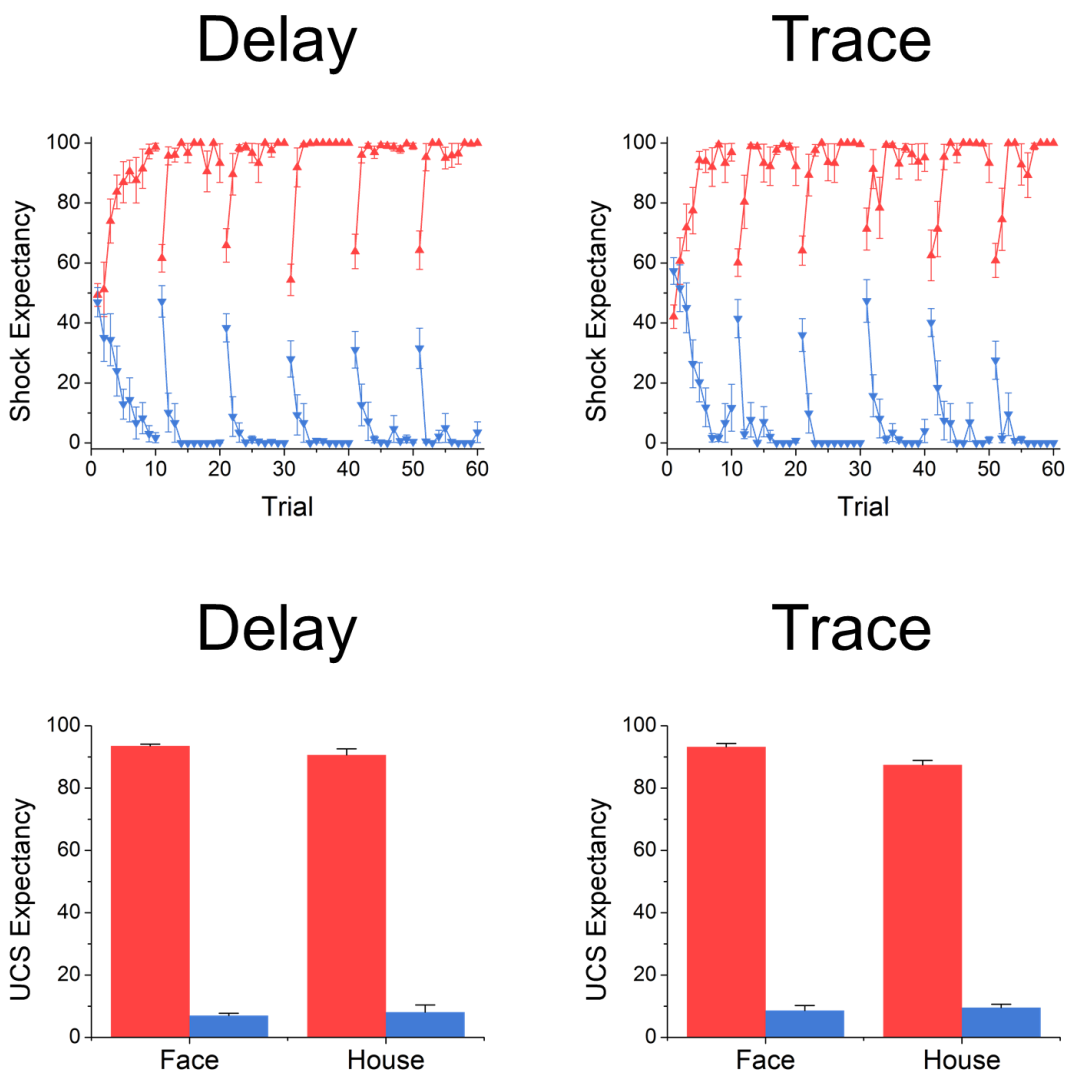

Figure 11. UCS expectancy performance across trials (top) and overall (bottom) for the conditioning session. Bars and symbols represent mean ± SEM. Red = CS+. Blue = CS-.

I followed up this interaction by performing post hoc picture content x training protocol (trace vs. delay) repeated-measures ANOVAs for the CS+ and the CS-. For the CS+ I found that subjects expected the shock more for faces than for houses ($F(1,14) =$

14.65; $p = 0.002$), but there were no effects for the CS-. Although significant, this effect is marginal when compared to the conditioning effect. Also, there were some differences in reaction time as well (See below), which may have played a part in the interaction.

3.2.2 Reaction time. In addition to measuring the degree to which subjects expected the shock, I also measured their latency to respond using the button box. To determine whether there were any differences in reaction time across conditions, I performed a CS x picture content (face vs. house) x training protocol (trace vs. delay) repeated-measures ANOVA, which is summarized in Figure 12. Overall, I found that subjects were faster for the CS- than the CS+ ($F(1,14) = 14.76$; $p = 0.002$). I also found a picture content by training protocol interaction ($F(1,14) = 7.03$; $p = 0.02$), which seemed to be driving a main effect for picture content ($F(1,14) = 52.68$; $p < 0.001$).

I followed up this interaction by performing *post hoc* CS x picture content repeated-measures ANOVAs for delay and trace conditioning. For both delay and trace, I see a main effect for CS, as described above. In addition, subjects responded more rapidly to faces than to houses during trace fear conditioning ($F(1,14) = 9$; $p = 0.01$).

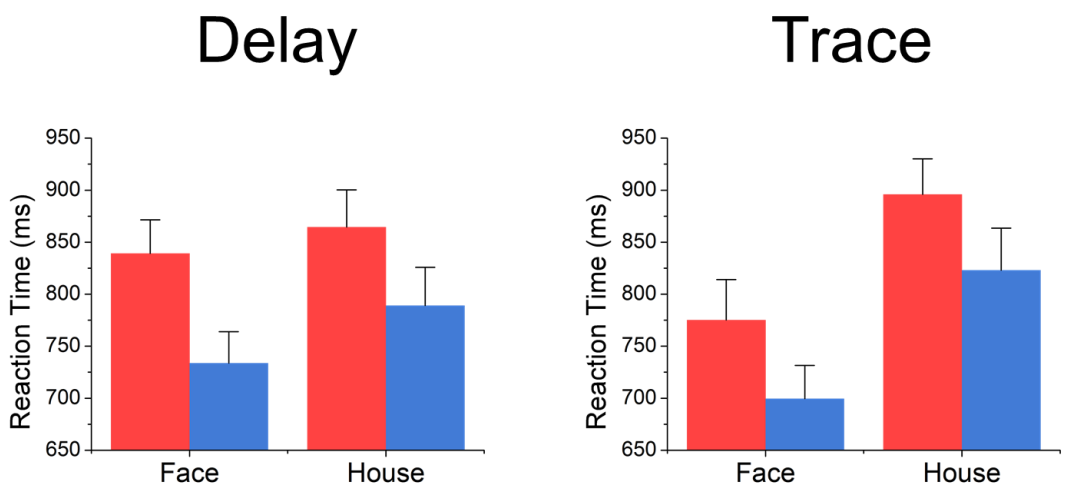

Figure 12. Latency to press a button to adjust the UCS expectancy scale during the conditioning session. Bars represent mean ± SEM. Red = CS+. Blue = CS-.

3.2.3 Pupil dilation. As an implicit measure of learning I included pupil dilation. To determine how our training protocol affected pupil dilation, I performed a CS x picture content (face vs. house) x training protocol (trace vs. delay) repeated-measures ANOVA, which is summarized in Figure 13. As you can see, subjects showed an increase in pupil diameter to the CS+ compared to the CS- ($F(1,14) = 21.25$; $p = 0.0001$). Subjects also showed larger pupils during trace trials than during delay trials ($F(1,14) = 21.99$; $p = 0.003$), however it is difficult to attribute this difference to the training protocol, because the data included in this ANOVA were recorded during the trace interval. Accordingly, there were viewing differences across the conditions.

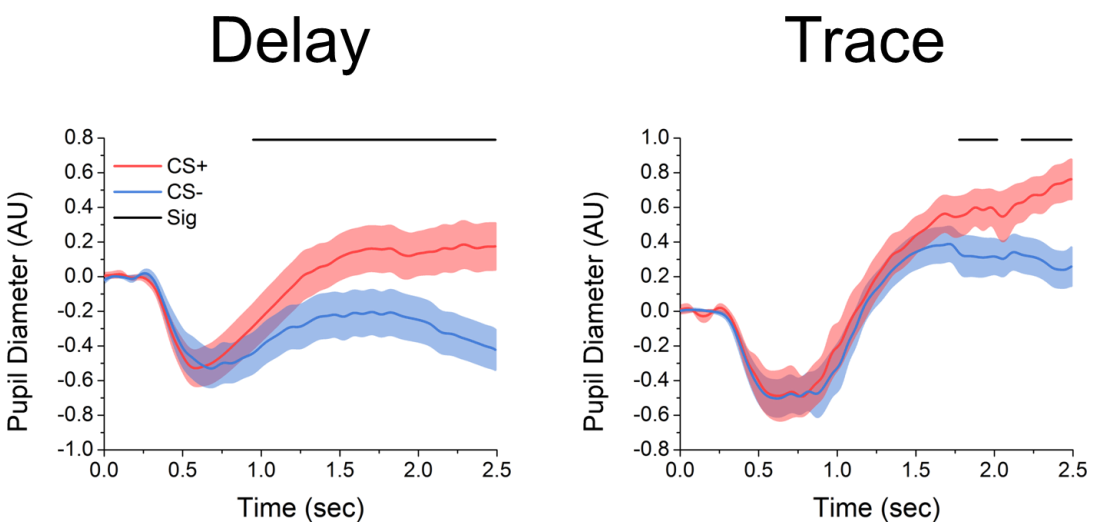

Figure 13. Pupil dilation during the conditioning session. Lines represent mean ± SEM. Red = CS+. Blue = CS-. Black lines represent significant results from paired sample t-tests conducted at each timepoint.

3.2.4 Heart rate. I also measured subjects' heart rate during the post-CS period. I recorded the interbeat interval between the two beats preceding the CS, and used that as a baseline. Next I recorded the interbeat interval between the following pairs of heartbeats: 1-2, 2-3, 3-4, 4-5. I then performed CS x picture content (face vs. house) x interbeat interval ANOVAs for delay and trace conditioning. For both delay and trace I find a main effect for heartbeat (Delay: $F(3,42) = 1140.35$; $p < 0.0001$; Trace: $F(3,42) = 1185.52$; $p < 0.0001$), which was characterized by an initial increase in interbeat interval, followed by a decrease across all conditions (See Figure 14).

For trace conditioning I also found a significant CS x picture content x heartbeat interaction ($F(3,42) = 3.64$; $p = 0.02$). To characterize this I divided the post CS interbeat intervals in to early (1-2, 2-3) and late (3-4, 4-5) bins. I then performed CS x picture content (face vs. house) ANOVAs for the early and late time bins. For the early time bin I found a significant interaction ($F(1,14) = 7.42$; $p = 0.017$), which I followed up on using

post hoc t-tests. There was no conditioning effect for faces ($t(14) = 0.76$; $p = 0.45$). In contrast, houses that predicted the shock lead to a shorter interbeat interval than houses that predicted no shock ($t(14) = 3.16$; $p = 0.007$). For the late time bin, I found that both faces and houses that predict the shock lead to longer interbeat intervals than faces and houses that predict no shock ($F(1,14) = 5.97$; $p = 0.029$).

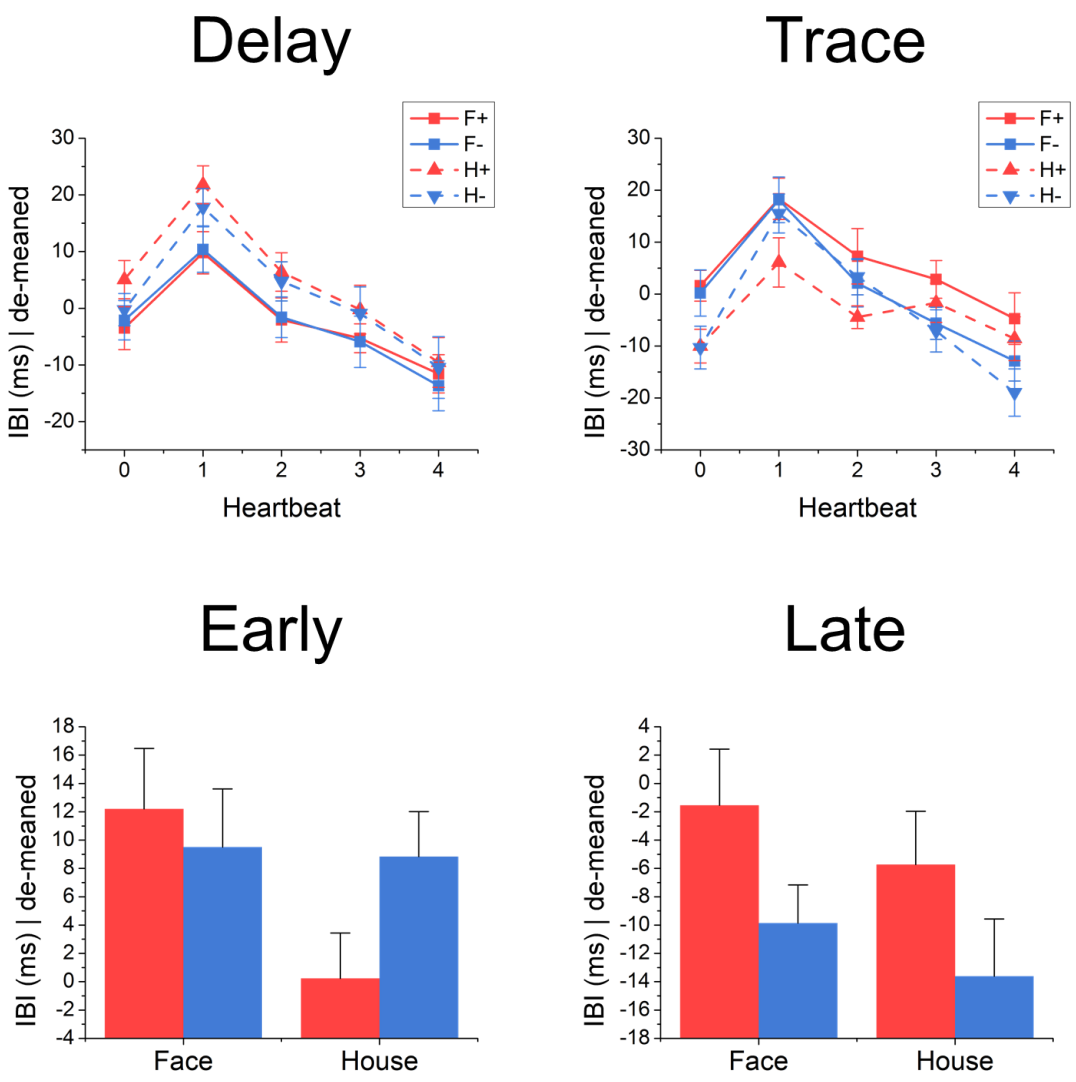

Figure 14. Heart rate interbeat interval during the conditioning session. Line graphs show the interbeat intervals for delay and trace conditioning plotted across heartbeats. Bars show the early (IBI = 1,2) and late (IBI = 3,4) interbeat intervals for trace conditioning. Bars and symbols represent mean ± SEM. Red = CS+. Blue = CS-.

3.2.5 Arousal and valence. In order to determine whether there were any evaluative conditioning effects, I asked the subjects to rate the pictures on arousal and valence scales. I performed a CS x picture content (face vs. house) x training protocol (trace vs. delay) repeated-measures ANOVA on these values, and the results are summarized in Figure 15. Subjects rated the CS+ pictures as more arousing ($F(1,14) = 14.17$; $p = 0.002$) and negative ($F(1,14) = 11.63$; $p = 0.004$) than the CS- pictures. They also rated the houses as slightly more positive than the faces ($F(1,14) = 8.46$; $p = 0.012$).

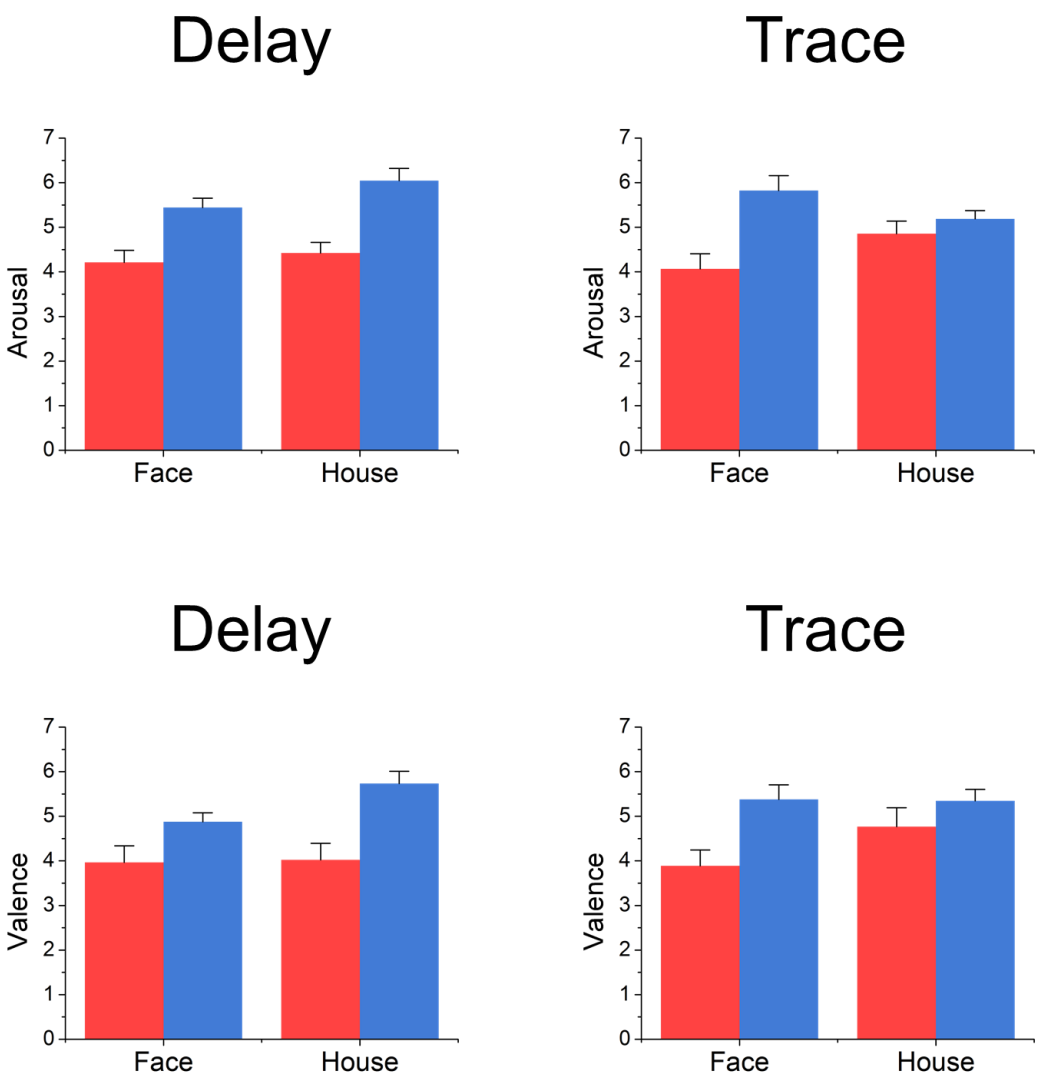

Figure 15. Evaluative (arousal = top; valence = bottom) ratings of the stimuli taken from the post experimental questionnaire. Bars represent mean ± SEM. Red = CS+. Blue = CS-.

3.3 Correlations

In order to understand the relationship between the behavioral measures, computed a set of cross correlations across subjects (See Figure 16). For measures of individual differences, I entered the scores directly into the matrix. For measures of

learning, I computed the CS+ > CS- difference scores for the delay and trace conditions, and entered these difference scores into the matrix. I computed the correlations, and thresholded the resulting correlation matrix ($\alpha = 0.05$).

Across experimental conditions, arousal and valence ratings tend to be highly correlated. Additionally, I find that the late differential interbeat interval tends to be correlated with shock intensity, but only for the trace condition. Finally, I see that differential UCS expectancy for the delay condition is correlated with reaction time.

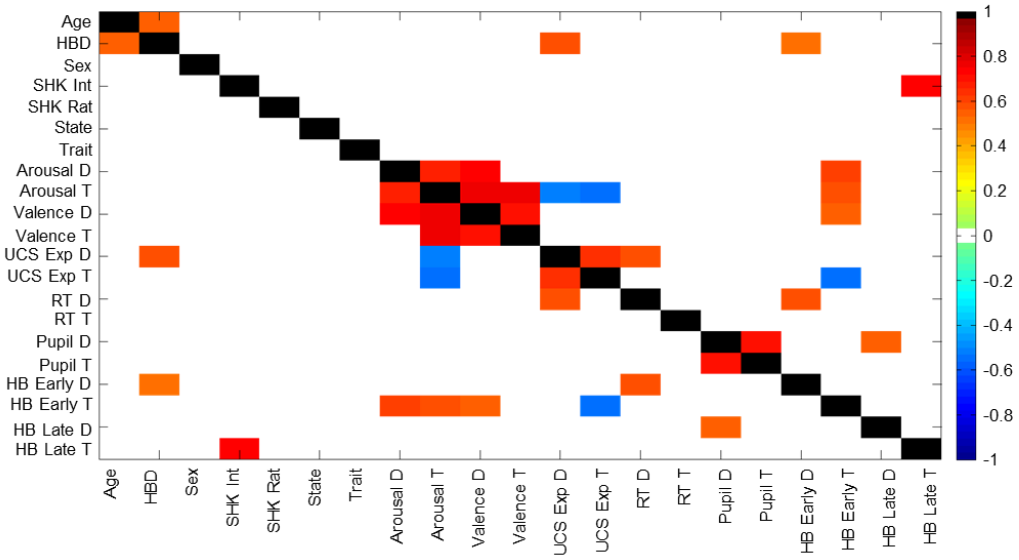

Figure 16. Significant correlations between behavioral measures. Colors represent the magnitude of the correlation coefficient. Warm colors represent positive correlations. Cool colors represent negative correlations. Non-significant correlations have been filtered and are shown in white. (D = delay; T = trace; HBD = heartbeat detection; SHK Int = shock intensity; SHK Rat = shock rating; UCS Exp = UCS expectancy; RT = reaction time; HB = heartbeat interbeat interval)

3.4 Evoked responses

For the analysis of the evoked responses, our primary goal was to determine whether there were any learning related effects based on stimulus content and

conditioning type. Therefore, I computed a series of CS+ > CS- t-tests for the different conditions in the experiment (Conditioning type: Delay, Trace; Stimulus content: Face, House). As a secondary goal, I wanted to determine whether there were learning related interactions between stimulus content and conditioning type. Therefore, I computed CS+ > CS- t-tests for the conditions in the experiment, broken down by both stimulus content and conditioning type (Face Delay, Face Trace, House Delay, House Trace). Finally, in order to be thorough I computed a series of t-tests corresponding to the main effects of the experiment (CS+ > CS-, Delay > Trace, Face > House), and a series of t-tests based on learning related difference scores (CS+ - CS-) for stimulus content (Face > House) and conditioning type (Delay > Trace). Once I computed the paired sample t-test for a given comparison, I identified temporal clusters that surpassed the summed t-statistic threshold. After inspecting these clusters, it became apparent that there were two types of temporal clusters identified by the analysis: 1) transient differences in specific components of the evoked response (i.e. the significant differential response contained both the rise and fall of a specific evoked component), 2) sustained non-specific differences, typically occurring later in the time window. I collected these results in graphs depicting the timecourse of significant responses across atlas regions for each comparison. In addition, for each of the effects identified as transient, I graphed the evoked response for the conditions being compared.

3.4.1 Learning related effects for conditioning type. For Delay, I found transient differences in activity in two regions (See Figure 19). For the left medial orbitofrontal cortex I found a larger response at ~100 ms for the CS+ than for the CS-. For the right entorhinal cortex, I found a larger response at ~150 ms for the CS+ than for

the CS-. The sustained responses are summarized in Figures 17-18.

For Trace, I found transient differences in activity in 4 regions (See Figure 22). First I find an early (~70 ms) CS+ > CS- difference in the right rostral middle frontal gyrus. I also found a CS+ > CS- difference in the right inferior parietal lobule at ~200 ms, a CS+ > CS- difference in the right parahippocampal gyrus at ~420 ms, and a CS+ > CS- difference in the right caudal anterior cingulate cortex beginning just prior to end of the period I were investigating. The sustained responses are summarized in Figures 20-21.

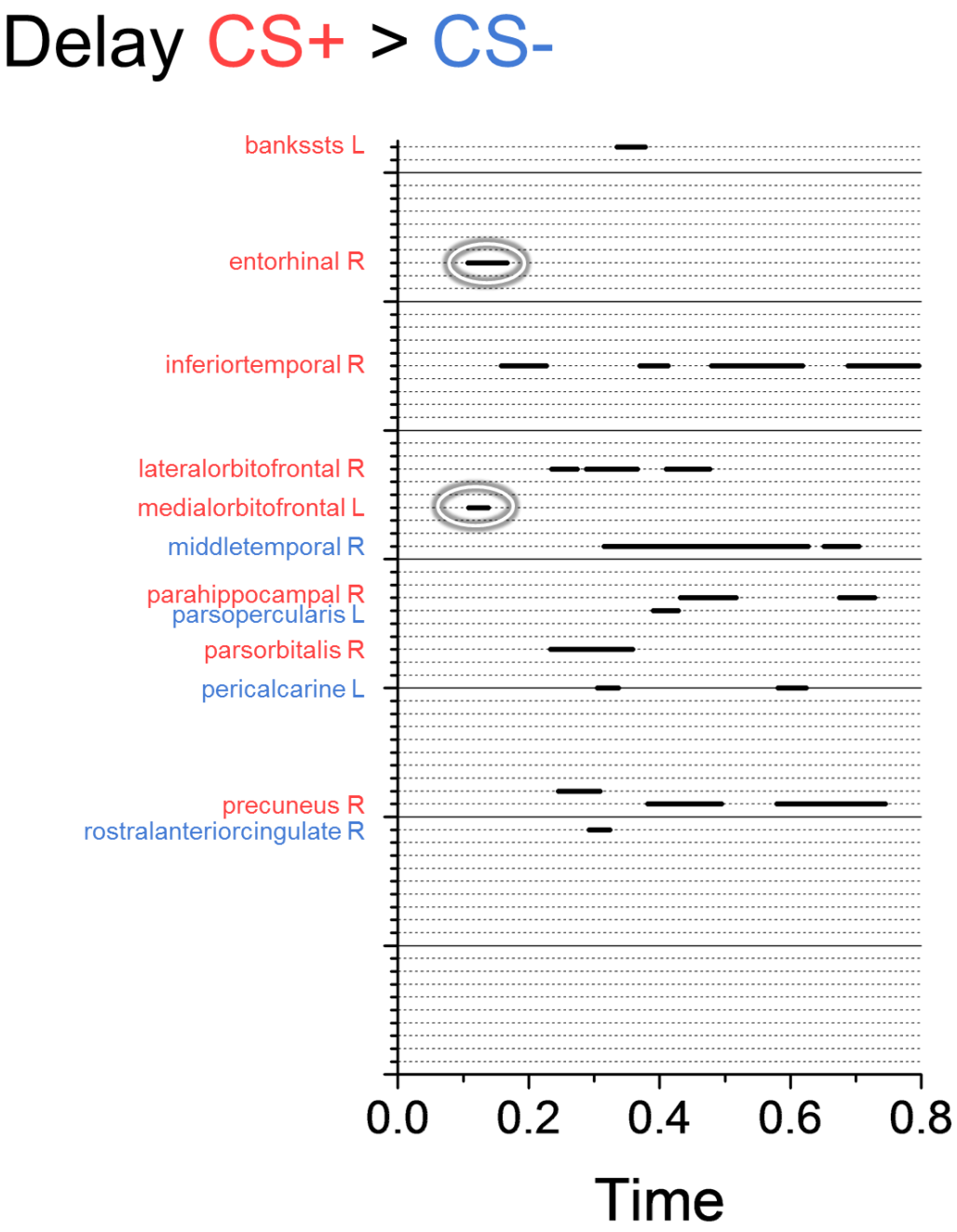

Figure 17. Timecourse of significant differential evoked responses for the Delay CS+ > Delay CS- comparison. Label color represents the direction of the effect. Circled effects were considered transient and graphed individually below.

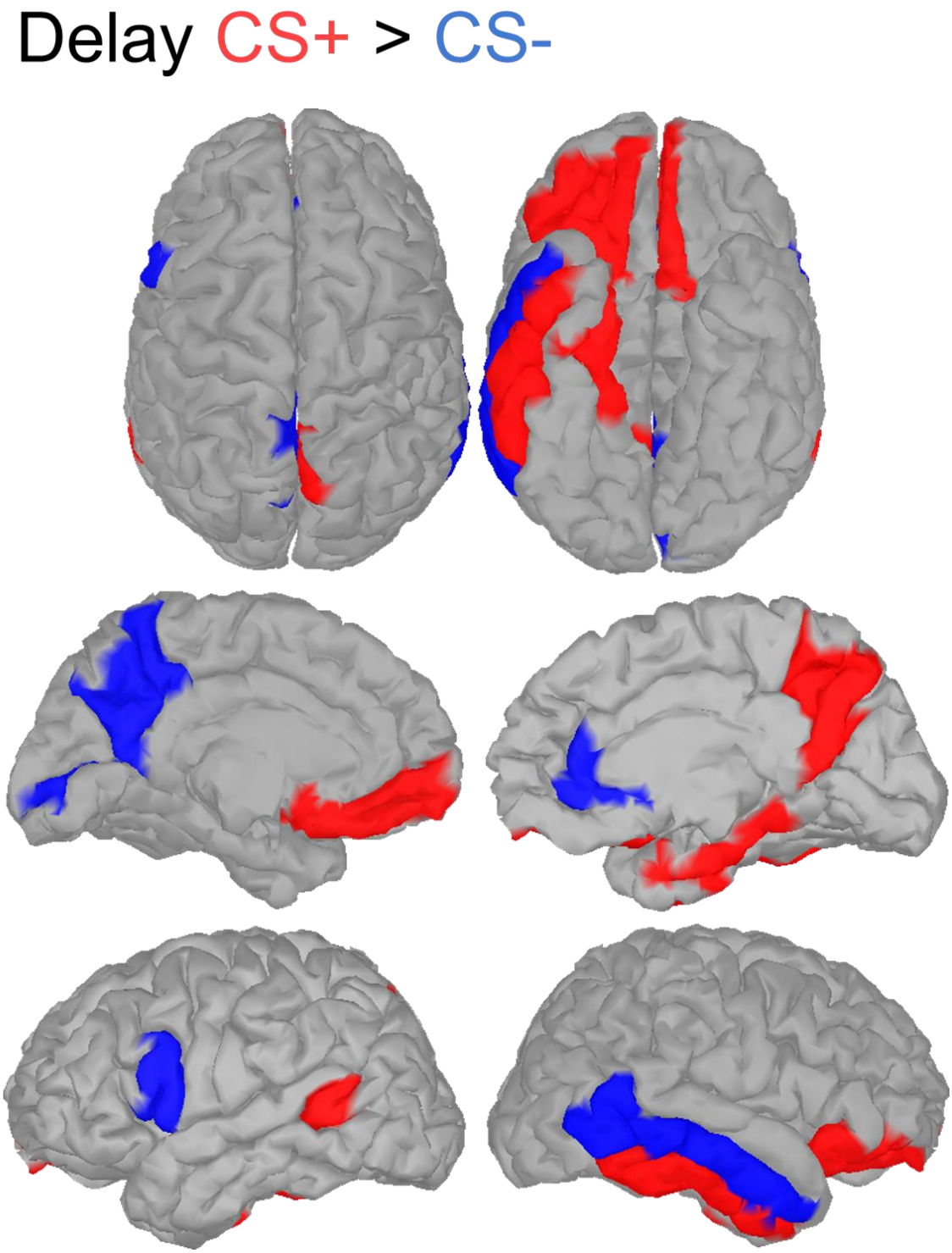

Figure 18. Regions showing differential activity for the Delay CS+ > Delay CS- comparison. Colors represent the direction of the effect.

Delay CS+ > CS-

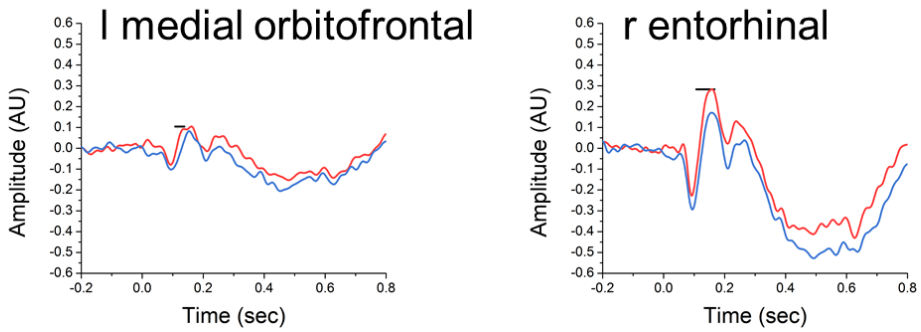

Figure 19. Evoked responses from regions showing transient differential activity for the Delay CS+ > Delay CS- comparison. Red = CS+. Blue = CS-.

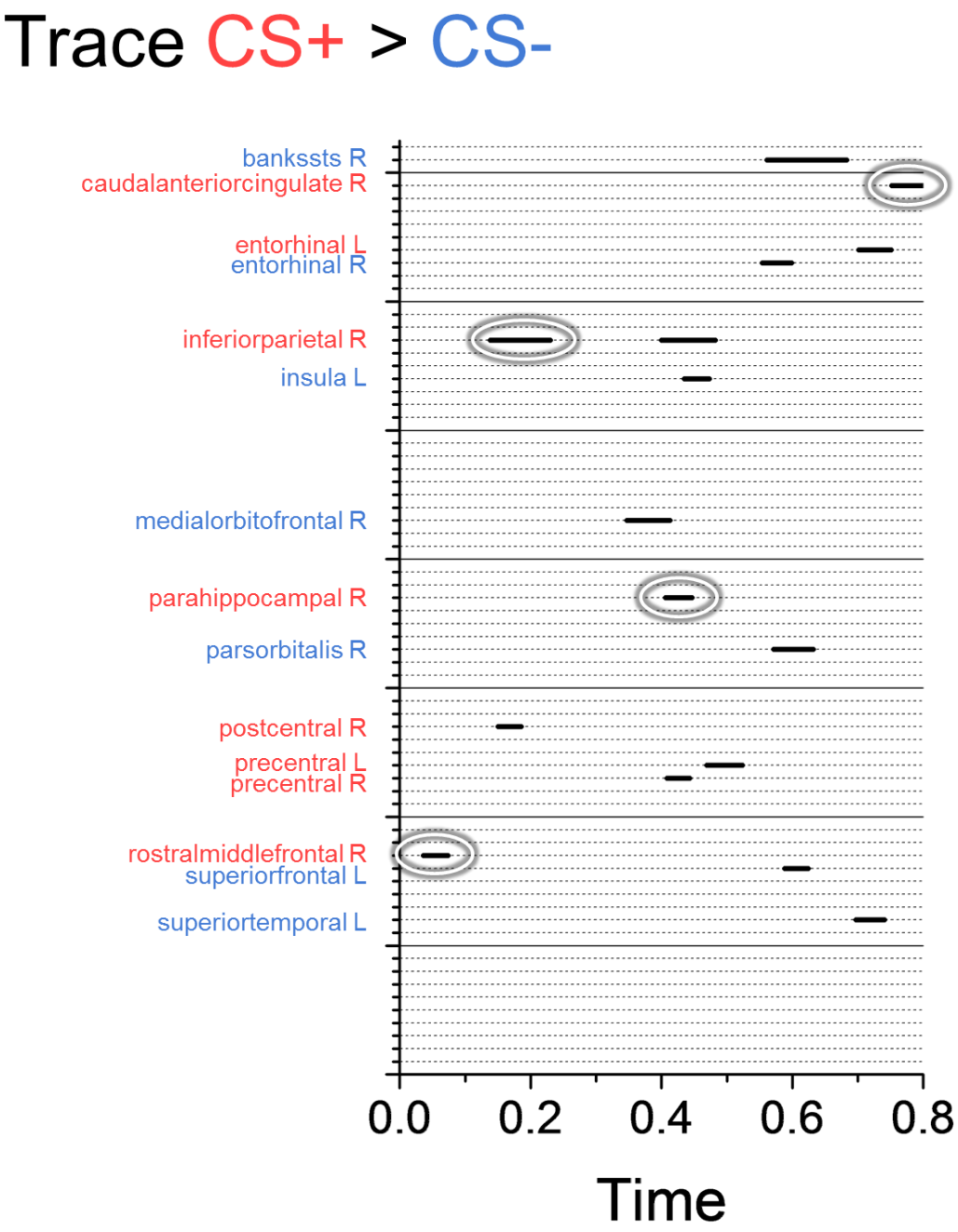

Figure 20. Timecourse of significant differential evoked responses for the Trace CS+ > Trace CS- comparison. Label color represents the direction of the effect. Circled effects were considered transient and graphed individually below.

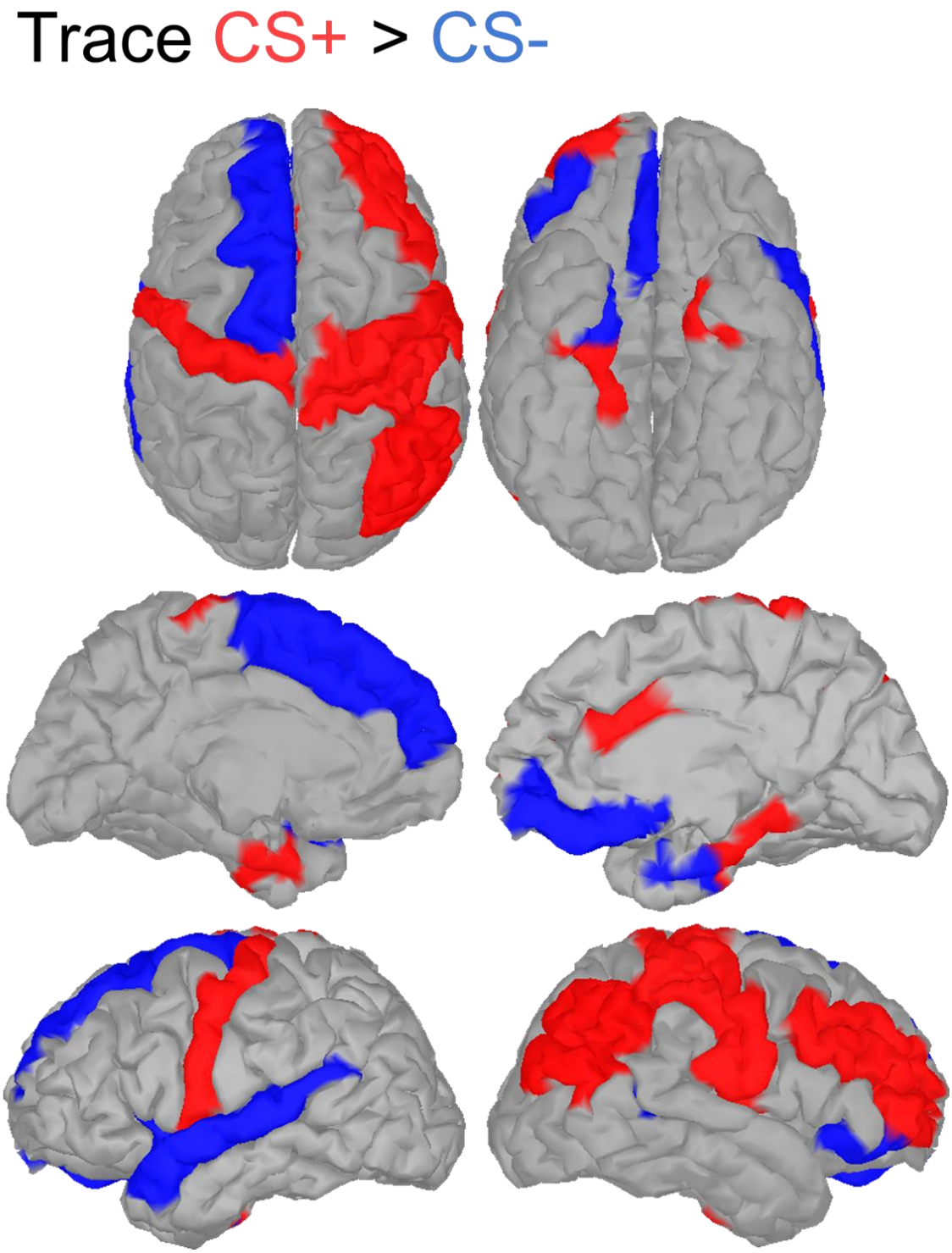

Figure 21. Regions showing differential activity for the Trace CS+ > Trace CS- comparison. Colors represent the direction of the effect.

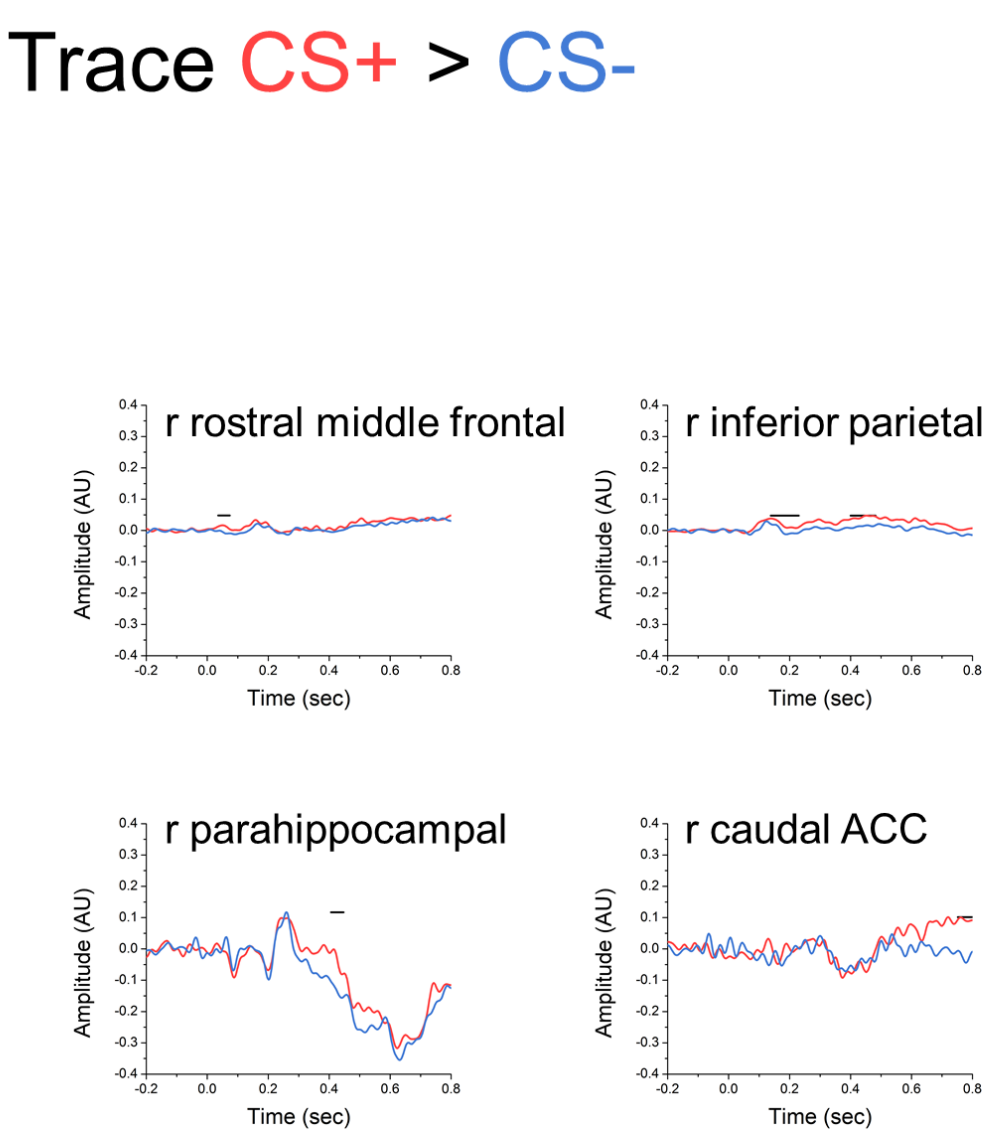

Figure 22. Evoked responses from regions showing transient differential activity for the Trace CS+ > Trace CS- comparison. Red = CS+. Blue = CS-.

3.4.2 Learning related effects for stimulus content. For faces, I found transient differential responses in three regions (Figure 25). First, I found a larger response for the CS- than the CS+ at ~250 ms in the left precuneus. Next I found offset related transient differences (CS+ > CS-) in the right parahippocampal gyrus and left temporal pole at ~550 ms and 600 ms respectively. The sustained responses are summarized in Figures 23-24.

For houses I found transient differences (CS+ > CS-) in both the left (300 ms) and the right (420 ms) parahippocampal gyrii (See Figure 28). In addition, I found transient differences in the opposite direction (CS- > CS+) in the right medial orbitofrontal gyrus at ~ 150 ms. The sustained responses are summarized in Figures 26-27.

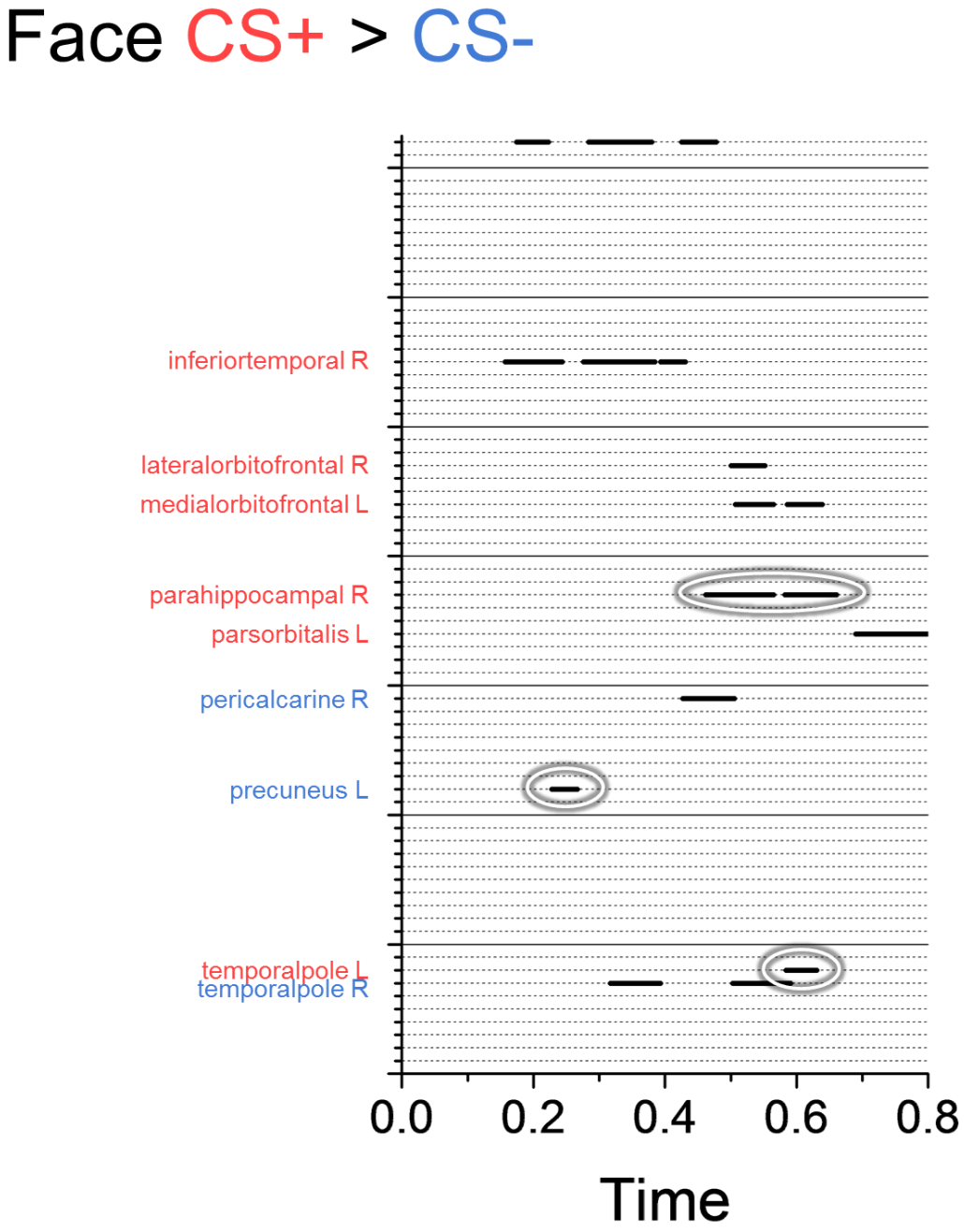

Figure 23. Timecourse of significant differential evoked responses for the Face CS+ > Face CS- comparison. Label color represents the direction of the effect. Circled effects were considered transient and graphed individually below.

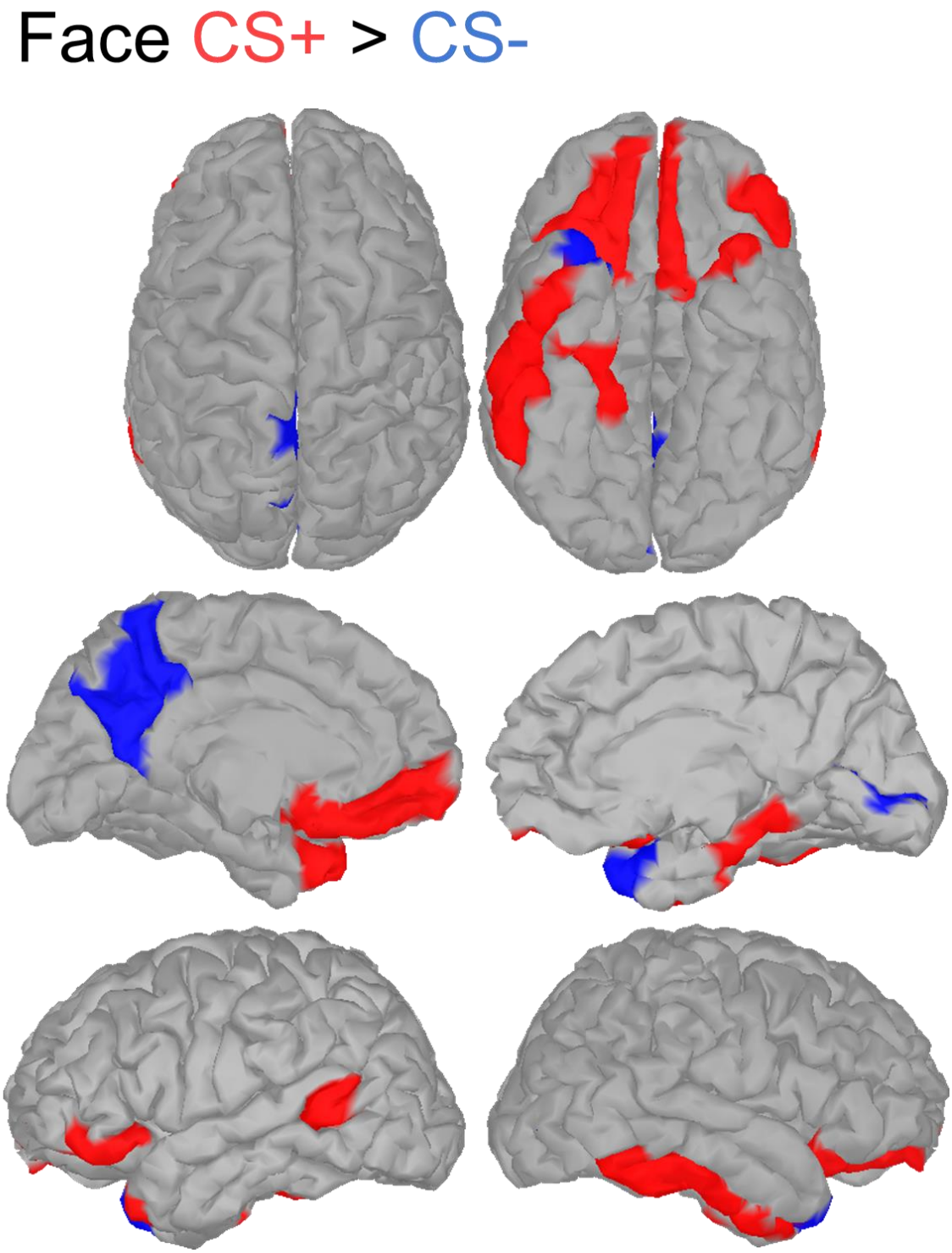

Figure 24. Regions showing differential activity for the Face CS+ > Face CS- comparison. Colors represent the direction of the effect.

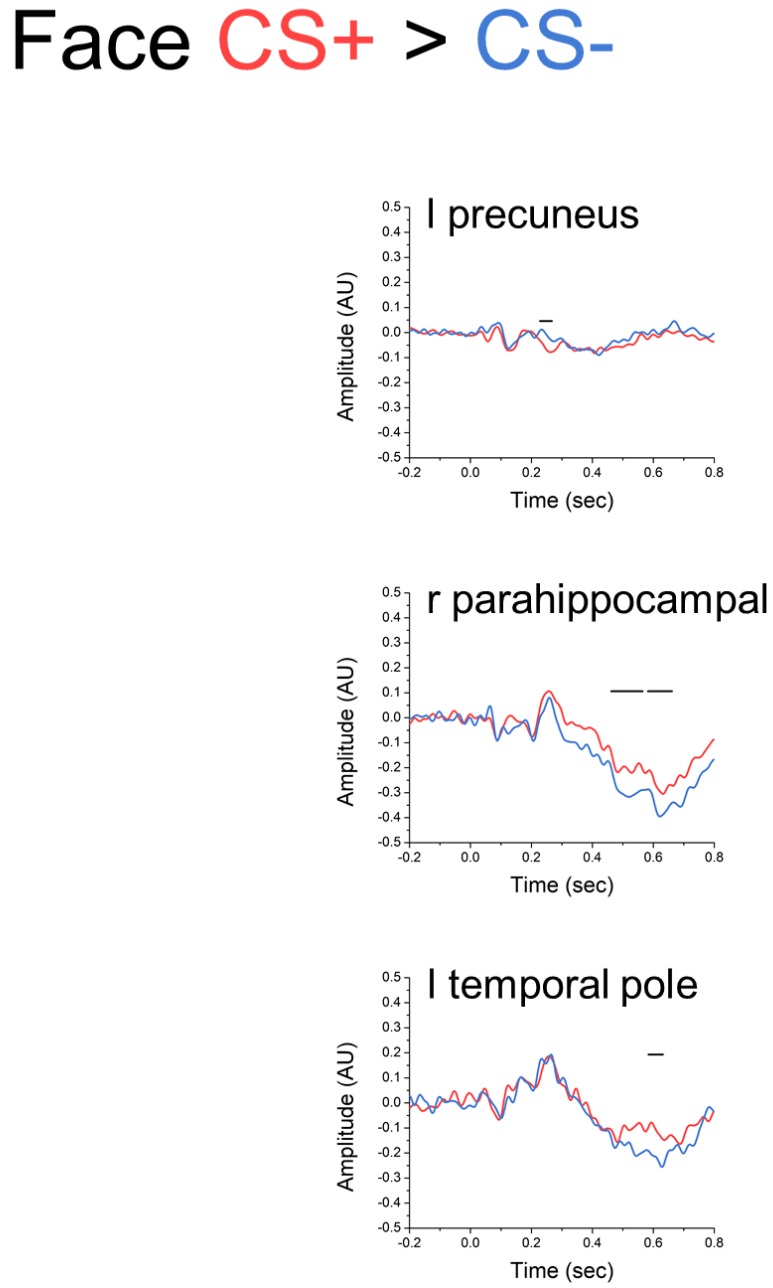

Figure 25. Evoked responses from regions showing transient differential activity for the Face CS+ > Face CS- comparison. Red = CS+. Blue = CS-.

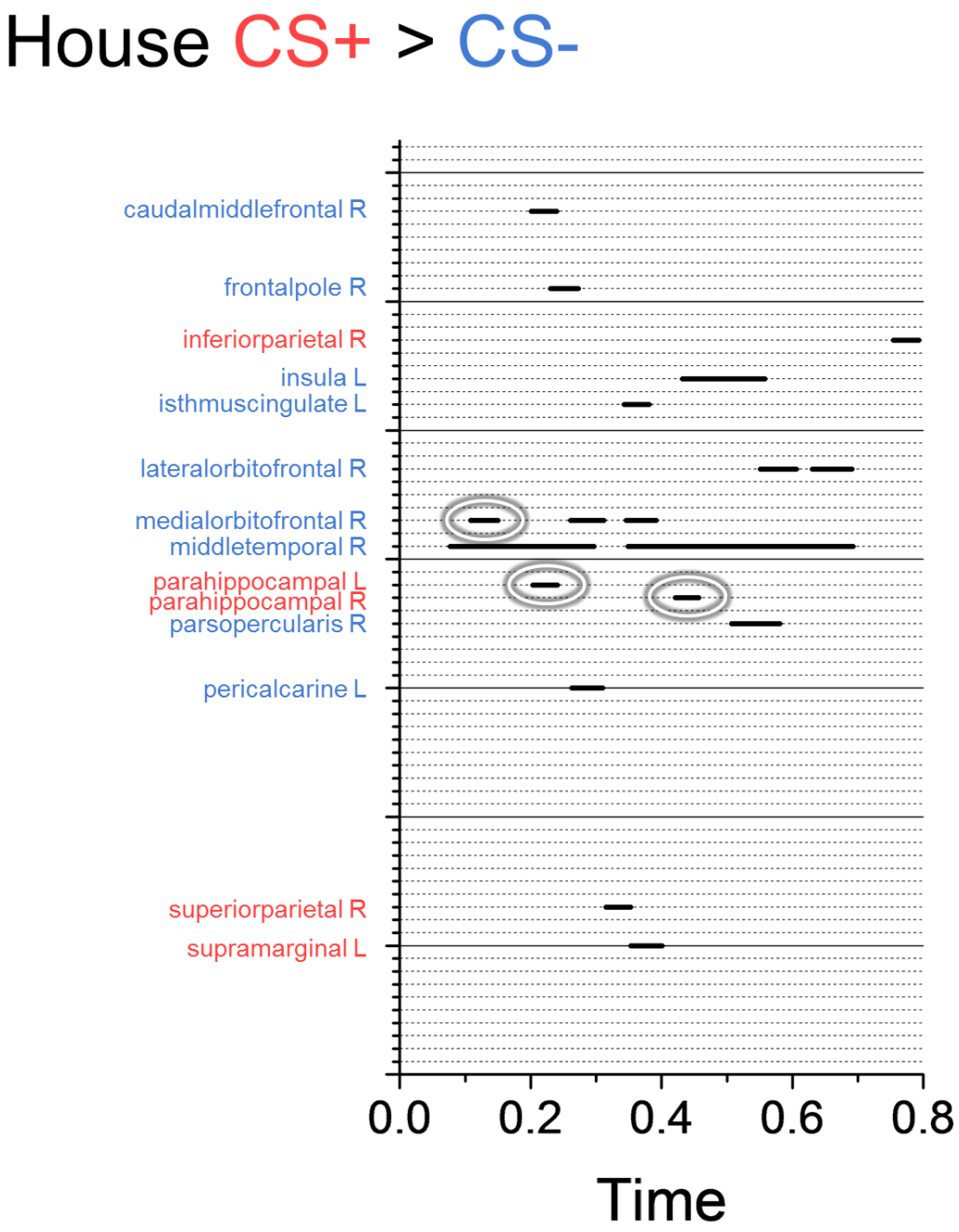

Figure 26. Timecourse of significant differential evoked responses for the House CS+ > House CS- comparison. Label color represents the direction of the effect. Circled effects were considered transient and graphed individually below.

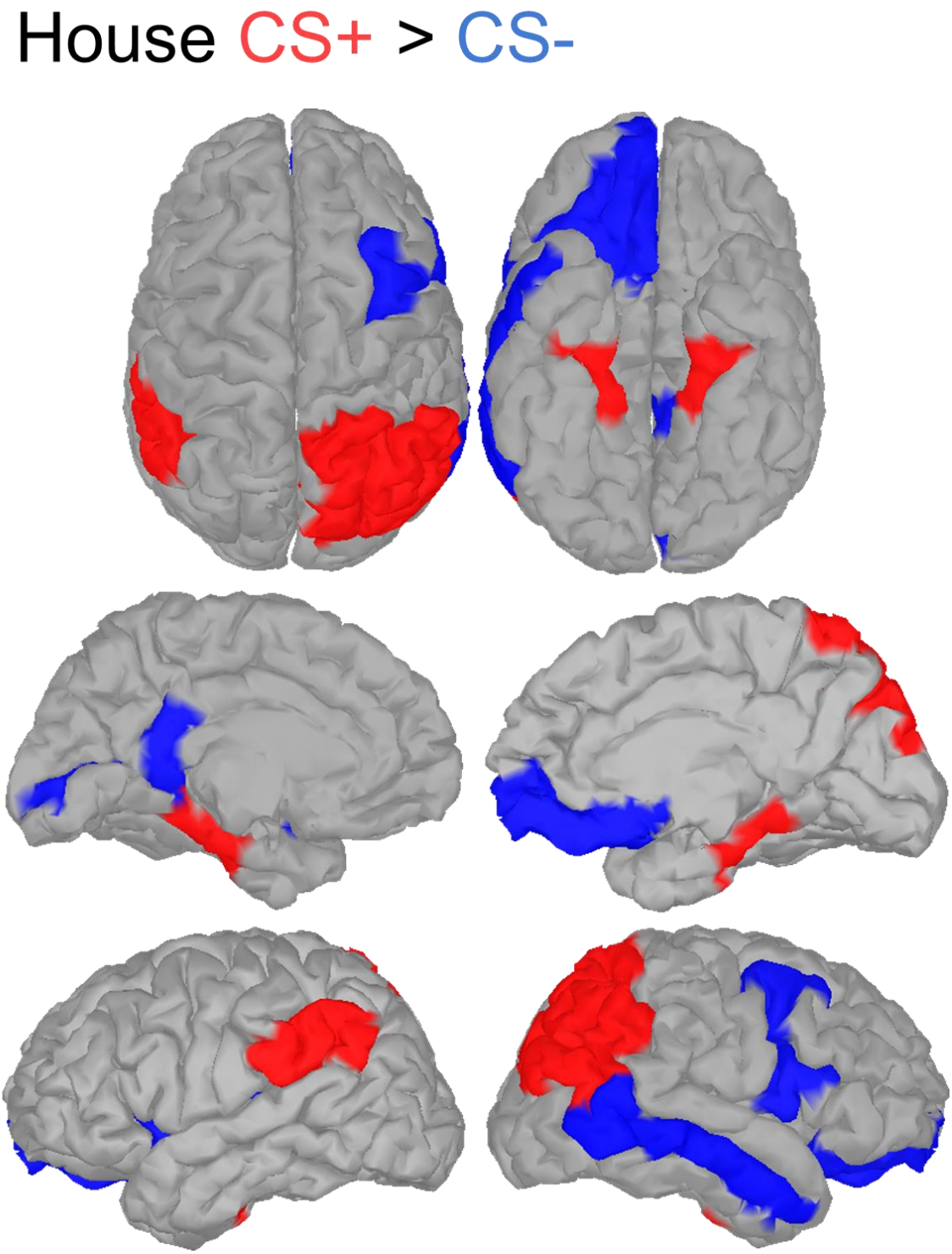

Figure 27. Regions showing differential activity for the House CS+ > House CS- comparison. Colors represent the direction of the effect.

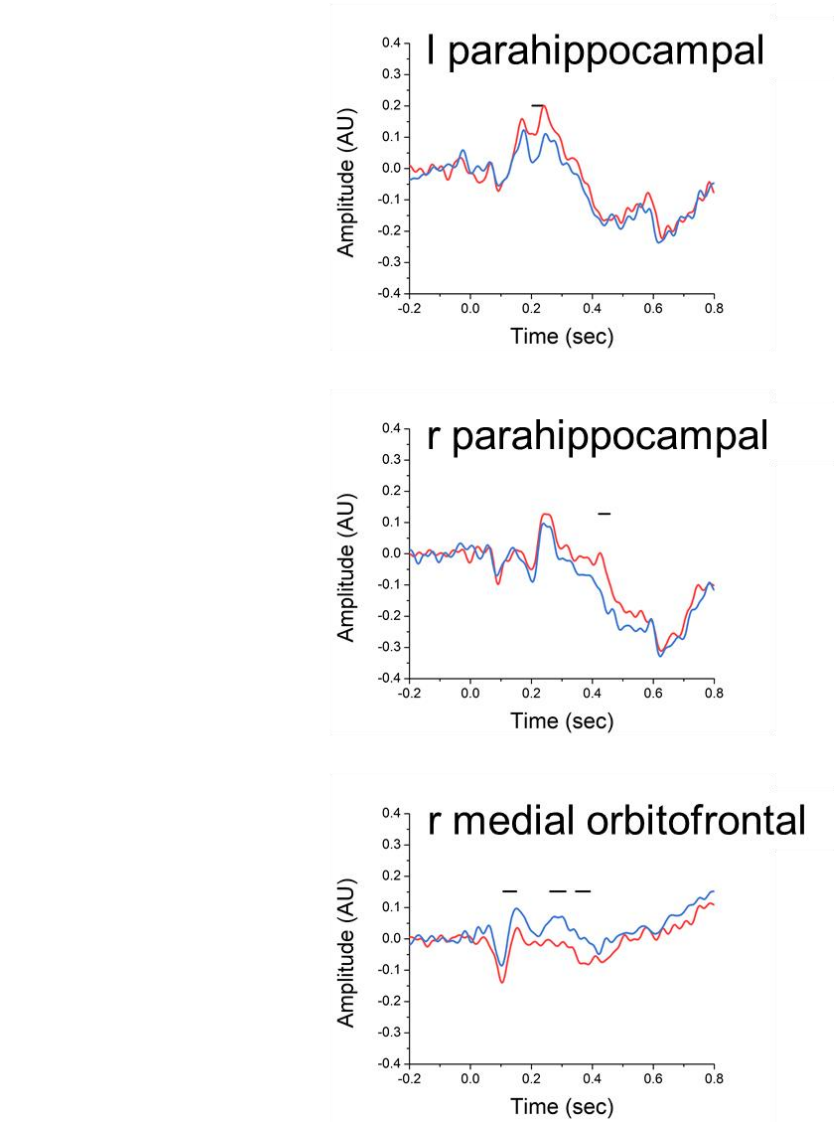

Figure 28. Evoked responses from regions showing transient differential activity for the House CS+ > House CS- comparison. Red = CS+. Blue = CS-.

3.4.3 Learning related interactions. Transient differential responses within the learning related interactions were scarcer. For delay conditioning with faces, I found a differential (CS- > CS+) effect in the right fusiform gyrus at ~100 ms (See Figure 31). In contrast for trace conditioning with faces I found a differential (CS+ > CS-) effect in the left insula at ~200 ms (See Figure 34). The sustained responses are summarized in Figures 29-30 (Delay), 32-33 (Trace).

For delay conditioning with houses I found two transient differential effects. The first differential (CS+ > CS-) effect was in the left precuneus at ~170 ms (See Figure 37). The second was in the left lateral orbitofrontal cortex at ~270 ms. For trace conditioning with houses there was only one differential (CS+ > CS-) effect in the right lingual gyrus at ~70 ms (See Figure 40). The sustained responses are summarized in Figures 35-36 (Delay), 38-39 (Trace).

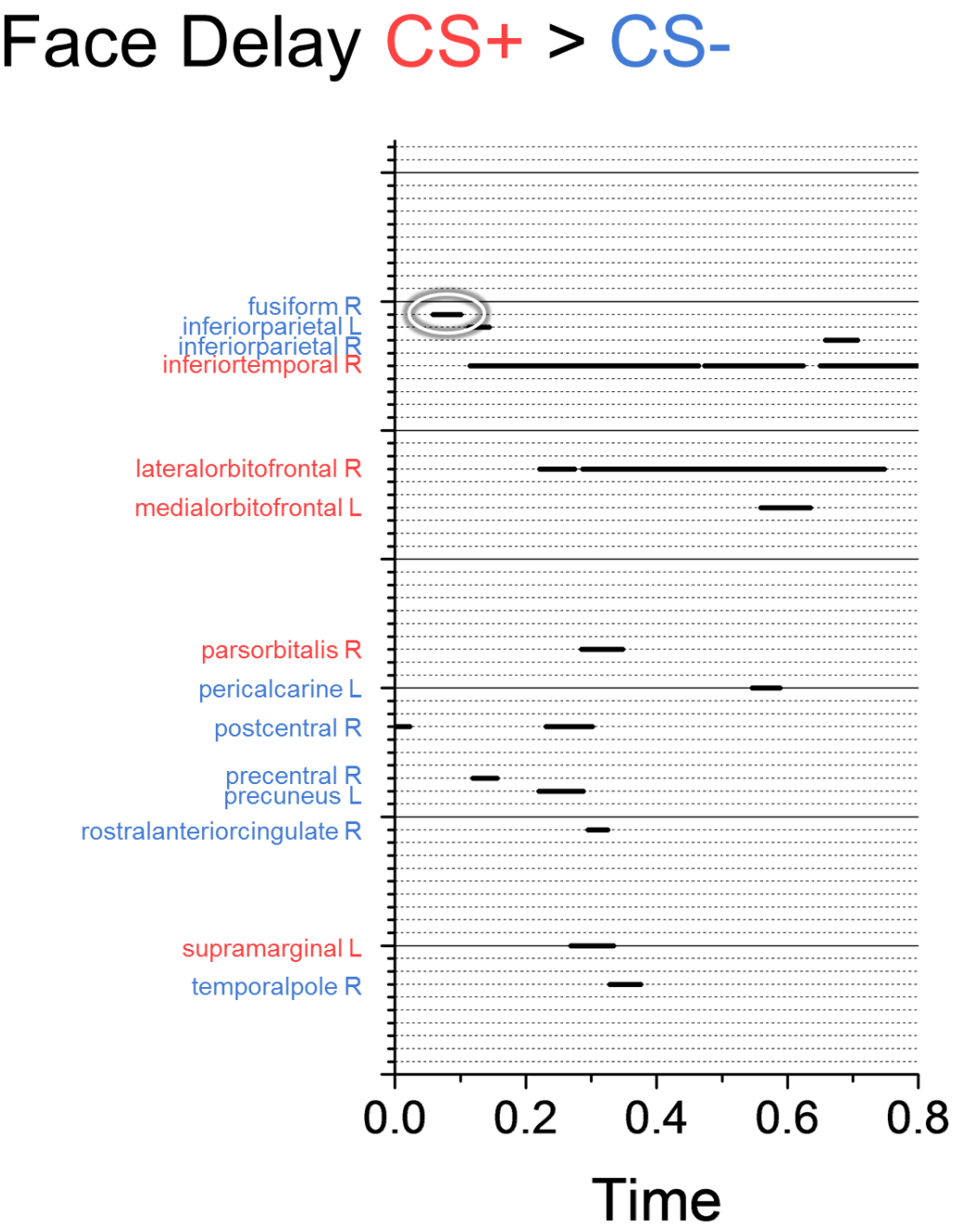

Figure 29. Timecourse of significant differential evoked responses for the Face Delay CS+ > Face Delay CS- comparison. Label color represents the direction of the effect. Circled effects were considered transient and graphed individually below.

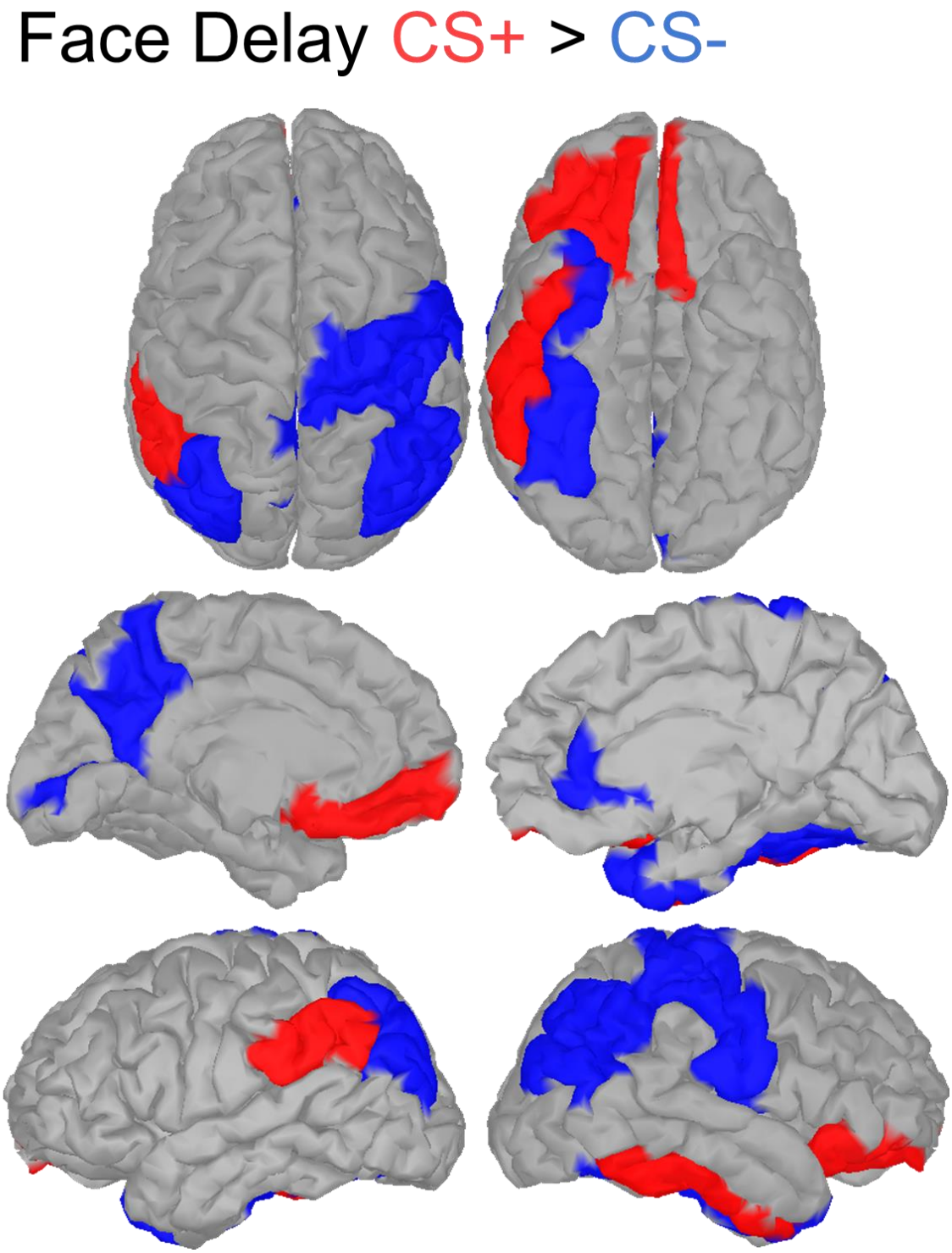

Figure 30. Regions showing differential activity for the Face Delay CS+ > Face Delay CS- comparison. Colors represent the direction of the effect.

Face Delay CS+ > CS-

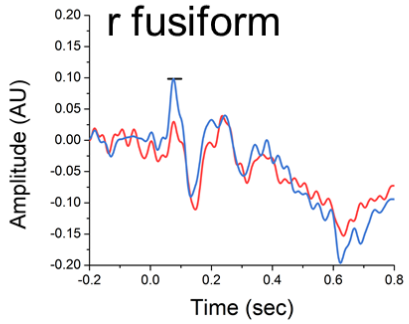

Figure 31. Evoked responses from region showing transient differential activity for the Delay CS+ > Face Delay CS- comparison. Red = CS+. Blue = CS-.

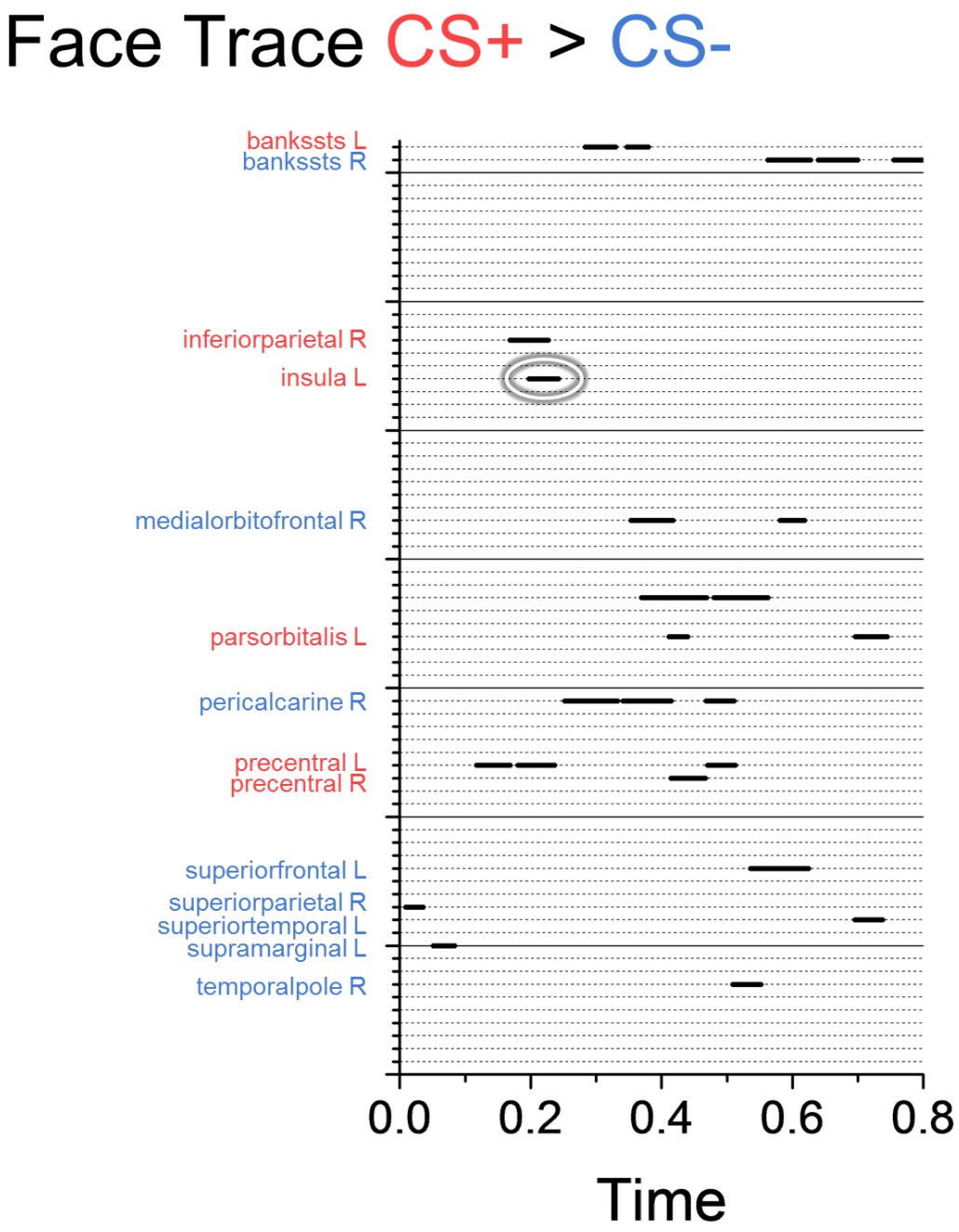

Figure 32. Timecourse of significant differential evoked responses for the Face Trace CS+ > Face Trace CS- comparison. Label color represents the direction of the effect. Circled effects were considered transient and graphed individually below.

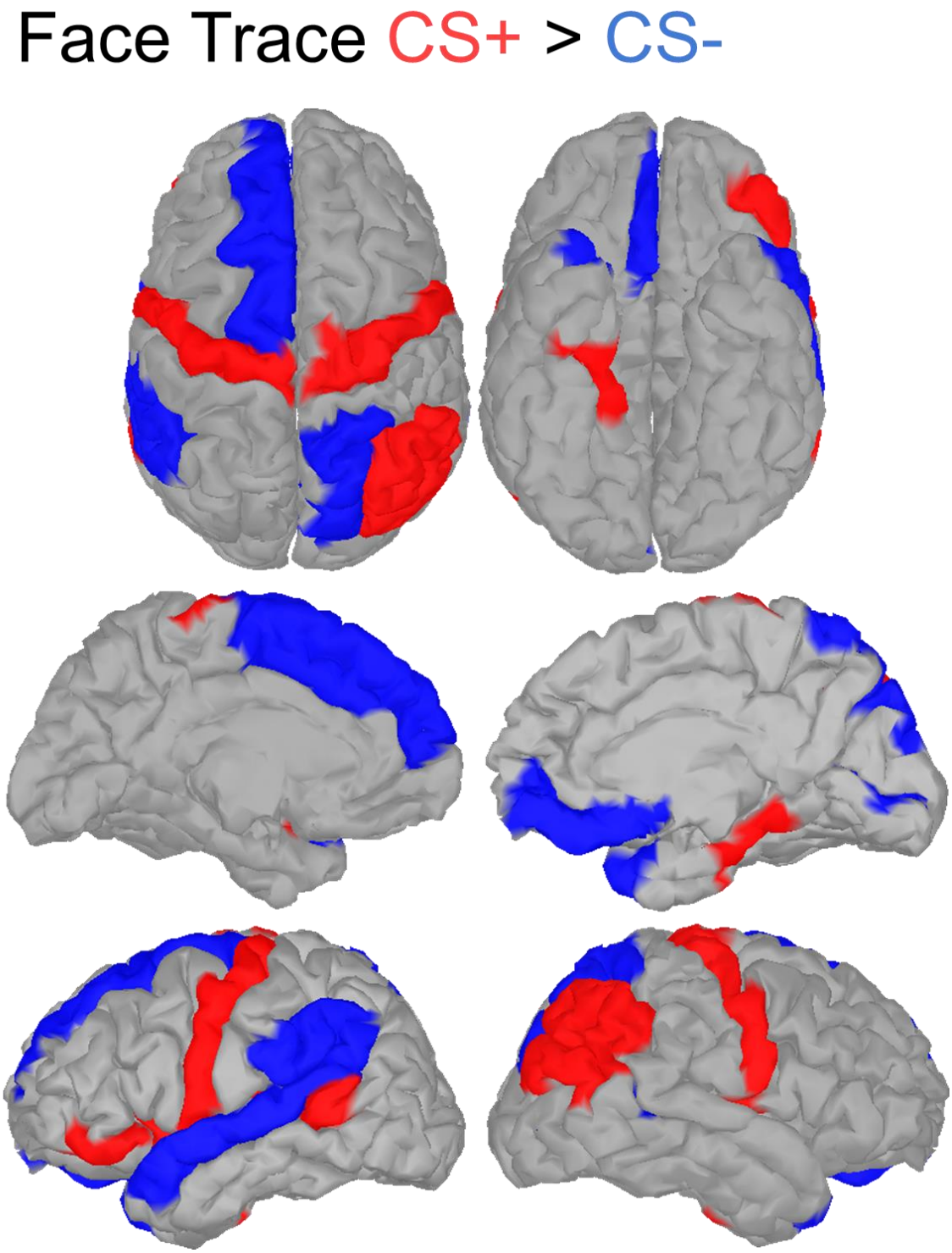

Figure 33. Regions showing differential activity for the Face Trace CS+ > Face Trace CS- comparison. Colors represent the direction of the effect.

Face Trace CS+ > CS-

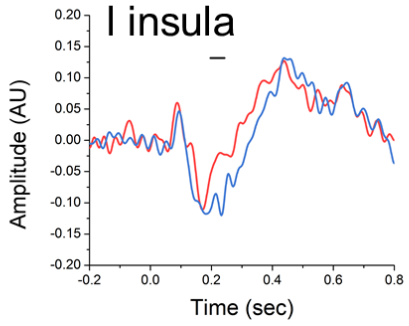

Figure 34. Evoked responses from region showing transient differential activity for the Face Trace CS+ > Face Trace CS- comparison. Red = CS+. Blue = CS-.

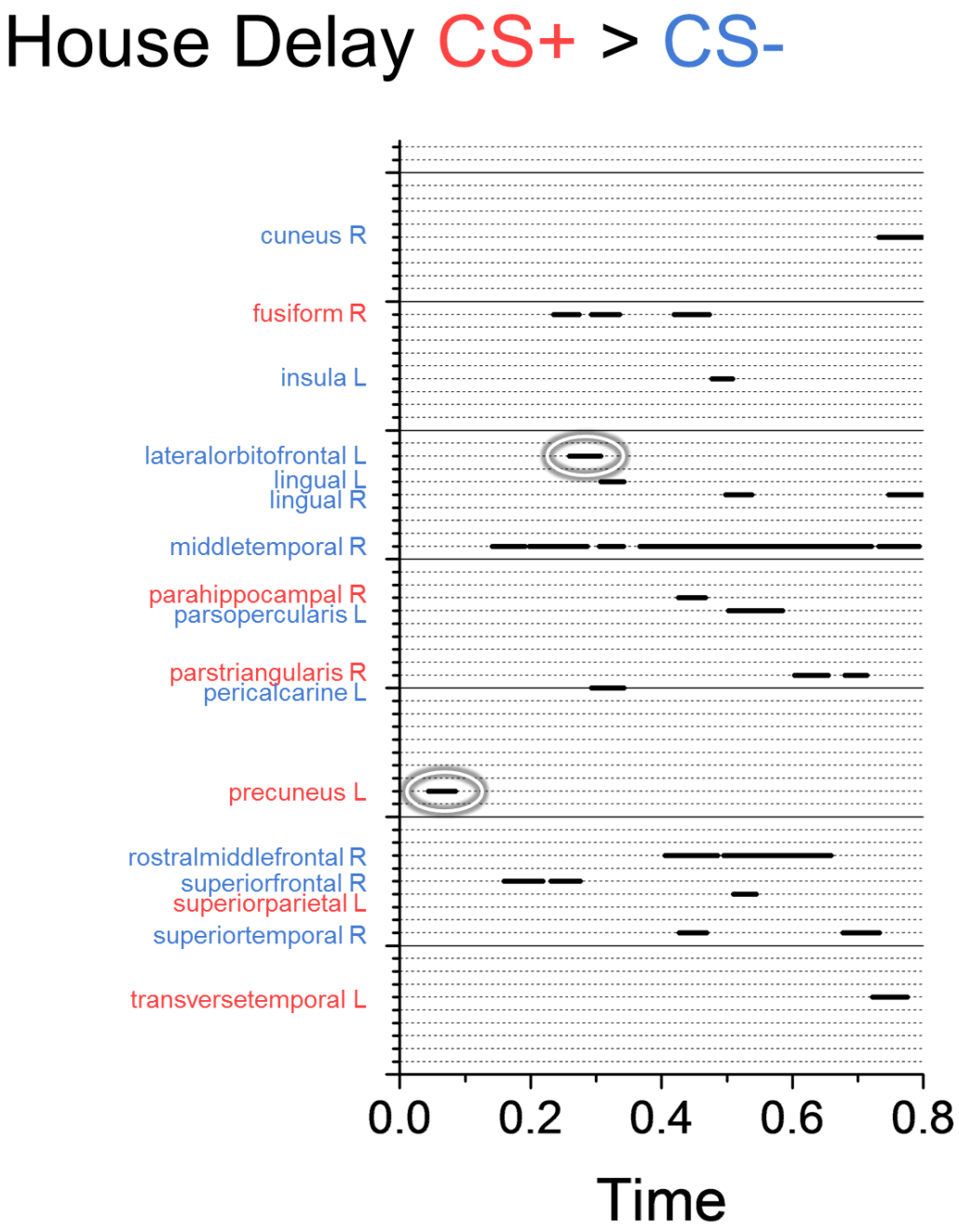

Figure 35. Timecourse of significant differential evoked responses for the House Delay CS+ > House Delay CS- comparison. Label color represents the direction of the effect. Circled effects were considered transient and graphed individually below.

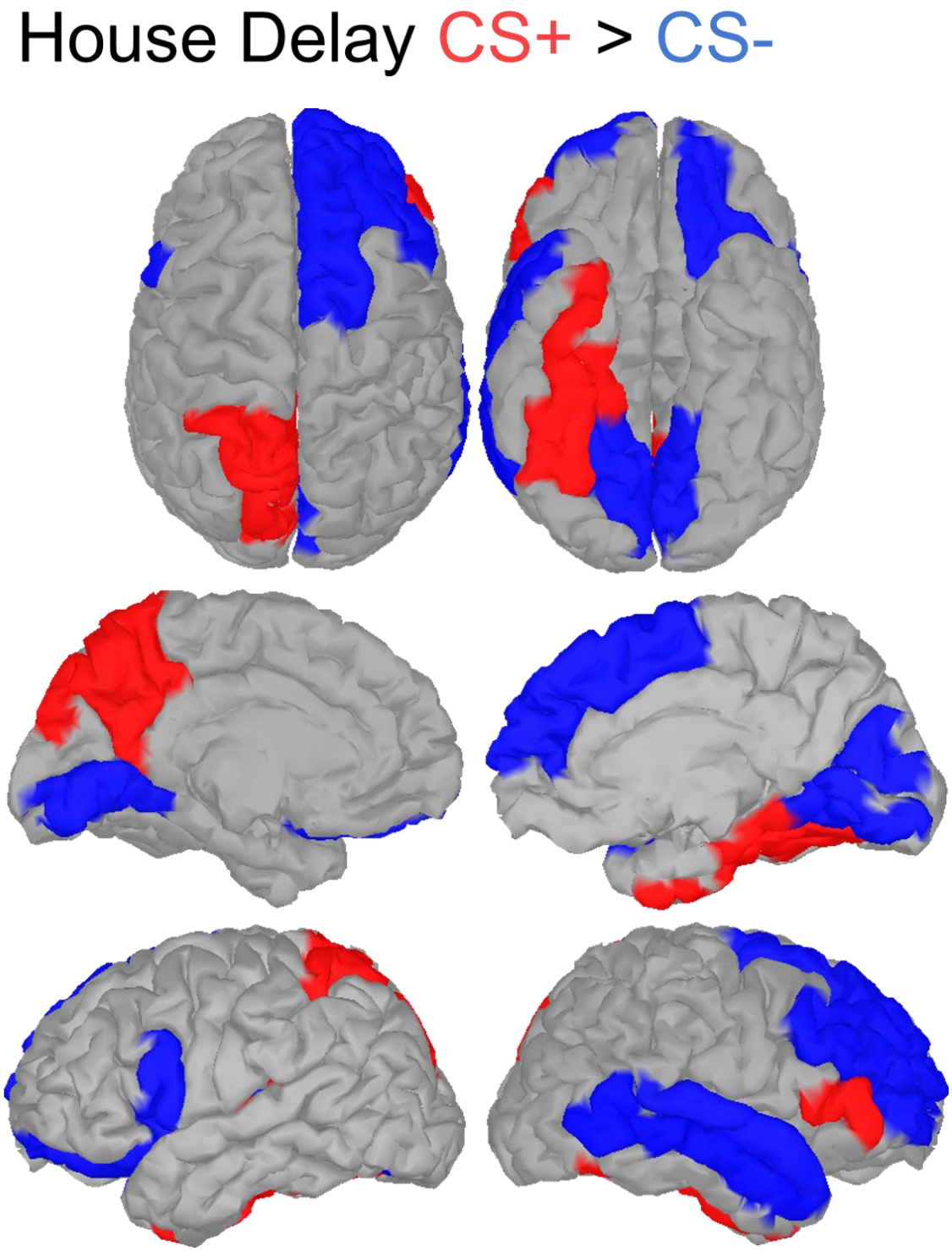

Figure 36. Regions showing differential activity for the House Delay CS+ > House Delay CS- comparison. Colors represent the direction of the effect.

House Delay CS+ > CS-

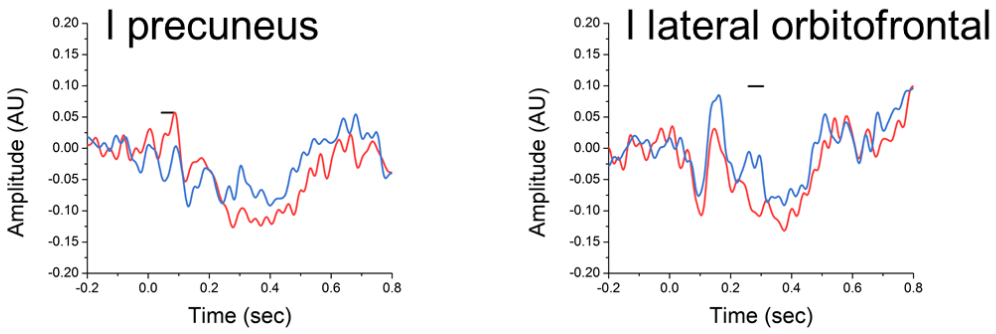

Figure 37. Evoked responses from regions showing transient differential activity for the House Delay CS+ > House Delay CS- comparison. Red = CS+. Blue = CS-.

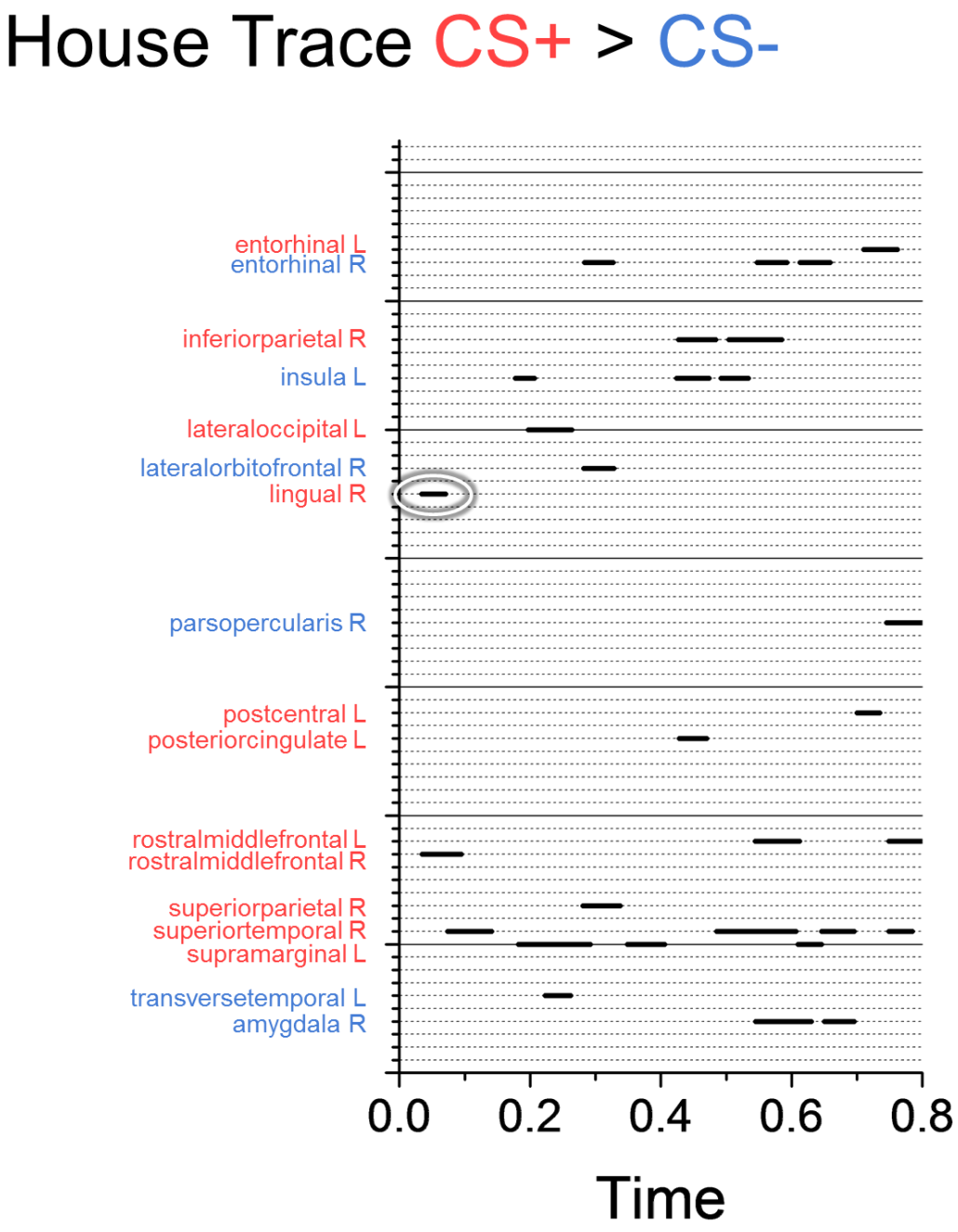

Figure 38. Timecourse of significant differential evoked responses for the House Trace CS+ > House CS- comparison. Label color represents the direction of the effect. Circled effects were considered transient and graphed individually below.

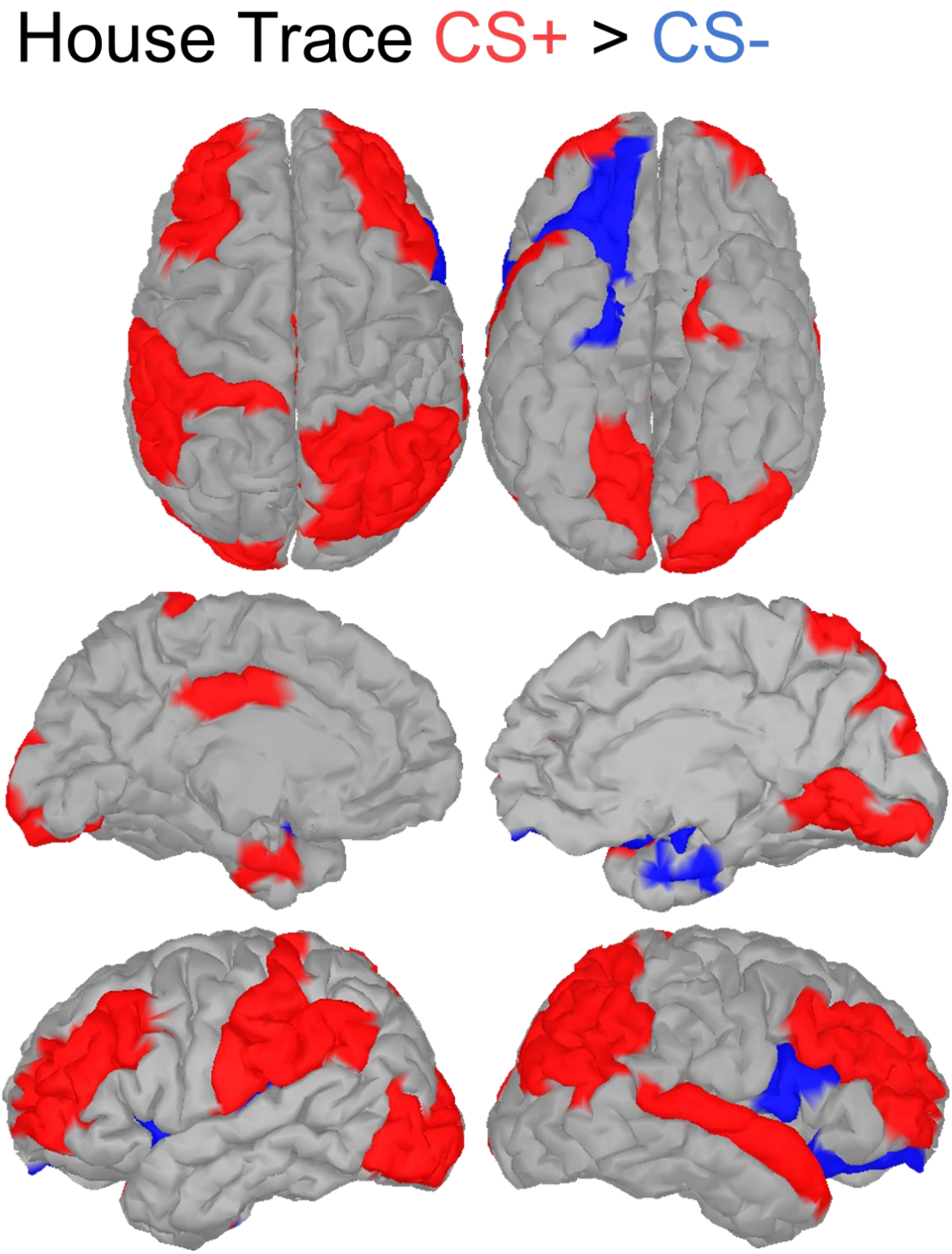

Figure 39. Regions showing differential activity for the House Trace CS+ > House CS- comparison. Colors represent the direction of the effect.

House Trace CS+ > CS-

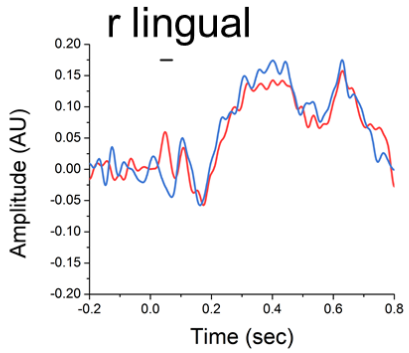

Figure 40. Evoked responses from region showing transient differential activity for the House Trace CS+ > House CS- comparison. Red = CS+. Blue = CS-.

3.4.4 Main effects. For the main effect for conditioning I found three basic effects (See Figure 43). First I found a transient differential (CS- > CS+) effect at ~270 ms in both the right medial orbitofrontal gyrus and the left precuneus. I also found a differential (CS- > C+) effect at ~350 ms in both the right temporal pole and the left isthmucingulate gyrus. Finally, I found a differential effect in the opposite direction (CS+ > CS-) in the right parahippocampal gyrus at ~400 ms. The sustained responses are summarized in Figures 41-42.

For the main effect for conditioning type, I found three basic effects (See Figure 46). The first two both occur at ~100 ms. I found a differential (Trace > Delay) effect in both the right medial orbitofrontal gyrus and the left parsopercularis. I also found an effect in the opposite direction (Delay > Trace) in the left supramarginal gyrus and left parstriangularis. Finally, I found an effect (Delay > Trace) in the right insular cortex at ~170 msec. The sustained responses are summarized in Figures 44-45.

For the main effect for stimulus content I found only one transient effect in the left caudal middle frontal gyrus at ~150 ms (See Figure 49). The sustained responses are summarized in Figures 47-48.

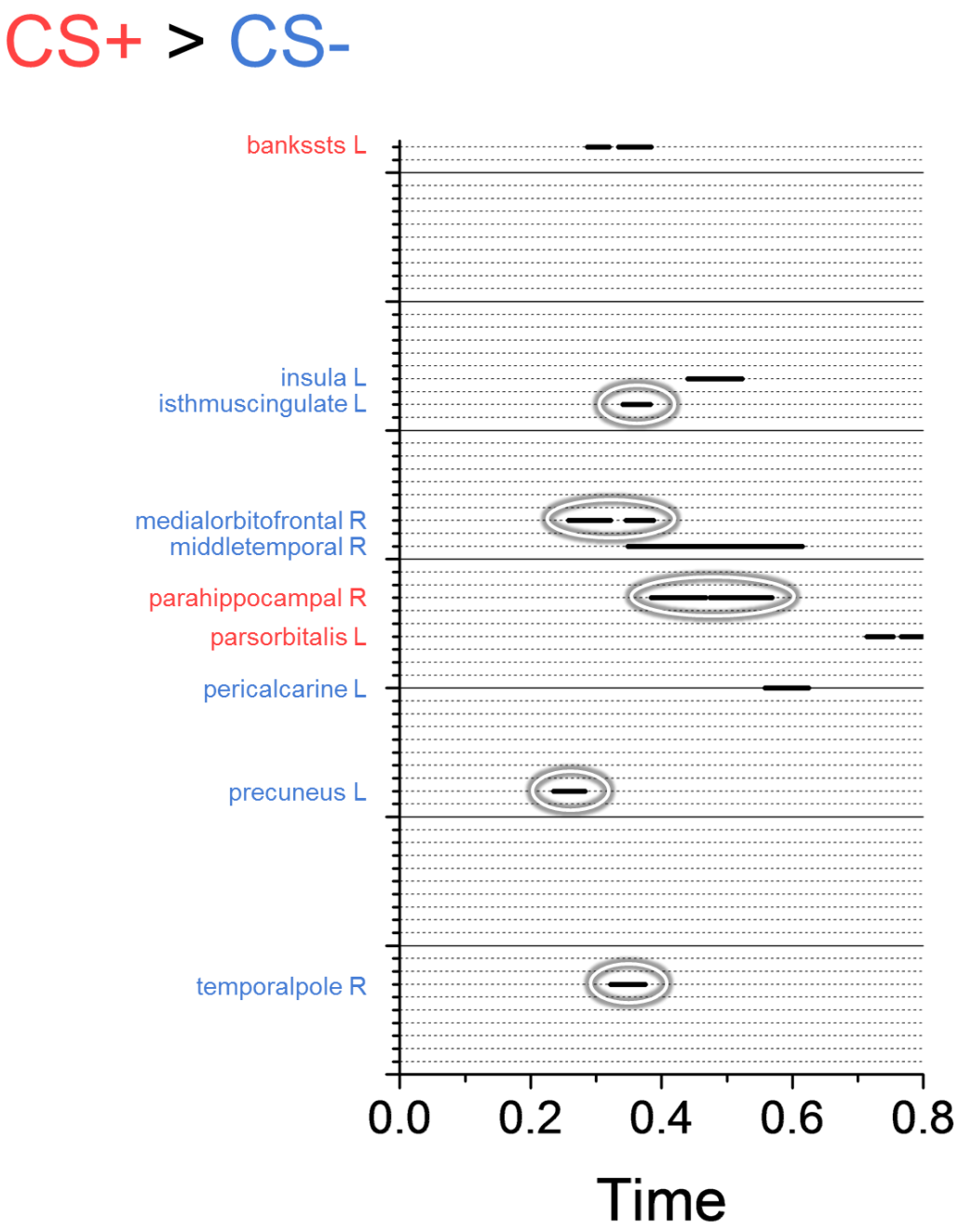

Figure 41. Timecourse of significant differential evoked responses for the CS+ > CS- comparison. Label color represents the direction of the effect. Circled effects were considered transient and graphed individually below.

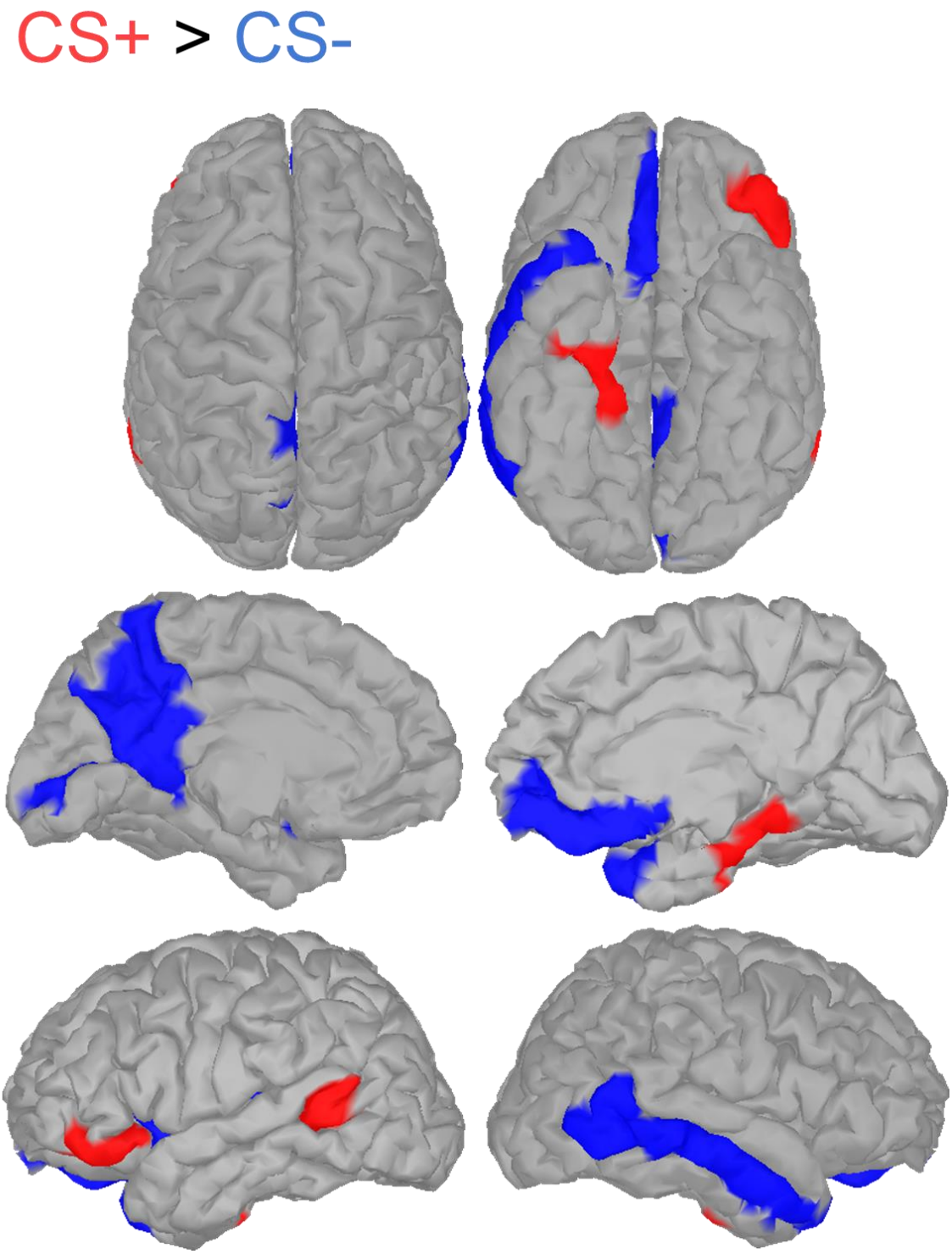

Figure 42. Regions showing differential activity for the CS+ > CS- comparison. Colors represent the direction of the effect.

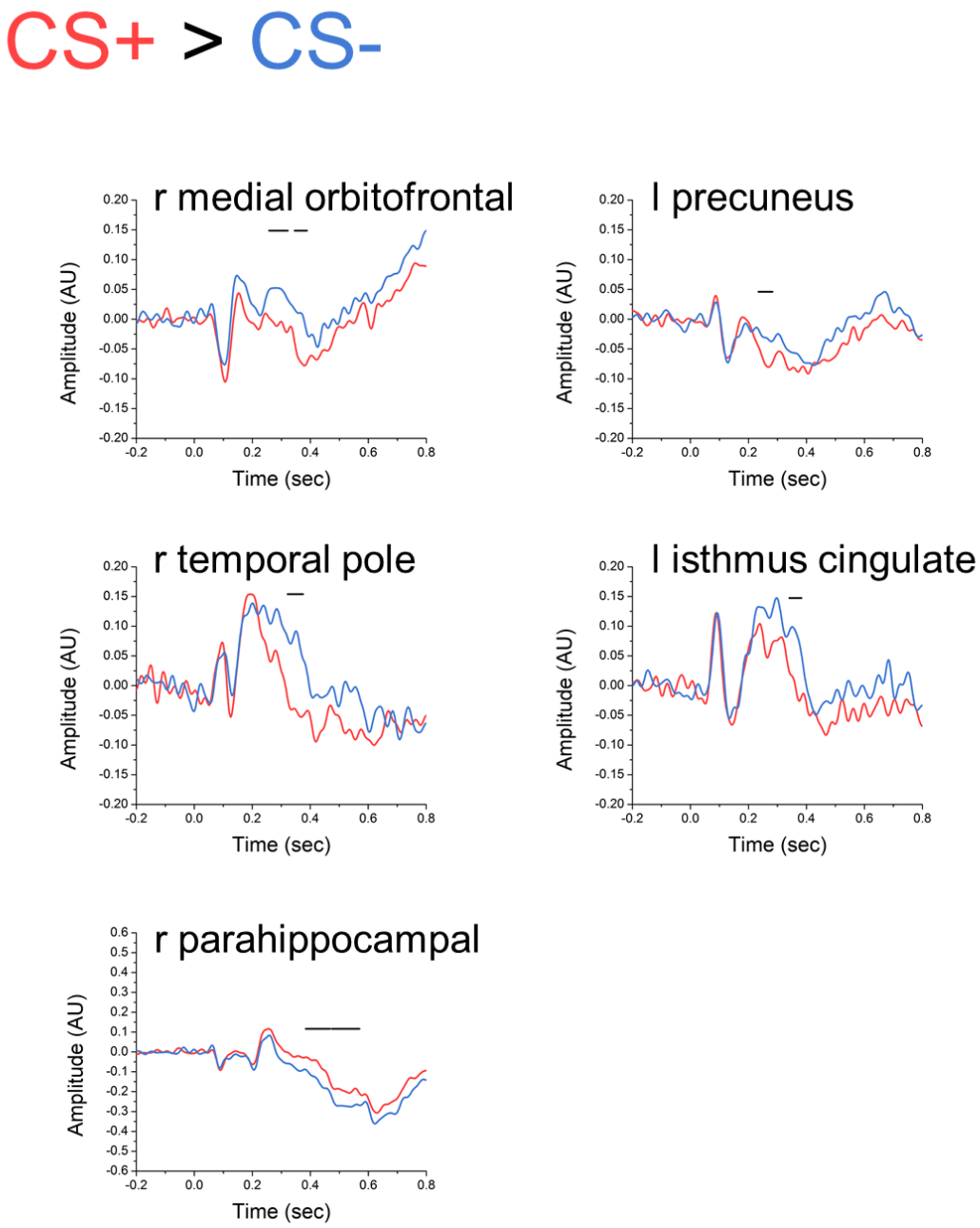

Figure 43. Evoked responses from regions showing transient differential activity for the CS+ > CS- comparison. Red = CS+. Blue = CS-.

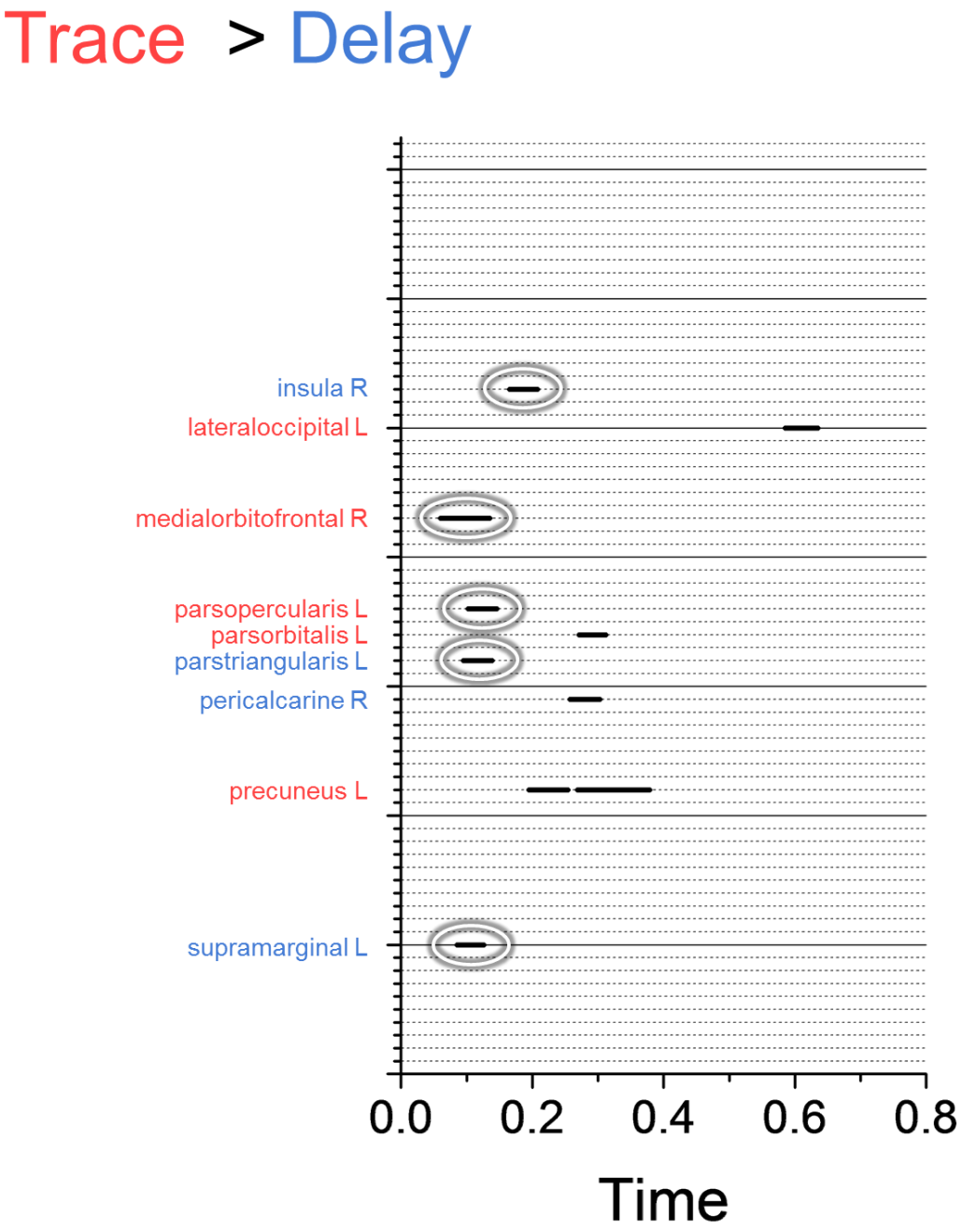

Figure 44. Timecourse of significant differential evoked responses for the Trace > Delay comparison. Label color represents the direction of the effect. Circled effects were considered transient and graphed individually below.

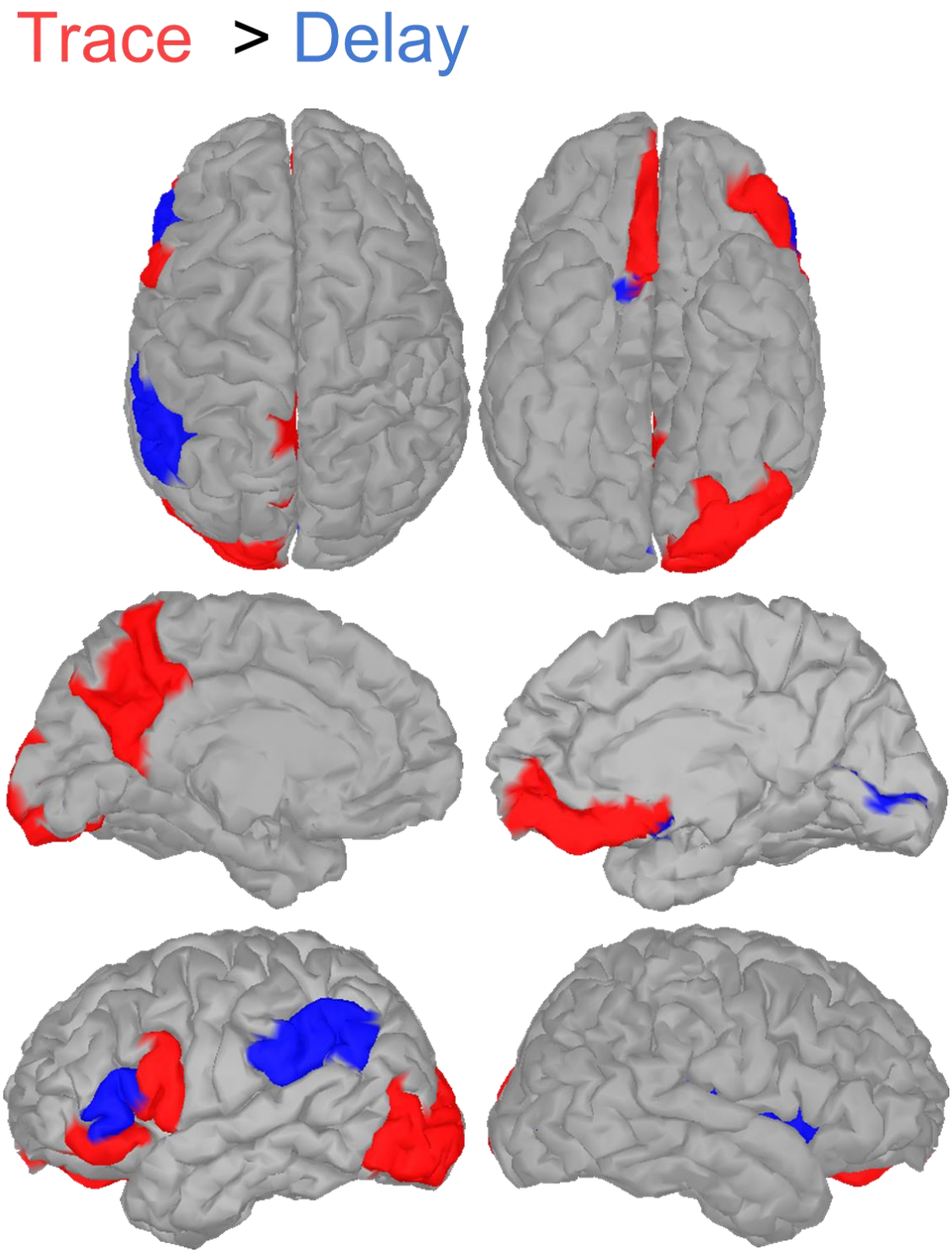

Figure 45. Regions showing differential activity for the Trace > Delay comparison. Colors represent the direction of the effect.

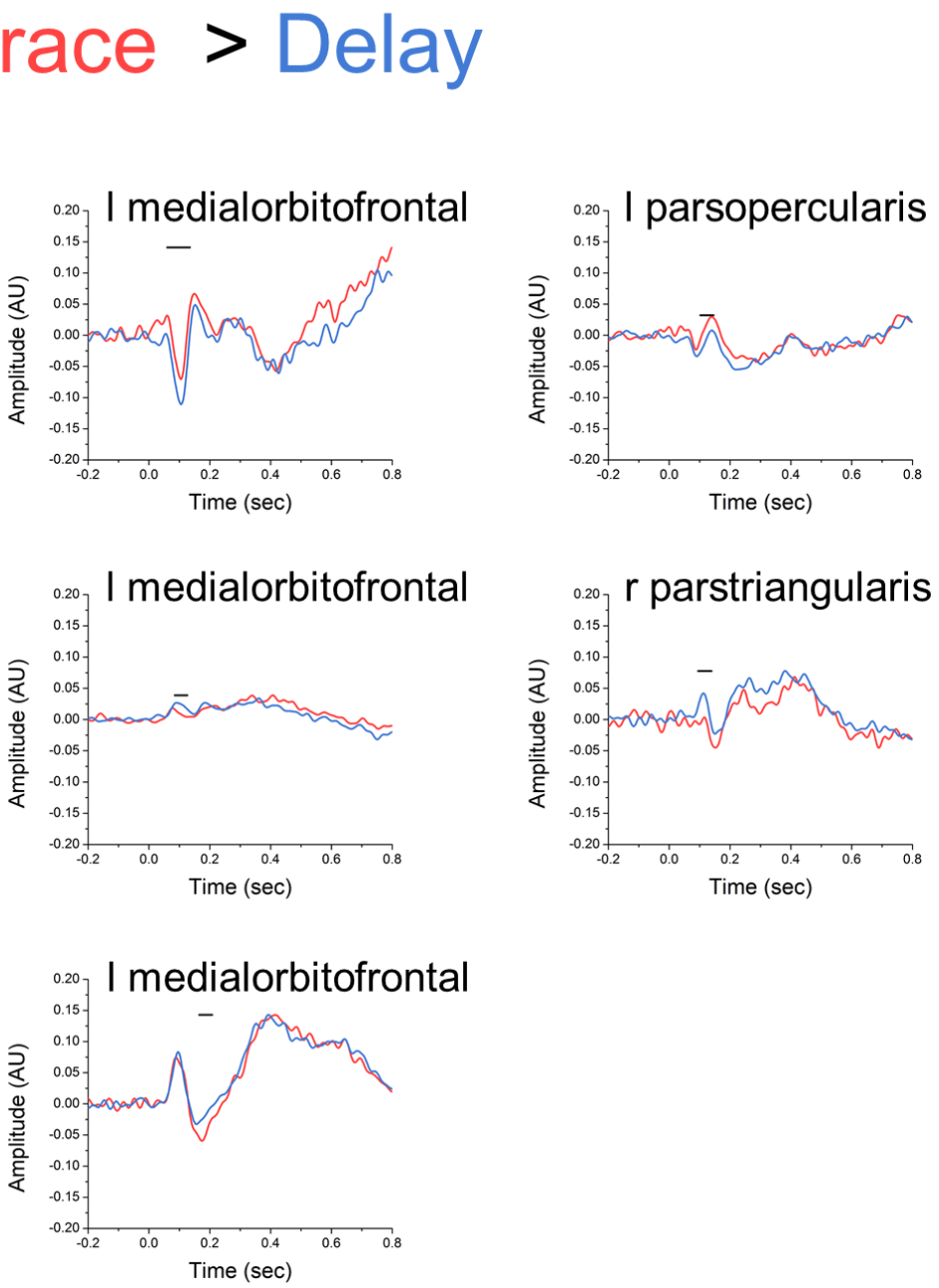

Figure 46. Evoked responses from regions showing transient differential activity for the Trace > Delay comparison. Red = Trace. Blue = Delay.

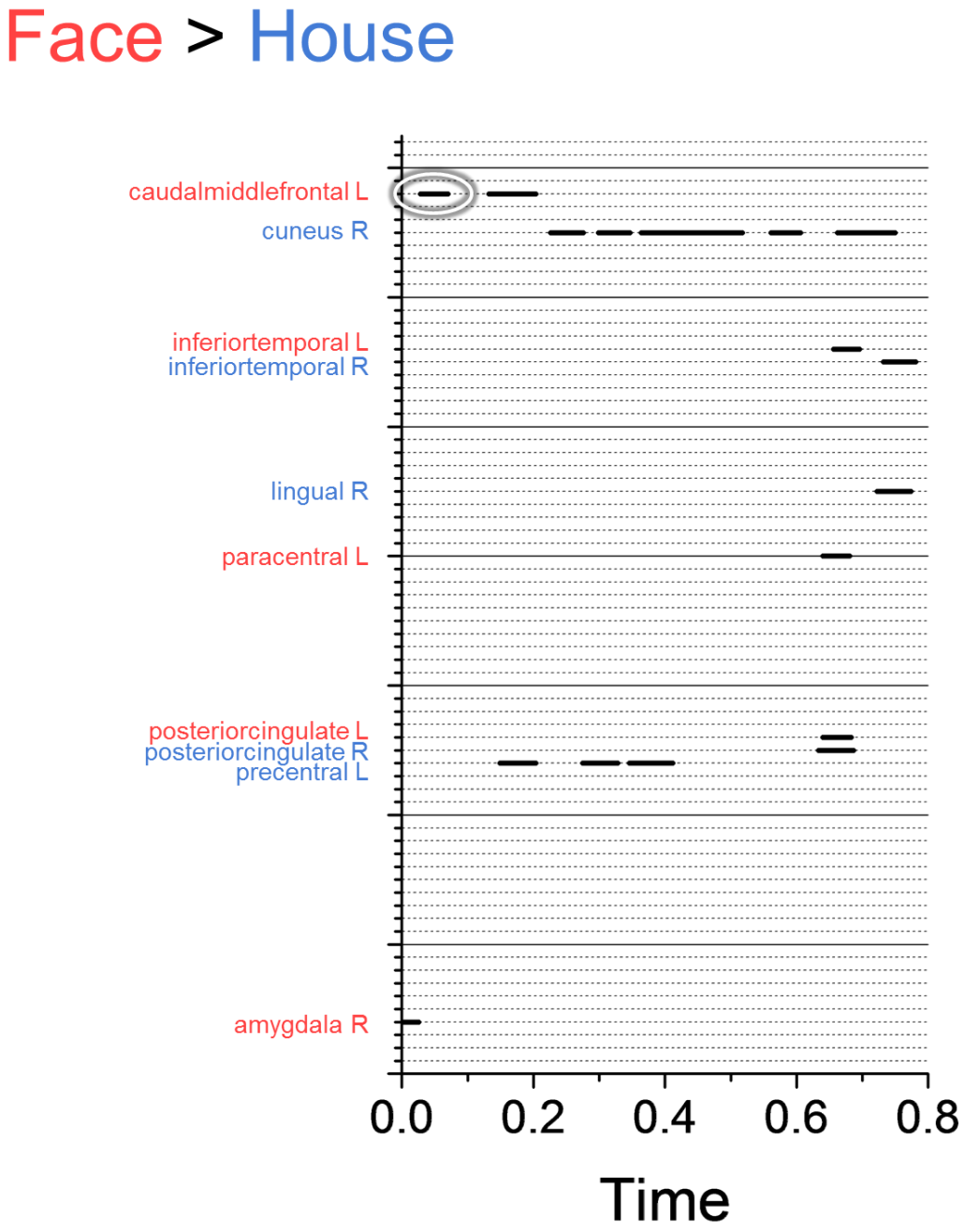

Figure 47. Timecourse of significant differential evoked responses for the Face > House comparison. Label color represents the direction of the effect. Circled effects were considered transient and graphed individually below.

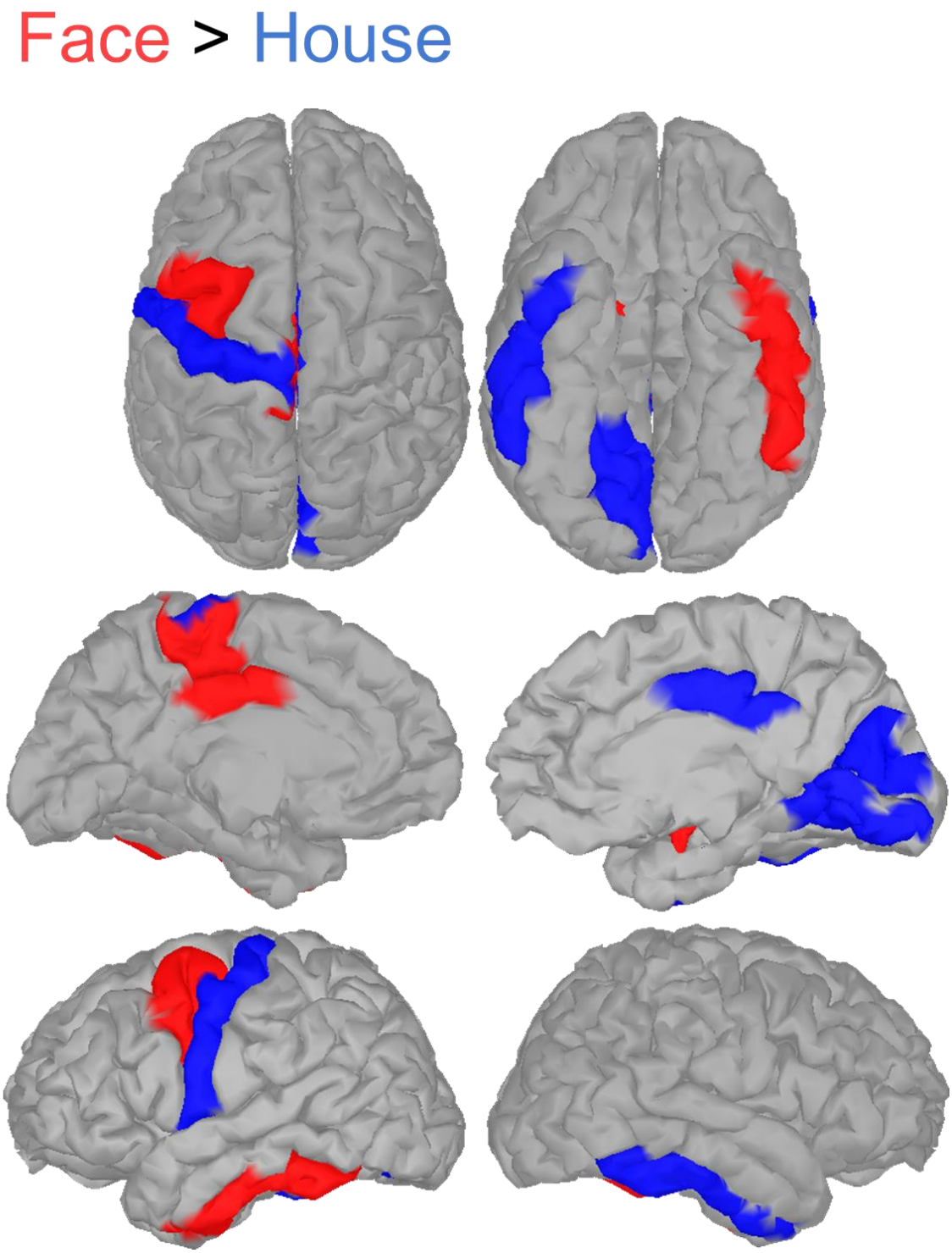

Figure 48. Regions showing differential activity for the Face > House comparison. Colors represent the direction of the effect.

Face > House

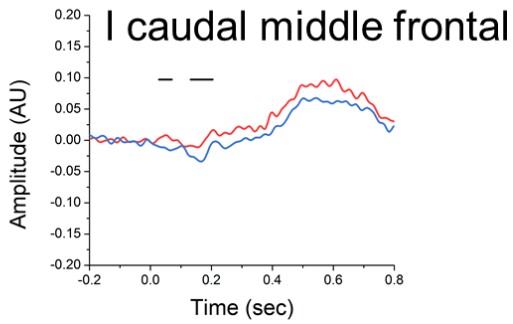

Figure 49. Evoked responses from region showing transient differential activity for the Face > House comparison. Red = Face. Blue = House.

3.4.5 CS+ - CS- Difference scores. I conducted the Delay > Trace and Face > House comparisons on the differential (CS+ - CS-) responses, but found no transient effects for either comparison. The sustained responses are summarized in Figures 50-53.

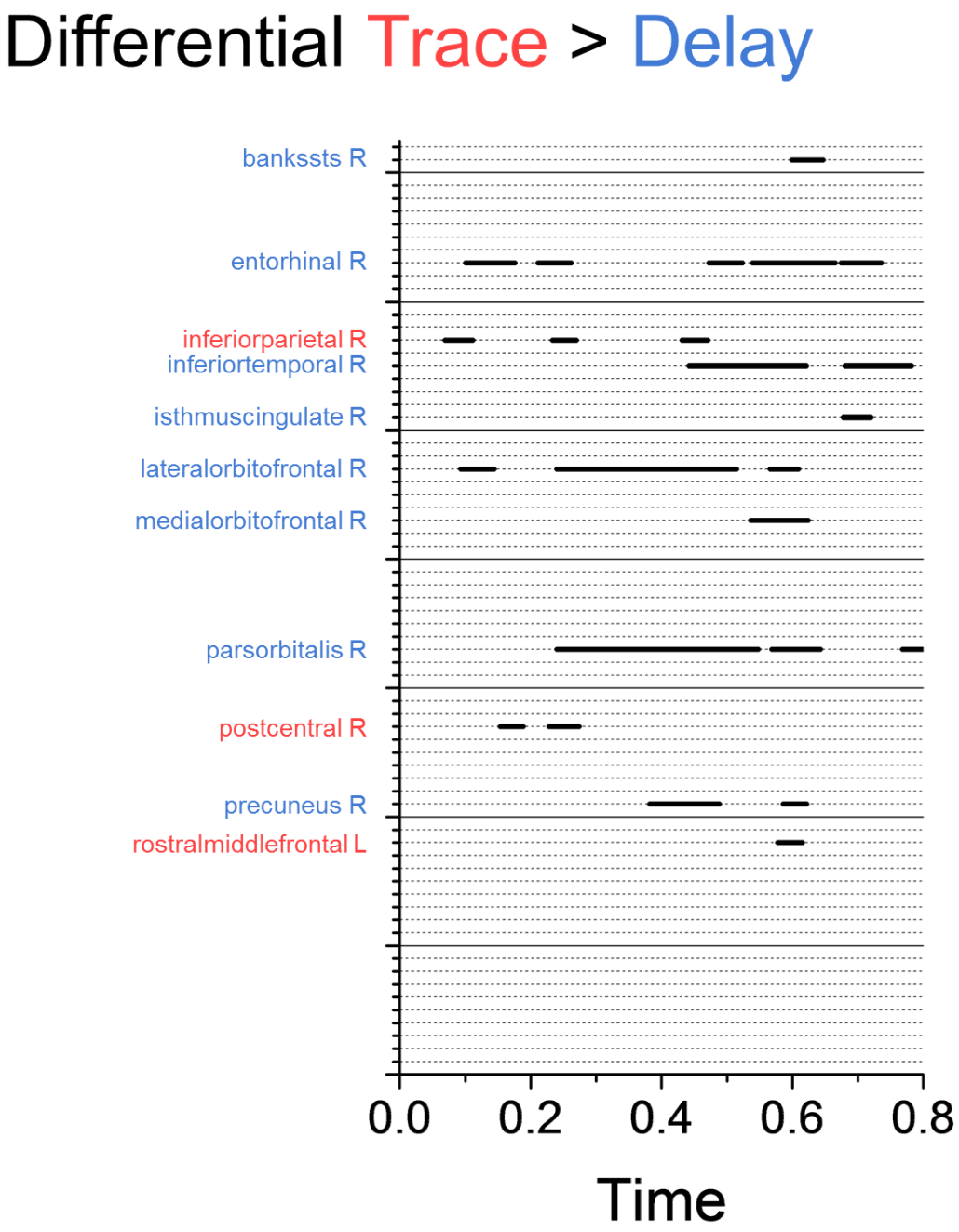

Figure 50. Timecourse of significant differential evoked responses for the Differential Trace > Differential Delay comparison. Label color represents the direction of the effect. Circled effects were considered transient and graphed individually below.

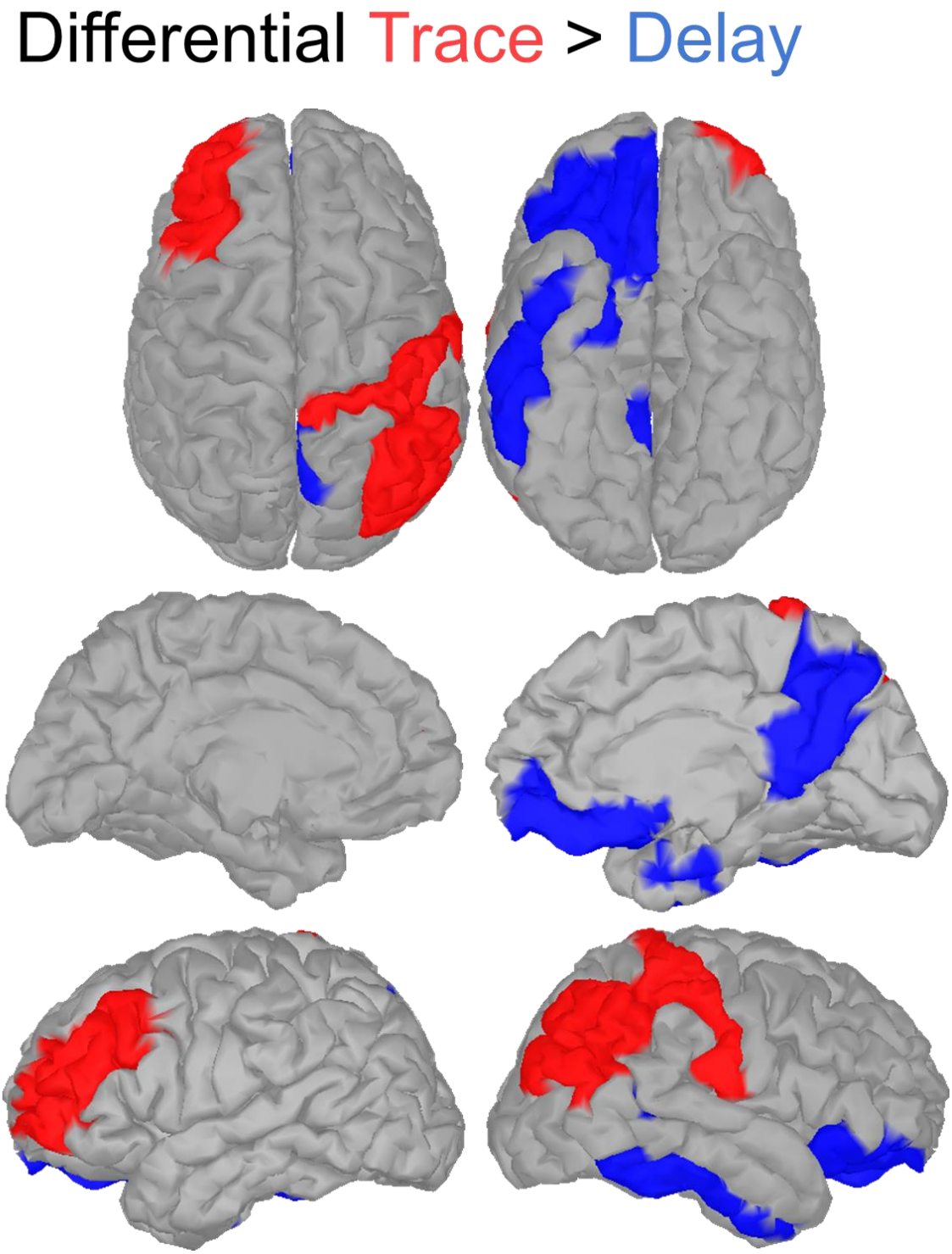

Figure 51. Regions showing differential activity for the Differential Trace > Differential Delay comparison. Colors represent the direction of the effect.

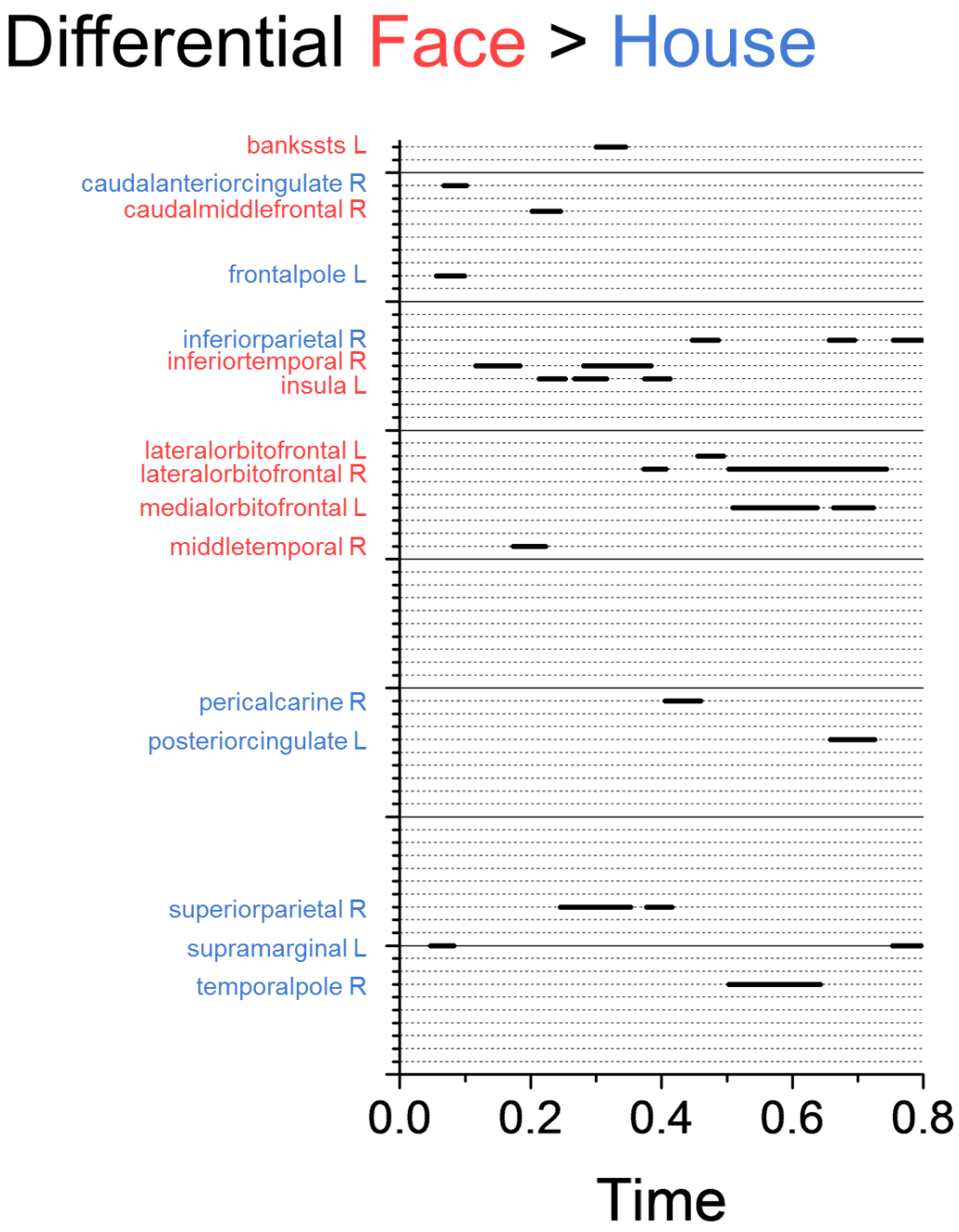

Figure 52. Timecourse of significant differential evoked responses for the Differential Face > Differential House comparison. Label color represents the direction of the effect. Circled effects were considered transient and graphed individually below.

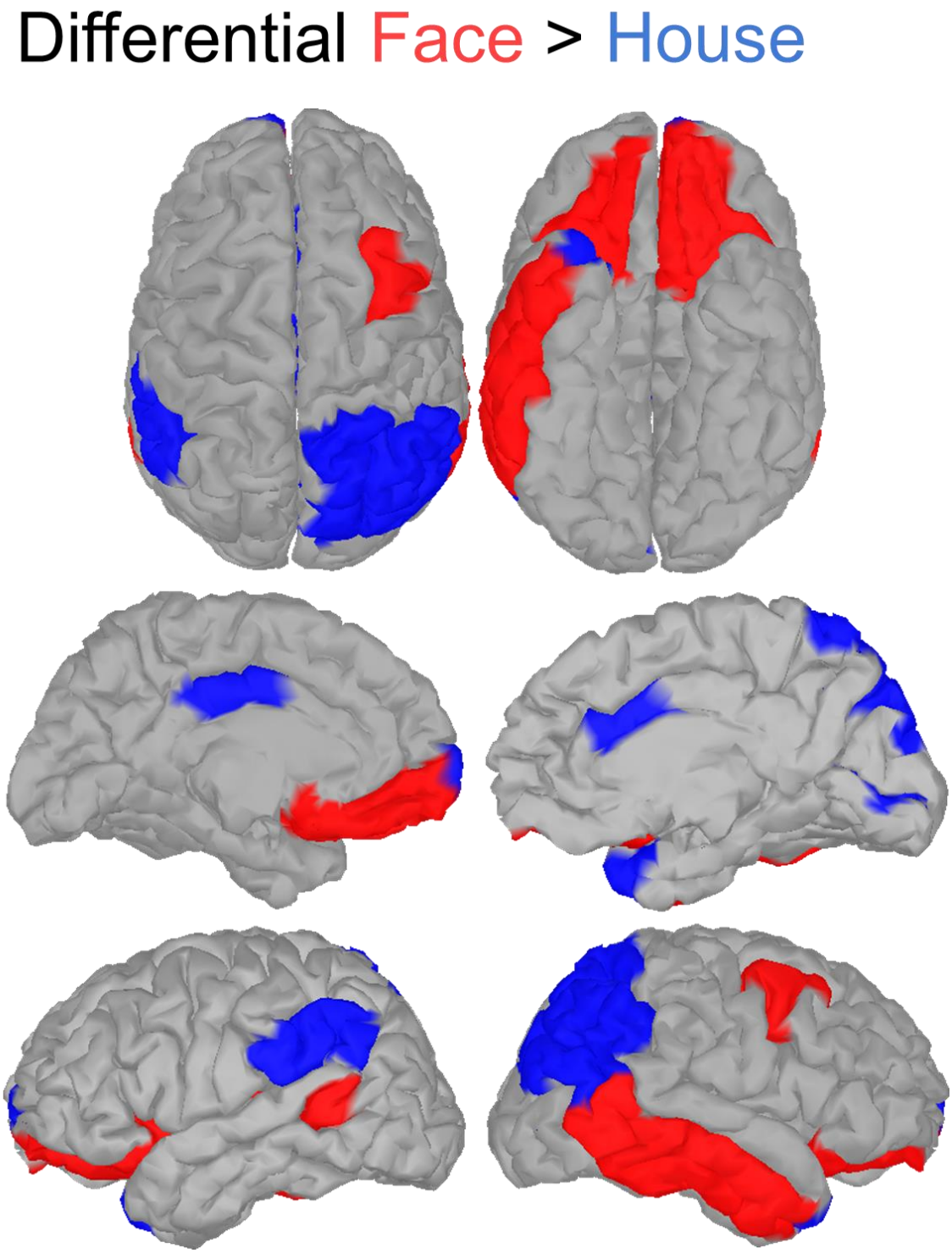

Figure 53. Regions showing differential activity for the Differential Face > Differential House comparison. Colors represent the direction of the effect.

3.5 Oscillations

For the time-frequency decompositions I conducted two comparisons: Delay CS+ > Delay CS-, and Trace CS+ > Trace CS-. The thresholding algorithm generally identified two types of clusters 1) those that reflected brief, broad spectrum increases in power, and 2) those that reflected sustained increases in power within a defined frequency band. I chose to focus on the latter. I identified four atlas regions that showed these types of responses, all within the beta frequency band (See Figure 54). First, the right insula and paracentral lobule show a differential increase (CS+ > CS-) in power as a function of delay but not trace conditioning. Similarly, the right lateral occipital cortex showed a differential decrease (CS+ < CS-) in power as a function of delay but not trace conditioning. Finally, the right superior frontal frontal gyrus showed a differential increase (CS+ > CS-) during the CS period and trace interval for trace but not delay conditioning.

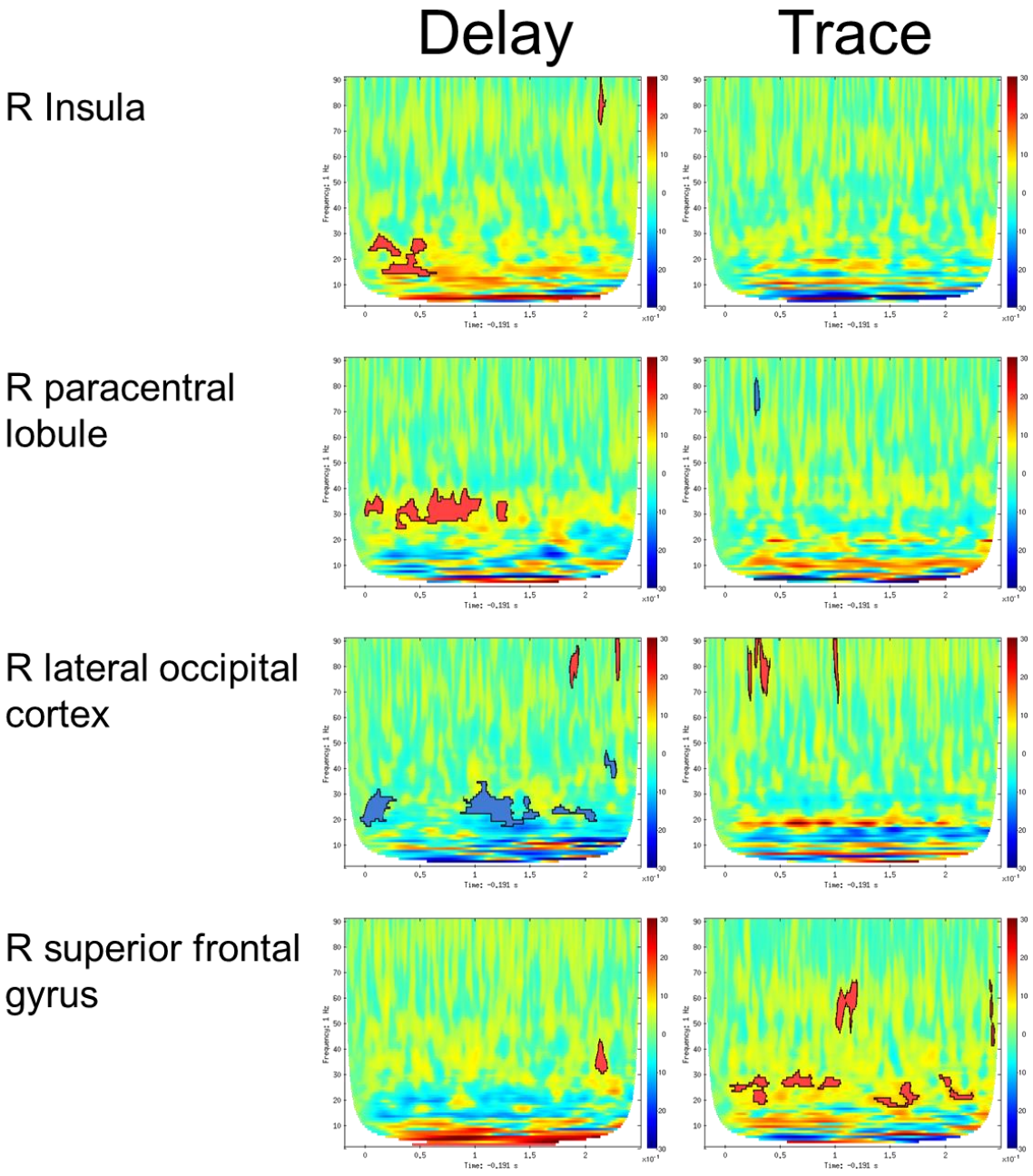

Figure 54. Differential power for the CS+ > CS- comparison for delay and trace conditioning. Warm colors represent CS+ > CS- values. Cool colors represent CS- > CS+ values. Red regions show significant CS+ > CS- difference. Blue regions show significant CS- > CS+ difference.

3.6 Coherence

For the coherence analyses I broke the data into 6 different frequency bands (delta, 2-4 Hz; theta, 5-7 Hz; alpha, 8-12 Hz; beta, 15-29 Hz; low gamma, 30-59 Hz; high gamma, 60-90 Hz). I then computed paired sample t-tests (CS+ > CS-) on the coherence estimates for the delay and trace conditions.

3.6.1 Delta-beta. Although there are distinct patterns of coherence across regions for delay and trace conditioning, these patterns seem to be consistent across the lower frequency bands (See Figures 55-58). For the delay condition I see greater coupling between the entorhinal cortex and fusiform gyrus for the CS+ than for the CS-. In general there seem to be more differences in low-frequency coupling for trace conditioning than for delay conditioning. Also, for the trace condition the left parahippocampal gyrus emerges as a hub region, showing differential coupling with several other regions (See Figure 57). Interestingly, among the regions that show low-frequency coherence with the left parahippocampal gyrus, there are several in the frontal and parietal cortices.

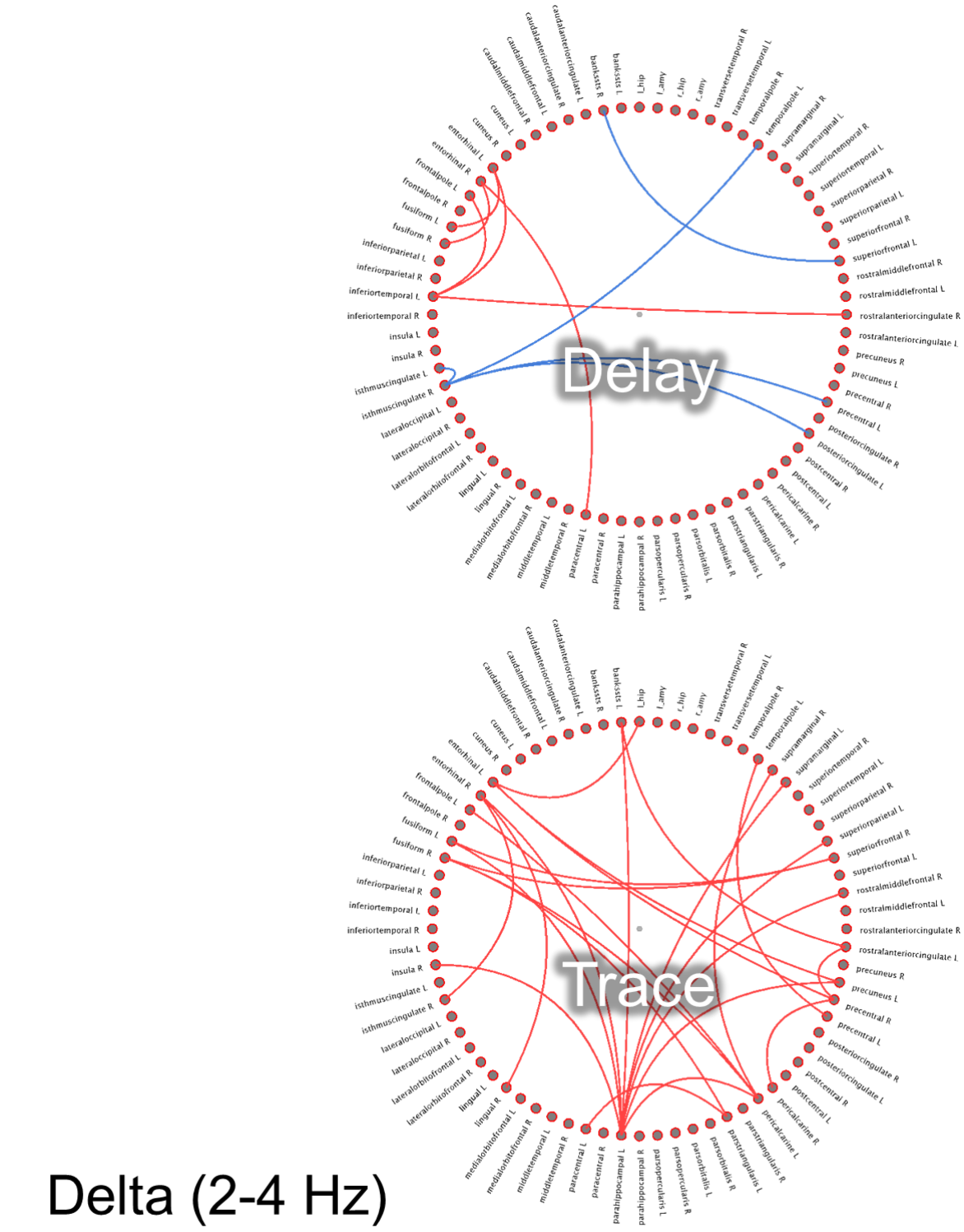

Figure 55. Differential coherence for the CS+ > CS- comparison for delay and trace conditioning. Red lines depict significant CS+ > CS- coherence difference. Blue lines depict significant CS- > CS+ difference.

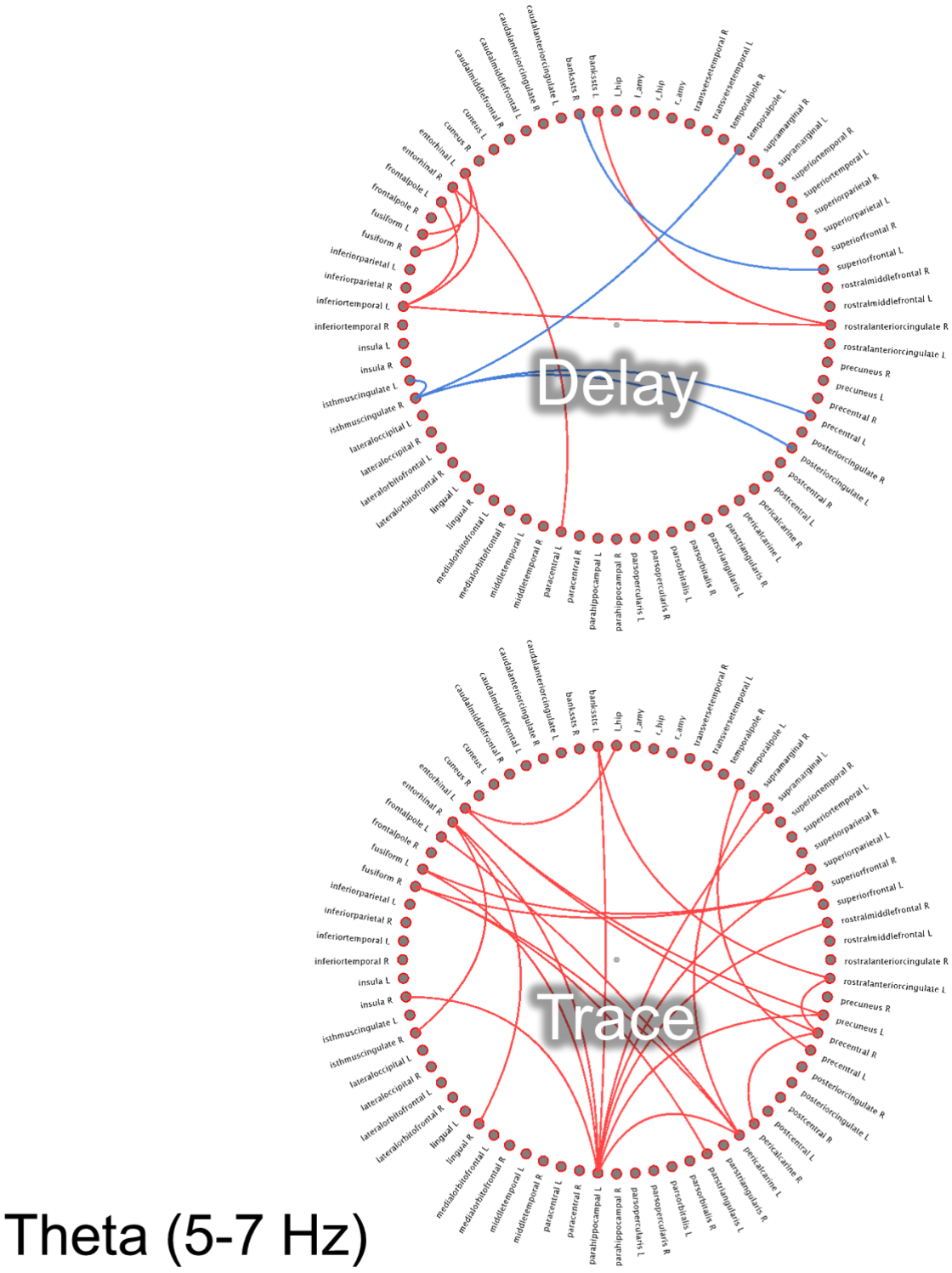

Figure 56. Differential coherence for the CS+ > CS- comparison for delay and trace conditioning. Red lines depict significant CS+ > CS- coherence difference. Blue lines depict significant CS- > CS+ difference.

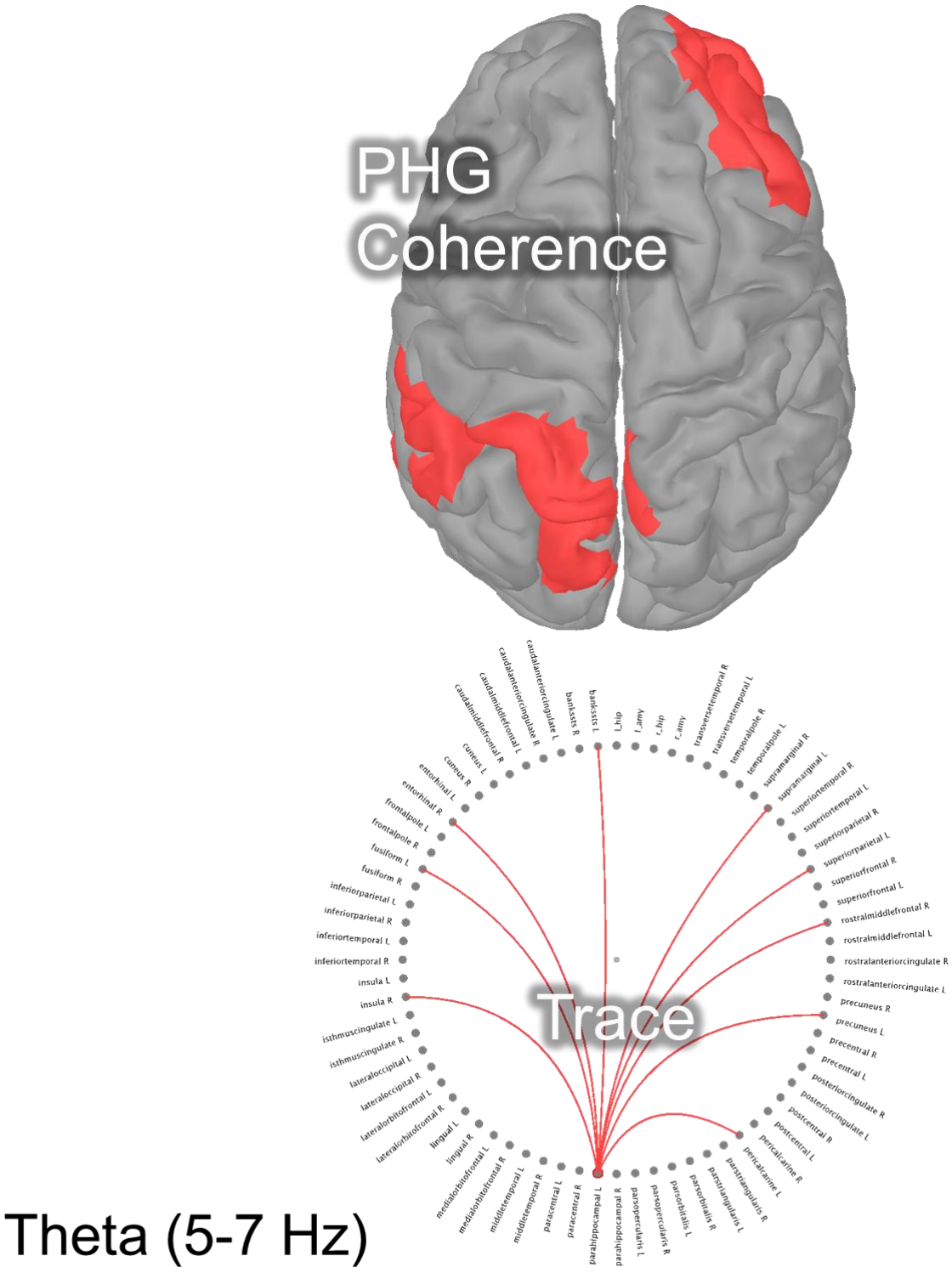

Figure 57. Regions showing differential theta coherence with the left parahippocampal gyrus. (Top) Regions plotted on cortical surface. (Bottom) Coherence map with regions what that differential theta coherence with the left parahippocampal gyrus for trace conditioning. Red lines and areas depict significant CS+ > CS- coherence difference.

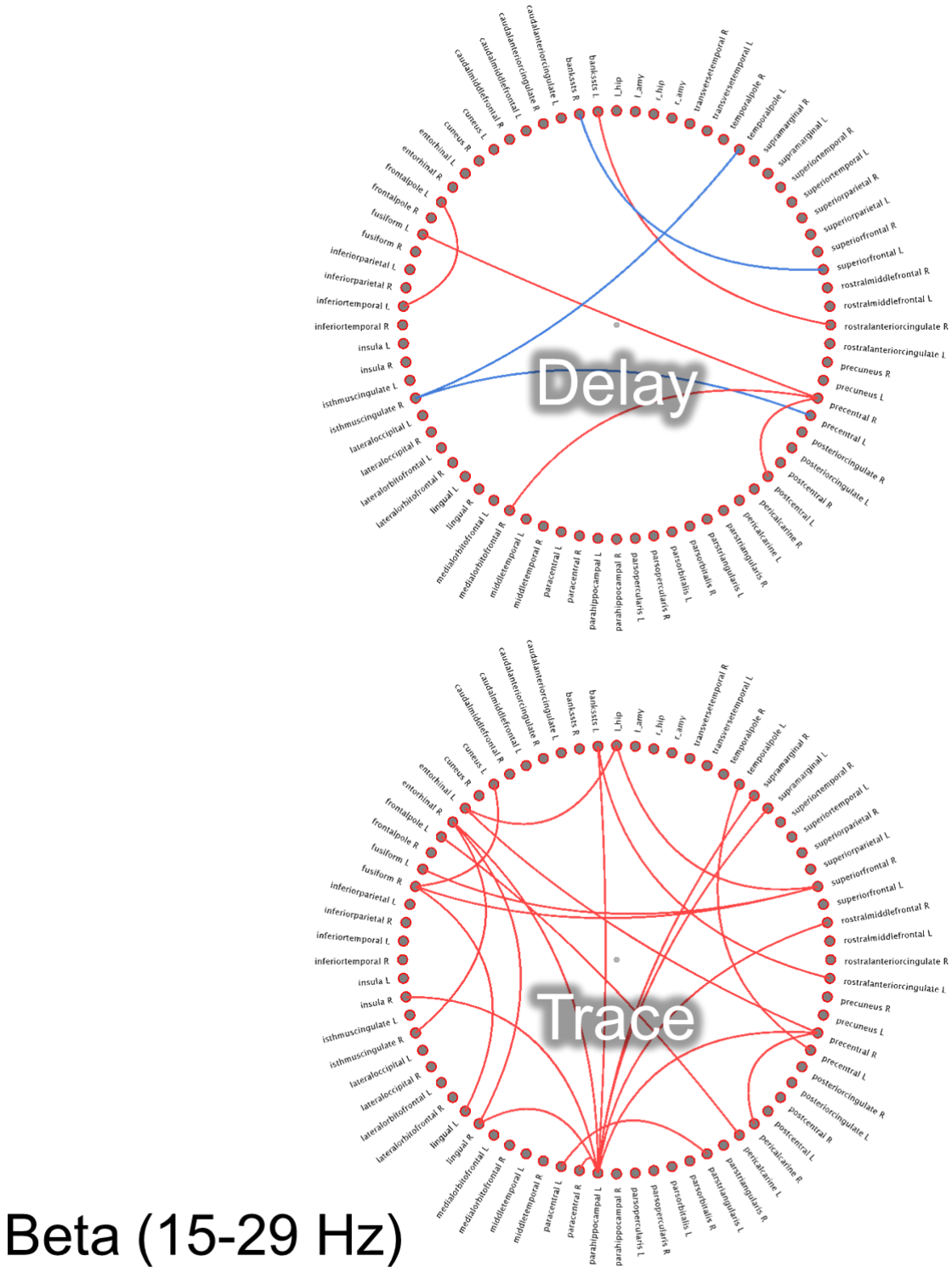

Figure 58. Differential coherence for the CS+ > CS- comparison for delay and trace conditioning. Red lines depict significant CS+ > CS- coherence difference. Blue lines depict significant CS- > CS+ difference.

3.6.2 Gamma. In the gamma frequency bands, the pattern of more differential coupling for trace than delay conditioning appears to hold (See Figures 59-60). For delay there are very few instances in differential coupling in these frequency bands, but for trace conditioning there are several. In the low gamma band, there is differential coupling between the entorhinal cortex and the caudal anterior cingulate cortex, as well as the insula. In addition, there is an increase in differential coupling between the left insula and two regions of the inferior frontal gyrus. In the high gamma band, there is coupling between the entorhinal cortex and the isthmus cingulate. In addition, there is coupling between the lateral occipital cortex and the fusiform gyrus.

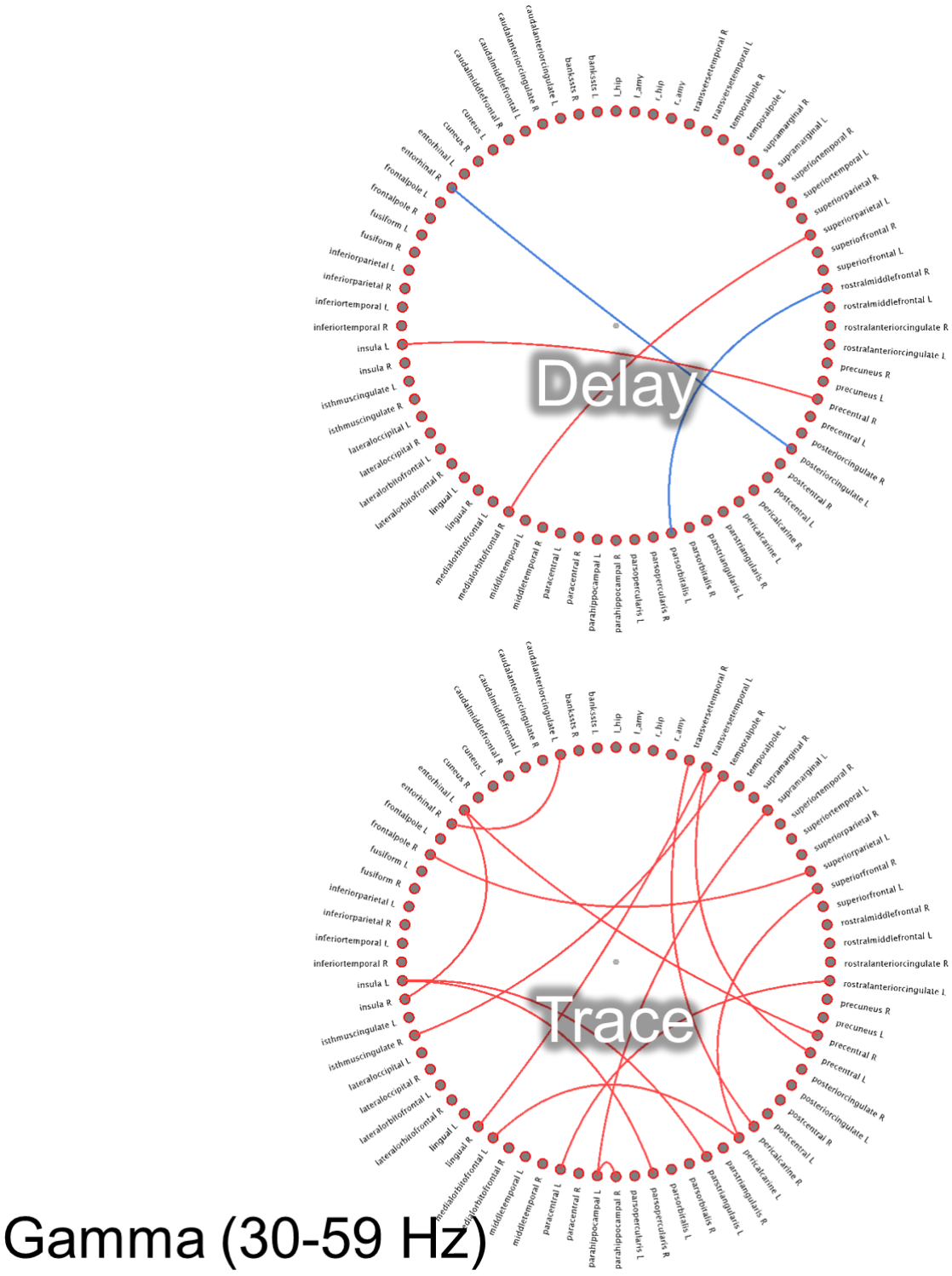

Figure 59. Differential coherence for the CS+ > CS- comparison for delay and trace conditioning. Red lines depict significant CS+ > CS- coherence difference. Blue lines depict significant CS- > CS+ difference.

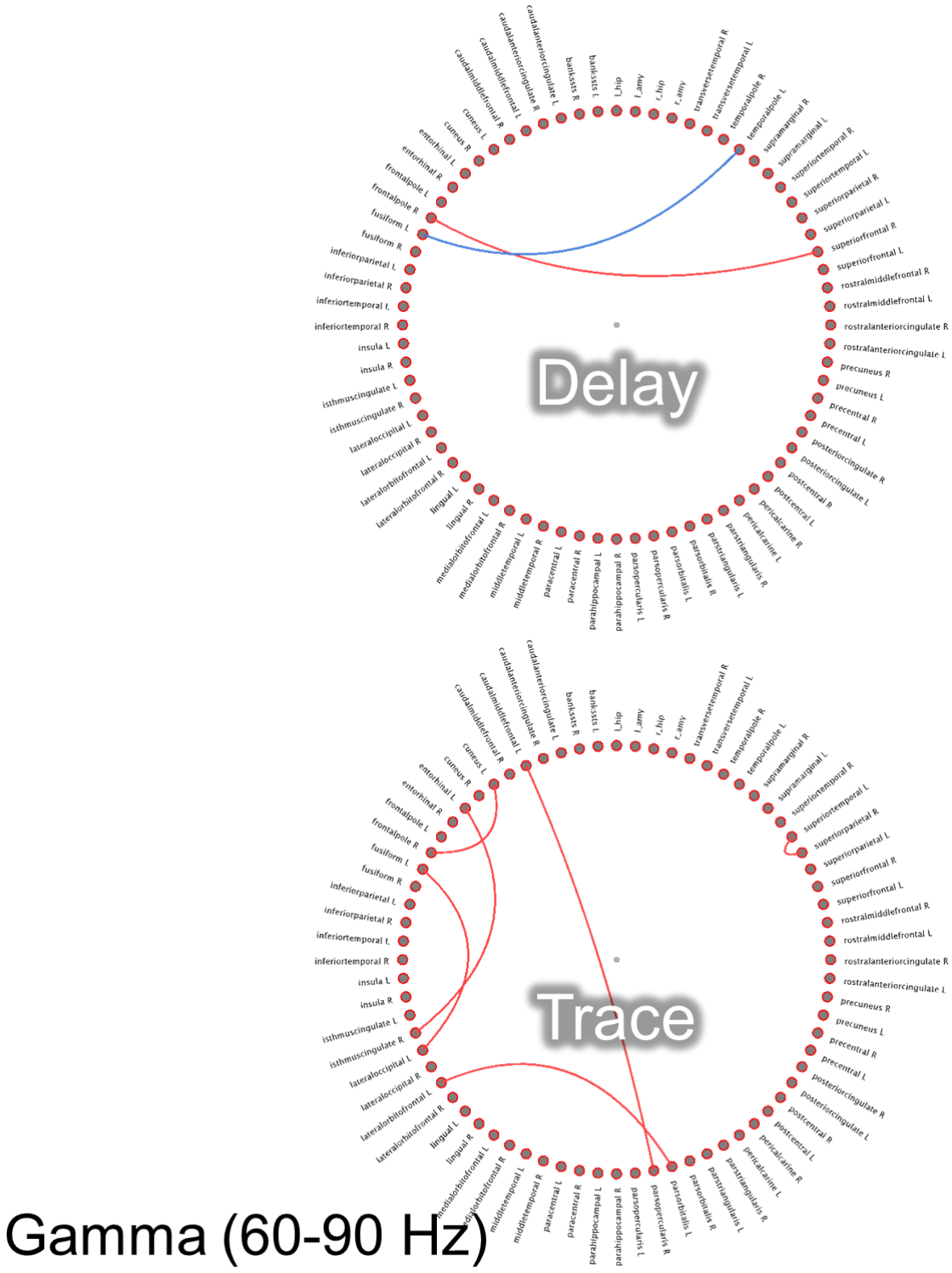

Figure 60. Differential coherence for the CS+ > CS- comparison for delay and trace conditioning. Red lines depict significant CS+ > CS- coherence difference. Blue lines depict significant CS- > CS+ difference.

4 Discussion

The purpose of this experiment was to investigate trace conditioning in humans using MEG to record brain activity at a high temporal resolution. I exposed subjects to differential delay and trace conditioning, using images of faces and houses as CSs. I found evidence of learning using both implicit (pupil dilation) and explicit (UCS expectancy) measures. Although behavioral measures of learning were similar for delay and trace conditioning, neural responses differed as a function of conditioning type. First, I found that trace but not delay conditioning resulted differences in evoked responses in frontal and parietal regions. Second, I found that delay conditioning induced beta oscillations in the insula and paracentral lobule, while trace conditioning induced beta oscillations in the superior frontal gyrus. Finally, I found that trace but not delay conditioning resulted in a learning related increase in low-frequency coupling between brain regions. In addition, this increase seems to be driven by an increase in coupling between the left parahippocampal gyrus and frontal and parietal regions.

Previous trace conditioning studies in humans (Büchel et al., 1999; Knight, Cheng, et al., 2004) and non-human animals (Gilmartin & McEchron, 2005b; Gilmartin et al., 2013) show that trace conditioning relies on activity in the hippocampus and prefrontal cortex. The prefrontal cortex is thought to bridge the gap between the CS and the UCS, but it is currently unclear what role the hippocampus plays. Consistent with these studies we find differential activity in the MTL and prefrontal cortex. Additionally, we show that a single source of activity within the MTL displays increased coherence with several frontal and parietal cortical regions. Taken together these results suggest that the MTL, possibly the hippocampus, coordinates the activity of a distributed network of

cortical regions during the trace interval.

Table 2. Summary of major findings.

Comparison	Effect
Delay	
	Differential activity inferior regions like OFC.
	Increased theta coherence between the MTL and visual cortex.
Trace	
	Differential evoked response in frontal and parietal regions.
	Increased theta coherence in a network of regions, coordinated by the MTL.

4.1 Implicit measures of learning.

As hypothesized subjects show differential pupil dilation during the training trials. Consistent with previous research (Reinhard et al., 2006; Reinhard & Lachnit, 2002), these results suggest that pupil dilation can serve as an alternative measure of conditioning when trial length is an issue for other methods like SCR. In addition, there were no learning related differences based on either conditioning type or stimulus content. These results suggest that learning was similar for these conditions. Although there were no learning related interactions, there was a significant main effect for conditioning type. Pupil diameter was slightly larger on trace trials than delay trails. However, this effect is likely due to the physical properties of the visual stimulation (i.e. viewing a picture vs. viewing a blank screen) rather than learning.

Based on previous work, we expected subjects to show conditioned bradycardia across all conditions (Headley & Weinberger, 2011; Hermans et al., 2012). However, this is not what we observed. Instead, we found an initial decrease in heart rate (i.e. increase

in interbeat interval), followed by a steady increase in heart rate (i.e. decrease in interbeat interval) for all conditions. In addition, we found that for trace conditioning, there was a different pattern on the early interbeat intervals than on the late interbeat intervals. For the early interbeat intervals, the initial decrease in heart rate was attenuated, but only for the house CS+. Although interesting, I do not have a good explanation for why this should be the case. For the late interbeat intervals, the pattern is a little easier to interpret. Although heart rate is generally increasing, this increase is attenuated for both the face and the house CS+. This pattern may represent the initial stage of a conditioned bradicardiac response, as others have observed (Headley & Weinberger, 2011; Hermans et al., 2012; Moratti et al., 2006; Moratti & Keil, 2005).

4.2 Explicit measures of learning.

As hypothesized, subjects rapidly learned the CS-UCS contingencies during the training trials. This is consistent across nearly every conditioning experiment that uses a similar online expectancy rating measure (Balderston, Schultz, Baillet, & Helmstetter, 2013; Cheng et al., 2006b, 2003, 2007a; Cheng, Richards, & Helmstetter, 2007b; Knight, Smith, et al., 2004; Knight et al., 1999; Schultz, Balderston, Geiger, & Helmstetter, 2013; Schultz, Balderston, & Helmstetter, 2012; Schultz & Helmstetter, 2010b). Unless there is a manipulation of awareness the learning process in differential conditioning is not complex, and these ratings reflect the simplicity of this approach. There was also a significant conditioning by stimulus content interaction. Although marginal, this effect was driven by the fact that subjects were slightly more confident about the face CS+ than the house CS+. It is possible that the faces were slightly easier to discriminate than the houses. Consistent with this hypothesis subjects were slightly faster to begin their rating

for faces than houses during the trace trials. In addition, it seemed that subjects' evaluation of the stimuli after the experiment may have been affected by stimulus content. In general, subjects showed typical evaluative conditioning effects (Tabbert et al., 2010). They rated the CS+ as more arousing and negative than the CS-. Although not significant, for both arousal and valence there appeared to be a trend toward a 3-way interaction, driven by the fact that subjects seemed to be less confident in their ratings of the houses that had been assigned to the trace condition.

Interestingly, subjects seemed to not only learn the specific picture – shock contingencies, they also seemed to learn the basic design of the experiment. This is evidenced by the fact that across training runs it appears that subjects seemingly gain the ability to correctly guess the contingencies on the first training trial. This is likely due to two aspects of the experimental design: 1) there is always one face and one house paired with a shock, and one face and one house not paired with the shock, 2) trial order was counterbalanced across subjects. What this means is that once a given subject has learned the design of the experiment he or she will rate the second face presentation based on the assignment of the first face presentation. That is, if a given subject gets the face CS+ first, they will likely correctly rate the subsequent face as a CS-.

4.3 Neural mechanisms supporting delay and trace fear conditioning.

4.3.1 Delay. The differential evoked responses for delay conditioning are primarily found in regions on the inferior portion of the brain. This is true for both transient and sustained responses. For instance, we see transient learning related differences during the M170 for both the left orbitofrontal gyrus and the right entorhinal

cortex. Additionally, we see sustained differences in the right parahippocampal gyrus and right inferior temporal gyrus.

Although this partially replicates previous work with delay fear conditioning (Knight, Cheng, et al., 2004; Moratti et al., 2006; Moratti & Keil, 2005), there are a number differences between our results, and those from previous fMRI and MEG studies. First, I did not see the expected learning related differences in evoked responding; however, it is possible that these regions are contributing differently to the learning process. For instance, I found differential beta activity in both the insula and the paracentral lobule for delay but not trace conditioning. These regions are commonly found in fear conditioning studies (Haritha, Wood, Ver Hoef, & Knight, 2012; Schultz et al., 2012; Simmons, Strigo, Matthews, Paulus, & Stein, 2006). Some have suggested that the insula is important for processing bottom-up signals from the body (Craig, 2009). Given that our subjects were shocked on the ankle, the beta activity in the paracentral lobule may represent activation of the UCS representation (Knight, Waters, King, & Bandettini, 2010).

Unlike previous studies, I did not observe differential evoked responses in visual cortical regions for delay conditioning. One possible reason for this is that I used faces and houses as CSs. It could be that this main effect has been reduced because these stimuli activate different visual cortical regions (Epstein, 2008; Kanwisher & Yovel, 2006). However, I did observe differences in beta activity in the right lateral occipital cortex. This structure has been previously shown to respond differentially to emotional and neutral stimuli (Gläscher, Rose, & Büchel, 2007). Interestingly, we also find a learning related increase in theta coherence between the entorhinal cortex and fusiform

gyrus, suggesting that communication between these regions is important for delay conditioning.

Work with laboratory animals has suggested that the orbitofrontal cortex plays an important role in both classical and operant conditioning (J. J. Clark, Hollon, & Phillips, 2012; Gottfried & Dolan, 2004; Moratti & Keil, 2005). However, activation in this region is not commonly seen in fMRI studies of fear conditioning. This is likely due to issues with signal dropout due to the fact that this region is so close to the sinuses. Interestingly, we find robust differential activity in this region for delay conditioning, suggesting that MEG may be better suited than fMRI to recover activity from this region.

There were a number of differences between our results and previous studies. One potential explanation for these results is the differences in the timescales used during training. For instance, we used a 2.5 second ISI for our experiments, while many fMRI studies of fear conditioning use ISIs of 8 to ten seconds (Schultz et al., 2012). Importantly, this difference in ISI may lead to different psychological processes. For evoked brain potentials, the precise timing of individual components has been thoroughly characterized (Kok, 1997), but this precise characterization includes approximately the first 500 ms. The functional significance of evoked brain potentials at longer latencies is less well understood. Furthermore, given the colinearity of the BOLD response, it is difficult to determine whether differences in BOLD magnitude are due to differences in the latency or the magnitude of neural activity (Logothetis, 2008).

4.3.2 Trace. Unlike delay, differences in evoked responses tend to occur primarily for superior regions. For instance, there are transient evoked responses early in the CS

period for both the middle frontal gyrus and the inferior parietal lobule. There activation of the dorsal anterior cingulate cortex and the right parahippocampal gyrus (this is similar to delay) during the trace interval. These results suggest that frontal and parietal regions are important for trace conditioning. Consistent with this hypothesis, I also see more differential activity in frontal and parietal regions for trace when I directly compare delay and trace conditioning. I also see differential beta power in the superior frontal gyrus during the trace interval. Most importantly, I see coherent low-frequency oscillations between the parahippocampal gyrus and these frontal and parietal regions.

Taken together, these results suggest that trace conditioning activates a network of frontal and parietal cortical regions that are coordinated by the MTL. Interestingly, a recent study of autobiographical memory recall found a similar network (Fuentemilla, Barnes, Düzel, & Levine, 2013). They asked subjects to recall autobiographical events while resting in the MEG. They then isolated a seed region in the MTL and computed theta coherence across the cortex. As with our results, they found greater theta coherence between their MTL region and the dorsolateral prefrontal cortex, and precuneus during autobiographical recall than during a semantic task. Interestingly, this theta coherence was also correlated the vividness of the recalled memories (Fuentemilla et al., 2013).

Some have suggested that theta coherence facilitates long-term bi-directional neural communication (Fell & Axmacher, 2011), and that the hippocampus has a particularly dominant theta rhythm (Buzsáki & Moser, 2013). Work with laboratory animals suggests that both the hippocampus and prefrontal cortex are necessary for trace conditioning (Gilmartin & Helmstetter, 2010; Gilmartin & McEchron, 2005a, 2005b; Gilmartin et al., 2013), and consistent with this fMRI studies often find activation of the

hippocampus and prefrontal cortex during trace fear conditioning (Haritha et al., 2012; Knight, Cheng, et al., 2004). This study extends these results by simultaneously recording neural activity in the prefrontal cortex and MTL, and demonstrating communication within the theta frequency range. Given that trace fear conditioning is thought to require awareness in humans (Knight et al., 2006), these results suggest that the hippocampus facilitates encoding of a declarative memory event by coordinating the activity of distinct cortical regions. This idea is consistent with the multiple trace theory of human memory (Nadel, Samsonovich, Ryan, & Moscovitch, 2000).

4.4 Conclusions

In this experiment I exposed subjects to delay and trace fear conditioning while recording their brain activity with magnetoencephalography. For delay conditioning I saw a learning related increase in coupling between the entorhinal cortex and the fusiform gyrus. For trace conditioning I saw a learning related increase in coupling between the left parahippocampal gyrus and several frontal and parietal cortical regions. These results suggest that trace conditioning recruits a network of frontal and parietal regions, and that the activity in these regions is coordinated by the medial temporal lobes.

References

Ahs, F., Frans, O., Tibblin, B., Kumlien, E., & Fredrikson, M. (2010). The effects of medial temporal lobe resections on verbal threat and fear conditioning. *Biological psychology*, *83*(1), 41–46. Retrieved from http://www.ncbi.nlm.nih.gov/entrez/query.fcgi?cmd=Retrieve&db=PubMed&dopt=Citation&list_uids=19836434

Asli, O., Kulvedrøsten, S., Solbakken, L. E., Flaten, M. A., & Kulvedrosten, S. (2009). Fear potentiated startle at short intervals following conditioned stimulus onset during delay but not trace conditioning. *Psychophysiology*, *46*(4), 880–8. doi:10.1111/j.1469-8986.2009.00809.x

Baddeley, A. (1992). Working memory. *Science*, *255*(5044), 556–559. Retrieved from http://www.ncbi.nlm.nih.gov/entrez/query.fcgi?cmd=Retrieve&db=PubMed&dopt=Citation&list_uids=1736359

Balderston, N. L., & Helmstetter, F. J. (2010). Conditioning with masked stimuli affects the timecourse of skin conductance responses. *Behavioral neuroscience*, *124*(4), 478–489. doi:10.1037/a0019927

Balderston, N. L., Schultz, D. H., Baillet, S., & Helmstetter, F. J. (2013). How to Detect Amygdala Activity with Magnetoencephalography using Source Imaging. *Journal of visualized experiments : JoVE*. doi:10.3791/50212

Bangasser, D. a, Waxler, D. E., Santollo, J., & Shors, T. J. (2006). Trace conditioning and the hippocampus: the importance of contiguity. *The Journal of neuroscience : the official journal of the Society for Neuroscience*, *26*(34), 8702–6. doi:10.1523/JNEUROSCI.1742-06.2006

Battaglia, F. P., Benchenane, K., Sirota, A., Pennartz, C. M. a, & Wiener, S. I. (2011). The hippocampus: hub of brain network communication for memory. *Trends in cognitive sciences*, *15*(7), 310–318. doi:10.1016/j.tics.2011.05.008

Bauer, M., Oostenveld, R., Peeters, M., & Fries, P. (2006). Tactile spatial attention enhances gamma-band activity in somatosensory cortex and reduces low-frequency activity in parieto-occipital areas. *The Journal of neuroscience : the official journal of the Society for Neuroscience*, *26*(2), 490–501. doi:10.1523/JNEUROSCI.5228-04.2006

Bechara, A., Tranel, D., Damasio, H., Adolphs, R., Rockland, C., & Damasio, A. (1995). Double dissociation of conditioning and declarative knowledge relative to the amygdala and hippocampus in humans. *Science*, *269*(5227), 1115–1118. Retrieved from http://www.ncbi.nlm.nih.gov/entrez/query.fcgi?cmd=Retrieve&db=PubMed&dopt=Citation&list_uids=7652558

Benchenane, K., Peyrache, A., Khamassi, M., Tierney, P. L., Gioanni, Y., Battaglia, F. P., & Wiener, S. I. (2010). Coherent theta oscillations and reorganization of spike

timing in the hippocampal- prefrontal network upon learning. *Neuron*, *66*(6), 921–36. doi:10.1016/j.neuron.2010.05.013

Bertrand, O., & Tallon-Baudry, C. (2000). Oscillatory gamma activity in humans: a possible role for object representation. *International Journal of Psychophysiology*, *38*(3), 211–23. Retrieved from http://www.ncbi.nlm.nih.gov/pubmed/11102663

Beylin, a V, Gandhi, C. C., Wood, G. E., Talk, a C., Matzel, L. D., & Shors, T. J. (2001). The role of the hippocampus in trace conditioning: temporal discontinuity or task difficulty? *Neurobiology of learning and memory*, *76*(3), 447–61. doi:10.1006/nlme.2001.4039

Bichot, N. P., Rossi, A. F., & Desimone, R. (2005). Parallel and serial neural mechanisms for visual search in macaque area V4. *Science (New York, N.Y.)*, *308*(5721), 529–34. doi:10.1126/science.1109676

Bledowski, C., & Kaiser, J. (2010). Basic operations in working memory: Contributions from functional imaging studies. *Behavioural brain research*, *214*(2), 172–179. Retrieved from http://www.sciencedirect.com/science/article/B6SYP-506W6HJ-5/2/b6dc2a6947970b1380dab6a4a3f1872a

Bradley, M. M., Miccoli, L., Escrig, M. a, & Lang, P. J. (2008). The pupil as a measure of emotional arousal and autonomic activation. *Psychophysiology*, *45*(4), 602–7. doi:10.1111/j.1469-8986.2008.00654.x

Büchel, C., Dolan, R. J., Armony, J. L., & Friston, K. (1999). Amygdala-hippocampal involvement in human aversive trace conditioning revealed through event-related functional magnetic resonance imaging. *Journal of Neuroscience*, *19*(24), 10869–10876. Retrieved from http://www.ncbi.nlm.nih.gov/entrez/query.fcgi?cmd=Retrieve&db=PubMed&dopt=Citation&list_uids=10594068

Buzsáki, G., & Moser, E. I. (2013). Memory, navigation and theta rhythm in the hippocampal-entorhinal system. *Nature neuroscience*, *16*(2), 130–8. doi:10.1038/nn.3304

Carter, R. M., Hofstotter, C., Tsuchiya, N., & Koch, C. (2003). Working memory and fear conditioning. *Proceedings of the National Academy of Sciences*, *100*(3), 1399–1404. doi:10.1073/pnas.0334049100

Carter, R. M., O'Doherty, J. P., Seymour, B., Koch, C., & Dolan, R. J. (2006). Contingency awareness in human aversive conditioning involves the middle frontal gyrus. *NeuroImage*, *29*(3), 1007–12. doi:10.1016/j.neuroimage.2005.09.011

Chaumon, M., Schwartz, D., & Tallon-Baudry, C. (2009). Unconscious learning versus visual perception: dissociable roles for gamma oscillations revealed in MEG. *Journal of cognitive neuroscience*, *21*(12), 2287–99. doi:10.1162/jocn.2008.21155

Cheng, D. T., Knight, D. C., Smith, C. N., & Helmstetter, F. J. (2006a). Human amygdala activity during the expression of fear responses. *Behavioral neuroscience*, *120*(6), 1187–95. doi:10.1037/0735-7044.120.5.1187

Cheng, D. T., Knight, D. C., Smith, C. N., & Helmstetter, F. J. (2006b). Human amygdala activity during the expression of fear responses. *Behavioral neuroscience*, *120*(6), 1187–1195. Retrieved from http://www.ncbi.nlm.nih.gov/entrez/query.fcgi?cmd=Retrieve&db=PubMed&dopt=Citation&list_uids=17201461

Cheng, D. T., Knight, D. C., Smith, C. N., Stein, E. A., & Helmstetter, F. J. (2003). Functional MRI of human amygdala activity during Pavlovian fear conditioning: Stimulus processing versus response expression. *Behavioral Neuroscience*, *117*(1), 3–10. doi:10.1037/0735-7044.117.1.3

Cheng, D. T., Richards, J., & Helmstetter, F. J. (2007a). Activity in the human amygdala corresponds to early, rather than late period autonomic responses to a signal for shock. *Learning & Memory*, *14*(7), 485–490. Retrieved from http://www.ncbi.nlm.nih.gov/entrez/query.fcgi?cmd=Retrieve&db=PubMed&dopt=Citation&list_uids=17626906

Cheng, D. T., Richards, J., & Helmstetter, F. J. (2007b). Activity in the human amygdala corresponds to early, rather than late period autonomic responses to a signal for shock. *Learning & memory (Cold Spring Harbor, N.Y.)*, *14*(7), 485–90. doi:10.1101/lm.632007

Clark, J. J., Hollon, N. G., & Phillips, P. E. M. (2012). Pavlovian valuation systems in learning and decision making. *Current opinion in neurobiology*, *22*(6), 1054–61. doi:10.1016/j.conb.2012.06.004

Clark, R. E., & Squire, L. R. (1998). Classical conditioning and brain systems: the role of awareness. *Science*, *280*(5360), 77–81. Retrieved from http://www.ncbi.nlm.nih.gov/entrez/query.fcgi?cmd=Retrieve&db=PubMed&dopt=Citation&list_uids=9525860

Courtney, S. M., Petit, L., Maisog, J. M., Ungerleider, L. G., & Haxby, J. V. (1998). An area specialized for spatial working memory in human frontal cortex. *Science*, *279*(5355), 1347–1351. Retrieved from http://www.ncbi.nlm.nih.gov/entrez/query.fcgi?cmd=Retrieve&db=PubMed&dopt=Citation&list_uids=9478894

Cox, R. W. (1996). AFNI: software for analysis and visualization of functional magnetic resonance neuroimages. *Computers and biomedical research*, *29*(3), 162–73. Retrieved from http://www.ncbi.nlm.nih.gov/pubmed/8812068

Craig, a D. B. (2009). How do you feel--now? The anterior insula and human awareness. *Nature reviews. Neuroscience*, *10*(1), 59–70. doi:10.1038/nrn2555

Dawson, M. E., Rissling, A. J., Schell, A. M., & Wilcox, R. (2007). Under what conditions can human affective conditioning occur without contingency awareness? Test of the evaluative conditioning paradigm. *Emotion*, *7*(4), 755–766. Retrieved from http://www.ncbi.nlm.nih.gov/entrez/query.fcgi?cmd=Retrieve&db=PubMed&dopt=Citation&list_uids=18039045

Desikan, R. S., Ségonne, F., Fischl, B., Quinn, B. T., Dickerson, B. C., Blacker, D., … Killiany, R. J. (2006). An automated labeling system for subdividing the human cerebral cortex on MRI scans into gyral based regions of interest. *NeuroImage*, *31*(3), 968–80. doi:10.1016/j.neuroimage.2006.01.021

Dunsmoor, J. E., Bandettini, P. a, & Knight, D. C. (2007). Impact of continuous versus intermittent CS-UCS pairing on human brain activation during Pavlovian fear conditioning. *Behavioral neuroscience*, *121*(4), 635–42. doi:10.1037/0735-7044.121.4.635

Dunsmoor, J. E., Kragel, P. a, Martin, A., & Labar, K. S. (2013). Aversive Learning Modulates Cortical Representations of Object Categories. *Cerebral cortex (New York, N.Y. : 1991)*, 1–14. doi:10.1093/cercor/bht138

Engell, A. D., & McCarthy, G. (2010). Selective attention modulates face-specific induced gamma oscillations recorded from ventral occipitotemporal cortex. *Journal of Neuroscience*, *30*(26), 8780–6. doi:10.1523/JNEUROSCI.1575-10.2010

Epstein, R. a. (2008). Parahippocampal and retrosplenial contributions to human spatial navigation. *Trends in cognitive sciences*, *12*(10), 388–96. doi:10.1016/j.tics.2008.07.004

Fell, J., & Axmacher, N. (2011). The role of phase synchronization in memory processes. *Nature reviews. Neuroscience*, *12*(2), 105–18. doi:10.1038/nrn2979

Fischl, B., Salat, D. H., Busa, E., Albert, M., Dieterich, M., Haselgrove, C., … Dale, A. M. (2002). Whole brain segmentation: automated labeling of neuroanatomical structures in the human brain. *Neuron*, *33*(3), 341–55. Retrieved from http://www.ncbi.nlm.nih.gov/pubmed/11832223

Fischl, B., Salat, D. H., van der Kouwe, A. J. W., Makris, N., Ségonne, F., Quinn, B. T., & Dale, A. M. (2004). Sequence-independent segmentation of magnetic resonance images. *NeuroImage*, *23 Suppl 1*, S69–84. doi:10.1016/j.neuroimage.2004.07.016

Fischl, B., van der Kouwe, A., Destrieux, C., Halgren, E., Ségonne, F., Salat, D. H., … Dale, A. M. (2004). Automatically parcellating the human cerebral cortex. *Cerebral Cortex*, *14*(1), 11–22. Retrieved from http://www.ncbi.nlm.nih.gov/pubmed/14654453

Fries, P., Reynolds, J. H., Rorie, a E., & Desimone, R. (2001). Modulation of oscillatory neuronal synchronization by selective visual attention. *Science (New York, N.Y.)*, *291*(5508), 1560–3. doi:10.1126/science.291.5508.1560

Fuentemilla, L., Barnes, G. R., Düzel, E., & Levine, B. (2013). Theta oscillations orchestrate medial temporal lobe and neocortex in remembering autobiographical memories. *NeuroImage*, 1–9. doi:10.1016/j.neuroimage.2013.08.029

Gilmartin, M. R., & Helmstetter, F. J. (2010). Trace and contextual fear conditioning require neural activity and NMDA receptor-dependent transmission in the medial prefrontal cortex. *Learning & Memory*, *17*(6), 289–296. Retrieved from

http://www.pubmedcentral.nih.gov/articlerender.fcgi?artid=2884289&tool=pmcentrez&rendertype=abstract

Gilmartin, M. R., & McEchron, M. D. (2005a). Single neurons in the medial prefrontal cortex of the rat exhibit tonic and phasic coding during trace fear conditioning. *Behavioral neuroscience*, *119*(6), 1496–510. doi:10.1037/0735-7044.119.6.1496

Gilmartin, M. R., & McEchron, M. D. (2005b). Single neurons in the dentate gyrus and CA1 of the hippocampus exhibit inverse patterns of encoding during trace fear conditioning. *Behavioral neuroscience*, *119*(1), 164–79. doi:10.1037/0735-7044.119.1.164

Gilmartin, M. R., Miyawaki, H., Helmstetter, F. J., & Diba, K. (2013). Prefrontal activity links nonoverlapping events in memory. *The Journal of neuroscience : the official journal of the Society for Neuroscience*, *33*(26), 10910–4. doi:10.1523/JNEUROSCI.0144-13.2013

Gläscher, J., Rose, M., & Büchel, C. (2007). Independent effects of emotion and working memory load on visual activation in the lateral occipital complex. *Journal of Neuroscience*, *27*(16), 4366–73. doi:10.1523/JNEUROSCI.3310-06.2007

Gottfried, J. a, & Dolan, R. J. (2004). Human orbitofrontal cortex mediates extinction learning while accessing conditioned representations of value. *Nature neuroscience*, *7*(10), 1144–52. doi:10.1038/nn1314

Gottlieb, D. (2004). Acquisition with partial and continuous reinforcement in pigeon autoshaping. *Learning & behavior*, *32*(3), 321–334. Retrieved from http://www.ncbi.nlm.nih.gov/entrez/query.fcgi?cmd=Retrieve&db=PubMed&dopt=Citation&list_uids=15672827

Gruber, T., Tsivilis, D., Montaldi, D., & Müller, M. M. (2004). Induced gamma band responses: an early marker of memory encoding and retrieval. *NeuroReport*, *15*(11), 1837–1841. Retrieved from http://journals.lww.com/neuroreport/Fulltext/2004/08060/Induced_gamma_band_responses__an_early_marker_of.30.aspx

Hämäläinen, M. S., & Ilmoniemi, R. J. (1994). Interpreting magnetic fields of the brain: minimum norm estimates. *Medical & biological engineering & computing*, *32*(1), 35–42. Retrieved from http://www.ncbi.nlm.nih.gov/pubmed/8182960

Haritha, A. T., Wood, K. H., Ver Hoef, L. W., & Knight, D. C. (2012). Human trace fear conditioning: right-lateralized cortical activity supports trace-interval processes. *Cognitive, affective & behavioral neuroscience*. doi:10.3758/s13415-012-0142-6

Headley, D. B., & Weinberger, N. M. (2011). Gamma-Band Activation Predicts Both Associative Memory and Cortical Plasticity. *Journal of Neuroscience*, *31*(36), 12748–12758. doi:10.1523/JNEUROSCI.2528-11.2011

Helmstetter, F. J., Parsons, R. G., & Gafford, G. M. (2008). Macromolecular synthesis, distributed synaptic plasticity, and fear conditioning. *Neurobiology of learning and memory*, *89*(3), 324–37. doi:10.1016/j.nlm.2007.09.002

Hermans, E. J., Henckens, M. J. a G., Roelofs, K., & Fernández, G. (2012). Fear bradycardia and activation of the human periaqueductal grey. *NeuroImage, 66C*, 278–287. doi:10.1016/j.neuroimage.2012.10.063

Hoffmann, L. C., & Berry, S. D. (2009). Cerebellar theta oscillations are synchronized during hippocampal theta-contingent trace conditioning. *Proceedings of the National Academy of Sciences of the United States of America*, *106*(50), 21371–6. doi:10.1073/pnas.0908403106

Huang, M. X., Mosher, J. C., & Leahy, R. M. (1999). A sensor-weighted overlapping-sphere head model and exhaustive head model comparison for MEG. *Physics in medicine and biology*, *44*(2), 423–40. Retrieved from http://www.ncbi.nlm.nih.gov/pubmed/10070792

Jarome, T. J., Werner, C. T., Kwapis, J. L., & Helmstetter, F. J. (2011). Activity dependent protein degradation is critical for the formation and stability of fear memory in the amygdala. *PloS one*, *6*(9), e24349. doi:10.1371/journal.pone.0024349

Kaiser, J., Ripper, B., Birbaumer, N., & Lutzenberger, W. (2003). Dynamics of gamma-band activity in human magnetoencephalogram during auditory pattern working memory. *NeuroImage*, *20*(2), 816–827. Retrieved from http://www.sciencedirect.com/science/article/pii/S1053811903003501

Kanwisher, N., & Yovel, G. (2006). The fusiform face area: a cortical region specialized for the perception of faces. *Philosophical transactions of the Royal Society of*

London. Series B, Biological sciences, *361*(1476), 2109–28. doi:10.1098/rstb.2006.1934

Kaplan, R., Doeller, C. F., Barnes, G. R., Litvak, V., Düzel, E., Bandettini, P. a, & Burgess, N. (2012). Movement-related theta rhythm in humans: coordinating self-directed hippocampal learning. *PLoS biology*, *10*(2), e1001267. doi:10.1371/journal.pbio.1001267

Kim, J. J., & Jung, M. W. (2006). Neural circuits and mechanisms involved in Pavlovian fear conditioning: a critical review. *Neuroscience and biobehavioral reviews*, *30*(2), 188–202. doi:10.1016/j.neubiorev.2005.06.005

Kluge, C., Bauer, M., Leff, A. P., Heinze, H.-J., Dolan, R. J., & Driver, J. (2011). Plasticity of human auditory-evoked fields induced by shock conditioning and contingency reversal. *Proceedings of the National Academy of Sciences of the United States of America*, *108*(30), 12545–50. doi:10.1073/pnas.1016124108

Knight, D. C., Cheng, D. T., Smith, C. N., Stein, E. A., & Helmstetter, F. J. (2004). Neural substrates mediating human delay and trace fear conditioning. *Journal of Neuroscience*, *24*(1), 218–28. doi:10.1523/JNEUROSCI.0433-03.2004

Knight, D. C., Nguyen, H. T., & Bandettini, P. A. (2005). The role of the human amygdala in the production of conditioned fear responses. *Neuroimage*, *26*(4), 1193–1200. doi:10.1016/j.neuroimage.2005.03.020

Knight, D. C., Nguyen, H. T., & Bandettini, P. A. (2006). The role of awareness in delay and trace fear conditioning in humans. *Cognitive, Affective, & Behavioral Neuroscience*, *6*(2), 157–162. Retrieved from http://www.ncbi.nlm.nih.gov/entrez/query.fcgi?cmd=Retrieve&db=PubMed&dopt=Citation&list_uids=17007236

Knight, D. C., Smith, C. N., Cheng, D. T., Stein, E. A., & Helmstetter, F. J. (2004). Amygdala and hippocampal activity during acquisition and extinction of human fear conditioning. *Cognitive, Affective, & Behavioral Neuroscience*, *4*(3), 317–25. Retrieved from http://www.ncbi.nlm.nih.gov/pubmed/15535167

Knight, D. C., Smith, C. N., Stein, E. A., & Helmstetter, F. J. (1999). Functional MRI of human Pavlovian fear conditioning: patterns of activation as a function of learning. *Neuroreport*, *10*(17), 3665–3670. Retrieved from http://www.ncbi.nlm.nih.gov/entrez/query.fcgi?cmd=Retrieve&db=PubMed&dopt=Citation&list_uids=10619663

Knight, D. C., Waters, N. S., & Bandettini, P. a. (2009). Neural substrates of explicit and implicit fear memory. *NeuroImage*, *45*(1), 208–14. doi:10.1016/j.neuroimage.2008.11.015

Knight, D. C., Waters, N. S., King, M. K., & Bandettini, P. A. (2010). Learning-related diminution of unconditioned SCR and fMRI signal responses. *NeuroImage*, *49*(1), 843–8. doi:10.1016/j.neuroimage.2009.07.012

Kok, a. (1997). Event-related-potential (ERP) reflections of mental resources: a review and synthesis. *Biological psychology*, *45*(1-3), 19–56. Retrieved from http://www.ncbi.nlm.nih.gov/pubmed/9083643

Koo, J. W., Han, J.-S., & Kim, J. J. (2004). Selective neurotoxic lesions of basolateral and central nuclei of the amygdala produce differential effects on fear conditioning. *Journal of Neuroscience*, *24*(35), 7654–62. doi:10.1523/JNEUROSCI.1644-04.2004

Krettek, J. E., & Price, J. L. (1977). Projections from the amygdaloid complex to the cerebral cortex and thalamus in the rat and cat. *Journal of Comparative Neurology*, *172*(4), 687–722.

Kwapis, J. L., Jarome, T. J., Schiff, J. C., & Helmstetter, F. J. (2011). Memory consolidation in both trace and delay fear conditioning is disrupted by intra-amygdala infusion of the protein synthesis inhibitor anisomycin. *Learning & Memory*, *18*(11), 728–32. doi:10.1101/lm.023945.111

Lang, P. J., Bradley, M. M., & Cuthbert, B. (2008). *International affective picture system (IAPS): Affective ratings of pictures and instruction manual*. *University of Florida*. Gainesville, FL.

LeDoux, J. (2000). Emotion circuits in the brain. *Annual review of neuroscience*, 155–184. Retrieved from http://www.annualreviews.org/doi/abs/10.1146/annurev.neuro.23.1.155

Ledoux, J. E. (2000). Emotion circuits in the brain. *Annual review of neuroscience*, *23*(1), 155–184. Retrieved from http://www.annualreviews.org/doi/abs/10.1146/annurev.neuro.23.1.155

Liddell, B. J., Brown, K. J., Kemp, A. H., Barton, M. J., Das, P., Peduto, A., … Williams, L. M. (2005). A direct brainstem-amygdala-cortical "alarm" system for subliminal signals of fear. *NeuroImage*, *24*(1), 235–43. doi:10.1016/j.neuroimage.2004.08.016

Logothetis, N. K. (2008). What we can do and what we cannot do with fMRI. *Nature*, *453*(7197), 869–878. doi:10.1038/nature06976

Lovibond, P. F., & Shanks, D. R. (2002). The role of awareness in Pavlovian conditioning: empirical evidence and theoretical implications. *Journal of Experimental Psychology Animal Behavior Processes*, *28*(1), 3–26. doi:10.1037//0097-7403.28.1.3

Mackintosh, N. J. (1983). *Conditioning and associative learning*. *Oxford psychology series ; no. 3* (p. 316 p.). Oxford: Clarendon Press.

Minati, L., Jones, C. L., Gray, M. a, Medford, N., Harrison, N. a, & Critchley, H. D. (2009). Emotional modulation of visual cortex activity: a functional near-infrared spectroscopy study. *Neuroreport*, *20*(15), 1344–50. doi:10.1097/WNR.0b013e328330c751

Moratti, S., & Keil, A. (2005). Cortical activation during Pavlovian fear conditioning depends on heart rate response patterns: an MEG study. *Brain research*, *25*(2), 459–471. doi:10.1016/j.cogbrainres.2005.07.006

Moratti, S., Keil, A., & Miller, G. a. (2006). Fear but not awareness predicts enhanced sensory processing in fear conditioning. *Psychophysiology*, *43*(2), 216–26. doi:10.1111/j.1464-8986.2006.00386.x

Morris, J. S., DeGelder, B., Weiskrantz, L., Dolan, R. J., & de Gelder, B. (2001). Differential extrageniculostriate and amygdala responses to presentation of emotional faces in a cortically blind field. *Brain*, *124*(Pt 6), 1241–52. Retrieved from http://www.ncbi.nlm.nih.gov/entrez/query.fcgi?cmd=Retrieve&db=PubMed&dopt=Citation&list_uids=11353739

Nadel, L., Samsonovich, a, Ryan, L., & Moscovitch, M. (2000). Multiple trace theory of human memory: computational, neuroimaging, and neuropsychological results. *Hippocampus*, *10*(4), 352–68. doi:10.1002/1098-1063(2000)10:4<352::AID-HIPO2>3.0.CO;2-D

Noguchi, Y., & Kakigi, R. (2005). Neural mechanisms of visual backward masking revealed by high temporal resolution imaging of human brain. *Neuroimage*, *27*(1), 178–187. doi:doi:10.1016/j.neuroimage.2005.03.032

Öhman, A., & Mineka, S. (2001). Fears, phobias, and preparedness: Toward an evolved module of fear and fear learning. *Psychological Review*, *108*(3), 483–522. Retrieved

from http://www.ncbi.nlm.nih.gov/entrez/query.fcgi?cmd=Retrieve&db=PubMed&dopt=Citation&list_uids=11488376

Öhman, A., Morris, J. S., & Dolan, R. J. (1999). A subcortical pathway to the right amygdala mediating “unseen” fear. *Proceedings of the National Academy of Sciences*, *96*(4), 1680–5. Retrieved from http://www.ncbi.nlm.nih.gov/pubmed/9990084

Osipova, D., Takashima, A., Oostenveld, R., Fernández, G., Maris, E., & Jensen, O. (2006). Theta and gamma oscillations predict encoding and retrieval of declarative memory. *The Journal of neuroscience : the official journal of the Society for Neuroscience*, *26*(28), 7523–31. doi:10.1523/JNEUROSCI.1948-06.2006

Ottersen, O. P., & Ben-Ari, Y. (1979). Afferent connections to the amygdaloid complex of the rat and cat. I. Projections from the thalamus. *Journal of Comparative Neurology*, *187*(2), 401–424.

Parsons, R. G., Gafford, G., & Helmstetter, F. J. (2006). Translational control via the mammalian target of rapamycin pathway is critical for the formation and stability of long-term fear memory in amygdala neurons. *Journal of Neuroscience*, *26*, 12977–12983.

Pascual-Marqui, R. D. (2002). Standardized low-resolution brain electromagnetic tomography (sLORETA): technical details. *Methods and findings in experimental*

and clinical pharmacology, *24 Suppl D*, 5–12. Retrieved from http://www.ncbi.nlm.nih.gov/pubmed/12575463

Pessoa, L., & Adolphs, R. (2010). Emotion processing and the amygdala: from a "low road" to "many roads" of evaluating biological significance. *Nature reviews. Neuroscience*, *11*(11), 773–83. doi:10.1038/nrn2920

Phelps, E. A., Delgado, M. R., Nearing, K. I., & LeDoux, J. E. (2004). Extinction learning in humans: role of the amygdala and vmPFC. *Neuron*, *43*(6), 897–905. doi:10.1016/j.neuron.2004.08.042

Pollatos, O., Kirsch, W., & Schandry, R. (2005). On the relationship between interoceptive awareness, emotional experience, and brain processes. *Brain research. Cognitive brain research*, *25*(3), 948–62. doi:10.1016/j.cogbrainres.2005.09.019

Popescu, A. T., Popa, D., & Paré, D. (2009). Coherent gamma oscillations couple the amygdala and striatum during learning. *Nature neuroscience*, *12*(6), 801–7. doi:10.1038/nn.2305

Reinhard, G., & Lachnit, H. (2002). Differential conditioning of anticipatory pupillary dilation responses in humans. *Biological Psychology*, *60*(1), 51–68. Retrieved from http://www.sciencedirect.com/science/article/pii/S030105110200011X

Reinhard, G., Lachnit, H., & König, S. (2006). Tracking stimulus processing in Pavlovian pupillary conditioning. *Psychophysiology*, *43*(1), 73–83. doi:10.1111/j.1469-8986.2006.00374.x

Sato, W., Kochiyama, T., Uono, S., Matsuda, K., Usui, K., Inoue, Y., & Toichi, M. (2011). Rapid amygdala gamma oscillations in response to fearful facial expressions. *Neuropsychologia*, *49*(4), 612–7. doi:10.1016/j.neuropsychologia.2010.12.025

Sato, W., Kochiyama, T., Uono, S., & Yoshikawa, S. (2010). Amygdala integrates emotional expression and gaze direction in response to dynamic facial expressions. *NeuroImage*, *50*(4), 1658–65. doi:10.1016/j.neuroimage.2010.01.049

Schultz, D. H., Balderston, N. L., Geiger, J. a, & Helmstetter, F. J. (2013). Dissociation between implicit and explicit responses in postconditioning UCS revaluation after fear conditioning in humans. *Behavioral neuroscience*, *127*(3), 357–68. doi:10.1037/a0032742

Schultz, D. H., Balderston, N. L., & Helmstetter, F. J. (2012). Resting-state connectivity of the amygdala is altered following Pavlovian fear conditioning. *Frontiers in Human Neuroscience*, *6*(August), 1–10. doi:10.3389/fnhum.2012.00242

Schultz, D. H., & Helmstetter, F. J. (2010a). Classical conditioning of autonomic fear responses is independent of contingency awareness. *Journal of Experimental Psychology Animal Behavior Processes*, *36*(4), 495–500. doi:10.1037/a0020263

Schultz, D. H., & Helmstetter, F. J. (2010b). Classical conditioning of autonomic fear responses is independent of contingency awareness. *J Exp Psychol Anim Behav Process*, *36*(4), 495–500. doi:10.1037/a0020263

Seager, M. a, Johnson, L. D., Chabot, E. S., Asaka, Y., & Berry, S. D. (2002). Oscillatory brain states and learning: Impact of hippocampal theta-contingent training. *Proceedings of the National Academy of Sciences of the United States of America*, *99*(3), 1616–20. doi:10.1073/pnas.032662099

Sederberg, P. B., Kahana, M. J., Howard, M. W., Donner, E. J., & Madsen, J. R. (2003). Theta and gamma oscillations during encoding predict subsequent recall. *The Journal of neuroscience : the official journal of the Society for Neuroscience*, *23*(34), 10809–14. Retrieved from http://www.ncbi.nlm.nih.gov/pubmed/14645473

Sederberg, P. B., Schulze-Bonhage, A., Madsen, J. R., Bromfield, E. B., McCarthy, D. C., Brandt, A., … Kahana, M. J. (2007). Hippocampal and neocortical gamma oscillations predict memory formation in humans. *Cerebral cortex (New York, N.Y. : 1991)*, *17*(5), 1190–6. doi:10.1093/cercor/bhl030

Simmons, A., Strigo, I., Matthews, S. C., Paulus, M. P., & Stein, M. B. (2006). Anticipation of aversive visual stimuli is associated with increased insula activation in anxiety-prone subjects. *Biological psychiatry*, *60*(4), 402–9. doi:10.1016/j.biopsych.2006.04.038

Steinmetz, P. N., Roy, A., Fitzgerald, P. J., Hsiao, S. S., & Johnson, K. O. (2000). Attention modulates synchronized neuronal ® ring in primate somatosensory cortex, 187–190.

Sterpenich, V., D'Argembeau, A., Desseilles, M., Balteau, E., Albouy, G., Vandewalle, G., … Maquet, P. (2006). The locus ceruleus is involved in the successful retrieval

of emotional memories in humans. *Journal of Neuroscience*, *26*(28), 7416–23. doi:10.1523/JNEUROSCI.1001-06.2006

Svartdal, F. (2003). Extinction after partial reinforcement: predicted vs. judged persistence. *Scand J Psychol*, *44*(1), 55–64. Retrieved from http://www.ncbi.nlm.nih.gov/entrez/query.fcgi?cmd=Retrieve&db=PubMed&dopt=Citation&list_uids=12603004

Tabbert, K., Merz, C. J., Klucken, T., Schweckendiek, J., Vaitl, D., Wolf, O. T., & Stark, R. (2010). Influence of contingency awareness on neural, electrodermal and evaluative responses during fear conditioning. *Social cognitive and affective neuroscience*. doi:10.1093/scan/nsq070

Tadel, F., Baillet, S., Mosher, J. C., Pantazis, D., & Leahy, R. M. (2011). Brainstorm: A User-Friendly Application for MEG/EEG Analysis. *Computational intelligence and neuroscience*, *2011*, 879716. doi:10.1155/2011/879716

Tallon-Baudry, C., & Bertrand, O. (1999). Oscillatory gamma activity in humans and its role in object representation. *Trends in cognitive sciences*, *3*(4), 151–162. Retrieved from http://www.ncbi.nlm.nih.gov/pubmed/10322469

Tamietto, M., Castelli, L., Vighetti, S., Perozzo, P., Geminiani, G., Weiskrantz, L., & de Gelder, B. (2009). Unseen facial and bodily expressions trigger fast emotional reactions. *Proceedings of the National Academy of Sciences*, *106*(42), 17661–6. doi:10.1073/pnas.0908994106

Taulu, S., & Hari, R. (2009). Removal of magnetoencephalographic artifacts with temporal signal-space separation: demonstration with single-trial auditory-evoked responses. *Human brain mapping*, *30*(5), 1524–34. doi:10.1002/hbm.20627

Taulu, S., Kajola, M., & Simola, J. (2004). Suppression of interference and artifacts by the Signal Space Separation Method. *Brain topography*, *16*(4), 269–75. Retrieved from http://www.ncbi.nlm.nih.gov/pubmed/15379226

Van Steenbergen, H., Band, G. P. H., & Hommel, B. (2011). Threat but not arousal narrows attention: evidence from pupil dilation and saccade control. *Frontiers in psychology*, *2*(October), 281. doi:10.3389/fpsyg.2011.00281

Wamsley, E. J., & Antrobus, J. S. (2009). The expression of trace conditioning during non-REM sleep and its relation to subjective experience. *Neurobiology of learning and memory*, *92*(3), 283–291. Retrieved from http://www.ncbi.nlm.nih.gov/entrez/query.fcgi?cmd=Retrieve&db=PubMed&dopt=Citation&list_uids=19254775

Weike, A. I. I., Schupp, H. T. T., & Hamm, A. O. (2007). Fear acquisition requires awareness in trace but not delay conditioning. *Psychophysiology*, *44*(1), 170–180. doi:10.1111/j.1469-8986.2006.00469.x

6 Curriculum Vitae

EDUCATION

University of West Florida
B.A. in Psychology **2004**

University of Wisconsin-Milwaukee
M.S. in Experimental Psychology - Neuroscience **2010**
Title: The effect of CS-UCS interval on masked conditioning with fear-relevant and fear-irrelevant stimuli.
Committee: Fred Helmstetter PhD.; Christine Larson, PhD.; Anthony Greene, PhD.

University of Wisconsin-Milwaukee
PhD in Experimental Psychology - Neuroscience **2013**
Title: Neural responses during trace conditioning with face and non-face stimuli recorded with magnetoencephalography
Committee: Fred Helmstetter PhD.; Christine Larson, PhD.; Ira Driscoll, PhD.; Deborah Hannula, PhD.; Catherine Tallon-Baudry, PhD.
Advisor: Dr. Fred Helmstetter PhD.
Major: Neuroscience
Minor: Neurobiology, Behavior Analysis

École normale supérieure
Chateaubriand Fellow **2012**
Advisor: Dr. Catherine Tallon-Baudry

PUBLICATIONS

Balderston, N. L., & Helmstetter, F. (2010). Conditioning with masked stimuli and without awareness affects timecourse of skin conductance response. *Behavioral Neuroscience*, *123*(4), 478-489.

Balderston, N. L., Schultz, D. H., & Helmstetter, F. (2011). The human amygdala plays a stimulus specific role in the detection of novelty. *Neuroimage, 55(4), 1889-1898.*

Balderston, N. L., Schultz, D. H., & Helmstetter, F. (2013). The effect of threat on novelty evoked amygdala responses*. PLoS ONE 8(5):* e63220.

Balderston, N. L., Schultz, D. H., Baillet, S., & Helmstetter, F. (2013). How to detect amygdala activity with magnetoencephalography using source imaging, *Journal of Visualized Experiments*. *76*, e50212, http://www.jove.com/video/50212/how-to-detect-amygdala-activity-with-magnetoencephalography-using?status=a52218k

Schultz, D. H., **Balderston, N. L.,** & Helmstetter, F. J. (2012). Resting-state connectivity of the amygdala is altered following Pavlovian fear conditioning. *Frontiers in Human Neuroscience*, 6(August), 1–10.

Schultz, D. H., **Balderston, N. L.,** Geiger, J. A., & Helmstetter, F. J. (2013). Dissociation between implicit and explicit responses in postconditioning UCS revaluation after fear conditioning in humans. *Behavioral Neuroscience, 127(3),* 357-368.

Larson, C. L., Baskin-Sommers, A. R., Stout, D. M., **Balderston, N. L.**, Curtin, J. J., Schultz D. H., Kiehl, K. A., & Newman, J. P. (2013), The interplay of attention and emotion: top-down attention modulates amygdala activation in psychopathy. Cognitive, Affective, & Behavioral Neuroscience, 1-14.

IN PREPARATION

Balderston, N. L., Schultz, D. H., Baillet, S., & Helmstetter, F. (Submitted to Neuroimage). Rapid amygdala responses during trace fear conditioning without awareness.

Balderston, N. L., Schultz, D. H., & Helmstetter, F. (In preparation). Identification of distinct functional subregions of the human amygdala using high-resolution BOLD imaging and probabilistic tractography.

Schultz, D. H., **Balderston, N. L.**, Cheng, D., Geiger, J. A., & Helmstetter, F. (In preparation). Conditional stimulus BOLD activation overlaps with shock evoked activity in somatosensory cortex.

Schultz, D., **Balderston, N. L.**, & Helmstetter, F. (In preparation). A direct comparison of auditory and visual fear conditioning in humans using FMRI.

Balderston, N. L., Schultz D. H., Baskin-Sommers, A. R., Newman, J. P. Larson, C. L., & Helmstetter, F (In preparation). Psychopaths display greater amygdala activation in a basic conditioning paradigm.

ABSTRACTS

Balderston, N. L., Schultz, D., & Helmstetter, F. Using DTI and high resolution BOLD to identify distinct functional subunits of the human amygdala. Program. No. 493.02. 2010 Neuroscience Meeting Planner. New Orleans, LA: Society for Neuroscience, 2012. Online

Balderston, N. L., Schultz, D., Baillet, S., & Helmstetter, F. (2012). Rapid amygdala responses during trace fear conditioning without awareness. *Poster presented at the Organization for Human Brain Mapping meeting in Beijing, China.*

Balderston, N. L., Schultz, D., Newman, J. P., Larson, C. L., & Helmstetter, F. (2012). Behavioral and amygdala BOLD responses in psychopaths during fear

conditioning. *Poster presented at the Organization for Human Brain Mapping meeting in Beijing, China.*

Balderston, N. L., Schultz, D., Baillet, S., & Helmstetter, F. Neuromagnetic amygdala responses during trace fear conditioning without awareness. Program. No. 287.04. 2010 Neuroscience Meeting Planner. Washington, DC: Society for Neuroscience, 2011. Online

Balderston, N. L., Schultz, D., & Helmstetter, F. The effect of threat on novelty evoked amygdala responses. Program. No. 602.13. 2010 Neuroscience Meeting Planner. San Diego, CA: Society for Neuroscience, 2010. Online

Balderston, N. L., Schultz, D., & Helmstetter, F. Novel faces but not scenes drive BOLD responses in the amygdala. Program. No. 674.22. 2009 Neuroscience Meeting Planner. Chicago, IL: Society for Neuroscience, 2009. Online

Balderston, N. L., Schultz, D., & Helmstetter, F. (2009). BOLD response to novelty in the human amygdala. *Poster presented at the Organization for Human Brain Mapping meeting in San Francisco, CA.*

Balderston, N. L., Schultz, D., Schramm, C., & Helmstetter, F. In a direct comparison of novelty and emotional valence, novelty evokes larger magnitude BOLD responses in the amygdala. Program. No. 119.6. 2008 Neuroscience Meeting Planner. Washington, DC: Society for Neuroscience, 2008. Online

Balderston, N.L., Geiger, J. A., Schultz, D.H., Helmstetter, F. J. Masked presentation of simple visual stimuli and learning without awareness in human fear conditioning Program. No. 526.19. 2007 Neuroscience Meeting Planner. San Diego, CA: Society for Neuroscience, 2007. Online

Balderston, N.L., Geiger, J. A., Schultz, D.H., Helmstetter, F. J. (2007). Learning without awareness in human fear conditioning. *Poster presented at the Pavlovian Society meeting in Austin, TX.*

Geiger, J. A., **Balderston, N.L.**, Schultz, D.H., Helmstetter, F. J. Functional neuroimaging of context dependent fear reinstatement in humans. Program No. 526.17. 2007 Neuroscience Meeting Planner. San Diego, CA: Society for Neuroscience, 2007. Online

Schultz, D., **Balderston, N.L.**, & Helmstetter, F. (2009). Somatosensory cortex activation by a visual stimulus that signals shock. Poster presented at the Organization for Human Brain Mapping meeting in San Francisco, CA.

Schultz, D., **Balderston, N.L.**, Schramm, C., & Helmstetter, F. Conditional stimulus evoked BOLD activation overlaps with shock evoked activity in somatosensory cortex.

Program. No. 190.8. 2008 Neuroscience Meeting Planner. Washington, DC: Society for Neuroscience, 2008. Online

Schultz, D.H., Geiger, J. A., **Balderston, N.L.**, Helmstetter, F. J. Classical conditioning of autonomic fear responses is independent of contingency awareness. Program No. 526.18. 2007 Neuroscience Meeting Planner. San Diego, CA: Society for Neuroscience, 2007. Online

Schultz, D.H., Geiger, J. A., **Balderston, N.L.**, Helmstetter, F. J. (2007). Classical conditioning of autonomic fear responses is independent of contingency Awareness. *Poster presented at the Pavlovian Society meeting in Austin, TX.*

Schultz, D.H., Geiger, J. A., **Balderston, N.L.**, Helmstetter, F. J. (2007). Contextual modulation of human brain activity during reinstatement of conditioned fear. *Poster presented at the Human Brain Mapping conference in Chicago, IL.*

Schramm, C., Schultz, D., **Balderston, N.L.**, & Helmstetter, F. Impact of repeated versus novel exposure to conditional stimuli on human brain activation during Pavlovian fear conditioning. Program. No. 190.7. 2008 Neuroscience Meeting Planner. Washington, DC: Society for Neuroscience, 2008. Online

COLLOQUIA AND SYMPOSIA

Rapid amygdala responses during trace fear conditioning without awareness. *Brainstorm User Symposium at BioMag 2012.* Paris, France. August 2012.

Differential effects of novelty and fear on activity within anatomically defined subregions of the human amygdala. *Graduate Student Research Symposium.* University of Wisconsin – Milwaukee, Milwaukee, WI. April 2012.

Novel Stimuli Evoke BOLD Responses in the Human Amygdala. *Center for Imaging Research seminar series.* Medical College of Wisconsin – Milwaukee, WI. April 2010.

BOLD response to novelty in the human amygdala. *Graduate Student Research Symposium.* University of Wisconsin – Milwaukee, Milwaukee, WI. April 2010.

BOLD response to novelty in the human amygdala. *Neuroscience and Physiology seminar series.* University of Wisconsin-Milwaukee, Milwaukee, WI. April 2010.

BOLD response to novelty in the human amygdala. *Milwaukee Area Neuroscience Meeting.* University of Wisconsin-Milwaukee, Milwaukee, WI. April 2010.

BOLD response to novelty in the human amygdala. *Milwaukee Area Neuroscience Meeting.* University of Wisconsin-Milwaukee, Milwaukee, WI. March 2010.

The effects of novelty and emotional valence on BOLD activity in the amygdala, hippocampus, and visual cortex. *Neuroscience and Physiology seminar series.* University of Wisconsin-Milwaukee, Milwaukee, WI. December 2008.

Masking blocks contingency awareness but not implicit learning in fear conditioning. *Graduate Student Research Symposium.* University of Wisconsin – Milwaukee, Milwaukee, WI. April 2008.

Fear learning does not depend on awareness. *Neuroscience and Physiology seminar series.* University of Wisconsin-Milwaukee, Milwaukee, WI. November 2007.

The role of awareness in fear acquisition. *Graduate Student Research Symposium.* University of Wisconsin – Milwaukee, Milwaukee, WI. April 2007.

The effects of visual masking on fear acquisition. *Neuroscience and Physiology seminar series.* University of Wisconsin-Milwaukee, Milwaukee, WI. April 2007.

PROFESSIONAL EXPERIENCE

Teaching Assistant: University of Wisconsin-Milwuakee

Fall 2006	Physiological Psychology (David Bauer, M.S.)
Spring 2007	Research Methods (Dr. Bob Hessling)
Fall 2007	Research Methods (Dr. Susan Lima)
Spring 2008	Research Methods (Dr. Marcellus Merritt)
Fall 2009	Research Methods (Dr. Susan Lima)

Research Assistant: University of Wisconsin-Milwuakee

2006-2013	Psychology Department (Dr. Fred Helmstetter)

Project Coordinator: University of West Florida

Summer 2006	Health Psychology Research Lab (Dr. Susan Walch)

Research Assistant: University of West Florida

Fall 2005	Center for Environmental Diagnostics and Bioremediation (Dr. Carl Mohrherr)

AWARDS

Chancellor's Graduate Student Award – University of Wisconsin-Milwaukee, 2006-2008
University of Wisconsin-Milwaukee Graduate School Travel Award, 2007
John and Lynn Schiek Award in Behavior Analysis, 2009, 2010
Chateaubriand Fellowship, 2012

MEMBERSHIPS

Society for Neuroscience
Human Brain Mapping
Pavlovian Society

Sigma Xi